

NONSEGMENTED NEGATIVE STRAND RNA VIRUSES: VIRAL RNA CAP
METHYLATION AND POTENTIAL APPLICATIONS AS AN ANTICANCER
THERAPY

by

Andrea Mary Murphy

A dissertation submitted to the faculty of
The University of North Carolina at Charlotte
in partial fulfillment of the requirements
for the degree of Doctor of Philosophy in
Biology

Charlotte

2012

Approved by:

Dr. Valery Grdzlishvili

Dr. Ian Marriott

Dr. Pinku Mukherjee

Dr. Laura Schrum

Dr. Michael Turner

© 2012
Andrea Mary Murphy
ALL RIGHTS RESERVED

ABSTRACT

ANDREA MARY MURPHY. Nonsegmented negative strand RNA viruses: viral RNA cap methylation and potential applications as an anticancer therapy. (Under the direction of DR. VALERY GRDZELISHVILI)

The viruses of the order *Mononegavirales* include important human, animal, and plant pathogens and additionally, have great potential as vaccine, oncolytic and gene therapy vectors. This dissertation focuses on two prototypic *Mononegavirales*, vesicular stomatitis virus (VSV) and Sendai virus (SeV), their virus-encoded cap methylation function, and potential applications as an anticancer therapy. The L protein of *Mononegavirales* has six conserved domains postulated to constitute the specific enzymatic activities of this multifunctional protein. We conducted a comprehensive mutational analysis by targeting the entire SeV L protein domain VI, creating twenty-four infectious L mutants. Our analysis identified several residues required for successful cap methylation and virus replication. This study confirms structural and functional similarity of this domain across different families of the order *Mononegavirales*. Additionally, the oncolytic potential of VSV was analyzed for the first time in a panel of human pancreatic ductal adenocarcinoma (PDA) cell lines and compared to other oncolytic viruses. VSV showed superior oncolytic abilities; however, cells were heterogeneous in their susceptibility to virus-induced oncolysis and several cell lines were resistant to all tested viruses. Four cell lines that varied in their permissiveness to VSV were tested in mice, and in vivo results closely mimicked those in vitro. While our results demonstrate VSV is a promising oncolytic agent against PDA, further studies are needed to better understand the molecular mechanisms of resistance to oncolytic virotherapy.

ACKNOWLEDGEMENTS

I would like to thank my advisor, Dr. Valery Grdzlishvili for his faith in me as a graduate student and his neverending support. I would like to thank Dr. Ian Marriott, Dr. Pinku Mukherjee, Dr. Laura Schrum, and Dr. Michael Turner for serving on my committee and providing encouragement and feedback. I would like to thank the members of the Grdzlishvili lab, Megan Moerdyk-Shauwecker, Nirav Shah, Eric Hastie, Natascha Moestl, and Carlos Molestino, for their support and friendship throughout my graduate career. I would also like to thank the Mukherjee lab for all of their help and input. I would like to thank the UNCC Graduate School for the Graduate Assistant Support Award for funding my graduate education. I would also like to thank the Lucille P. and Edward C. Giles Foundation for awarding me a generous dissertation-year fellowship. Lastly, I would like to thank my husband, Frank, my parents, Jim and Laura, and all my family and friends who encouraged and supported me while I pursued my graduate degree.

TABLE OF CONTENTS

LIST OF FIGURES	vi
LIST OF TABLES	viii
LIST OF ABBREVIATIONS	ix
CHAPTER 1: INTRODUCTION	1
CHAPTER 2: SEQUENCE-FUNCTION ANALYSIS OF THE SENDAI VIRUS L PROTEIN DOMAIN VI	26
2.1 Objective of the study	26
2.2 Materials and Methods	29
2.3 Results	40
2.4 Conclusions	62
2.5 Figures	76
2.6 Tables	88
CHAPTER 3: VESICULAR STOMATITIS VIRUS AS AN ONCOLYTIC AGENT AGAINST PANCREATIC DUCTAL ADENOCARCINOMA	92
3.1 Objective of the study	92
3.2 Materials and Methods	96
3.3 Results	104
3.4 Conclusions	114
3.5 Figures	121
3.6 Tables	133
CHAPTER 4: DISSERTATION SUMMARY	136
REFERENCES	148

LIST OF FIGURES

FIGURE 1: Proposed 5' capping mechanisms for eukaryotes and viruses of <i>Mononegavirales</i> .	11
FIGURE 2: Recognition of viral RNA by RIG-I and MDA5 results in production of IFN- β .	16
FIGURE 3: IFN- $\alpha\beta$ is recognized by IFNAR and a subsequent signaling cascade leads to the production of ISGs.	17
FIGURE 4: Schematic of oncolytic virus (OV) therapy.	20
FIGURE 5: SeV L protein mutants generated and analyzed in this study.	76
FIGURE 6: In vitro mRNA synthesis and genome replication with SeV mutant L proteins using a VVT7 expression system.	78
FIGURE 7: Host range and temperature sensitivity analysis of SeV mutants.	79
FIGURE 8: Multistep growth kinetics of wt and recombinant SeV in Vero and HEp-2 cells at 34°C.	80
FIGURE 9: Growth analysis of recombinant SeV mutants in Vero cells.	81
FIGURE 10: One-step growth kinetics of SeV mutants in Vero cells.	82
FIGURE 11: In vitro mRNA synthesis with purified mutant SeV.	83
FIGURE 12: Cap methylation analysis using tobacco acid pyrophosphatase.	84
FIGURE 13: Superinfection of Vero cells with SeV mutants.	85
FIGURE 14: SeV infectivity of MEFs.	86
FIGURE 15: Western blot analysis of MEFs infected with SeV mutants.	87
FIGURE 16: Viruses used in the PDA study.	121
FIGURE 17: PDA cell viability following infection with viruses.	122
FIGURE 18: Kinetics of cytopathogenicity of VSV- Δ M51-GFP in PDA cells.	123
FIGURE 19: Permissiveness of PDA cell lines to different viruses.	124

FIGURE 20: Permissiveness of selected PDA cell lines to virus infection.	125
FIGURE 21: Surface expression of adenovirus CAR receptor.	126
FIGURE 22: Analysis of viral protein accumulation in cells at 16 h p.i.	127
FIGURE 23: Early viral RNA levels in infected cells.	128
FIGURE 24: One-step growth kinetics of VSVs in PDA cell lines.	129
FIGURE 25: Type I interferon sensitivity of PDA cell lines.	130
FIGURE 26: Type I interferon production by PDA cell lines.	131
FIGURE 27: Efficacy of VSV- Δ M51-GFP and CRAd-dl1520 in nude mice bearing human PDA tumors.	132

LIST OF TABLES

TABLE 1: Sequences of primers used in this study to generate SeV mutant L genes	88
TABLE 2: Comparative titers of recombinant Sendai viruses in Vero or HEp2 cells at 34°C or 40°C.	90
TABLE 3: Cap methylation analysis using SeV detergent-activated purified virions.	91
TABLE 4: PDA cell lines used in this study.	133
TABLE 5: Early viral RNA synthesis in cells infected with VSV- Δ M51-GFP.	134
TABLE 6: Correlation between IFN sensitivity, production and resistance of PDA cells to VSV.	135

LIST OF ABBREVIATIONS AND SYMBOLS

4 CN	4-chloro-1-naphthol
aa	amino acid
AdoHcy	S-adenosylhomocysteine
AdoMet	S-adenosylmethionine
BSA	bovine serum albumin
CBC	cap binding complex
CE	capping enzyme
CIU	cell infectious units
CPE	cytopathic effects
CRAd	conditionally replicative adenovirus
CTD	C-terminal domain
DAB	3,3'-diaminobenzidine tetrahydrochloride hydrate
DI	defective-interfering
DNA	deoxyribonucleic acid
DMEM	Dulbecco's modified Eagle's medium
ECL	Enhanced Chemiluminescence
eIF	eukaryotic initiation factor
F	fusion protein
FBS	fetal bovine serum
G	glycoprotein
GDP	guanosine diphosphate
GFP	green fluorescent protein

GMP	guanosine monophosphate
GTP	guanosine triphosphate
GTPase	guanosine 5'-triphosphatase
H ³	tritium
HN	hemagglutinin/neuraminidase
h p.i.	hours post infection
<i>hr</i>	host range
HRP	horseradish peroxidase
hTERT	human telomerase reverse transcriptase
IACUC	Institutional Animal Care and Use Committee
ICC	immunocytochemistry
IF	immunofluorescence
IFN	interferon
IFNAR	IFN- $\alpha\beta$ receptor
ISG	interferon-stimulated gene
IT	intratumoral
KO	knock out
L	large polymerase protein
M	matrix protein
MDA5	melanoma differentiated-associated gene 5
MDSC	myloid-derived suppressor cells
MEFs	mouse embryonic fibroblasts
MEM	modified Eagle's medium

MOI	multiplicity of infection
mRNA	messenger RNA
MTase	methyltransferase
MTT	3-(4,5-dimethylthiazol-2-yl)-2,5-diphenyltetrazolium bromide
N	nucleoprotein
NIH	National Institutes of Health
NNS	nonsegmented, negative strand
NTP	nucleotide triphosphate
ORF	open reading frame
OV	oncolytic virus
P	phosphoprotein
PanIN	pancreatic intraepithelial neoplasias
PBS	phosphate-buffered saline
PDA	Pancreatic ductal adenocarcinoma
PFA	paraformaldehyde
PRNTase	polyribonucleotidyltransferase
PVDF	polyvinylidene difluoride
RdRp	RNA-dependent RNA polymerase
RIG-I	retinoic-acid inducible gene I
RNA	ribonucleic acid
RNGTT	RNA guanylyltransferase and 5' triphosphatase
RNMT	RNA guanine-7 methyltransferase
RNP	ribonucleoprotein

RPMI	Roswell Park Institute medium-1640
SDS-PAGE	sodium-dodecyl sulfate polyacrylamide gel electrophoresis
SeV	Sendai virus
SFM	serum-free media
STAT	signal transducers and activators
T _{reg}	regulatory T cells
TAM	tumor-associated macrophages
TAP	tobacco acid pyrophosphatase
TBST	Tris-buffered saline with Tween-20
<i>ts</i>	temperature sensitive
VSV	Vesicular stomatitis virus
VV	Vaccinia virus
wt	wild type

CHAPTER 1: INTRODUCTION

The nonsegmented negative strand (NNS) RNA viruses of the order *Mononegavirales* include many important human, animal, and plant pathogens such as rabies virus, Ebola and Marburg viruses, measles, mumps and respiratory syncytial virus. Most of our current understanding of the biology of *Mononegavirales* comes from studying two prototypic members of this order, vesicular stomatitis virus (VSV, Family *Rhabdoviridae*) and Sendai virus (SeV, Family *Paramyxoviridae*) (Lamb and Parks 2007; Lyles 2007). There are several advantages to using VSV and SeV as research models for the less tractable members of this order including: i) the ability to safely study them in the laboratory ii) their simple genome structure; iii) their ability to replicate in a wide range of cell types; iv) the development of in vitro systems for the study of RNA synthesis; and v) available reverse genetic systems (Lyles 2007). Further study of the molecular biology of these viruses is important because it can lead to the development of new effective antiviral therapies for medically related viruses. Moreover, VSV and SeV have great potential as vaccine, gene therapy and oncolytic vectors (von Messling and Cattaneo 2004; Finke and Conzelmann 2005; Bukreyev et al. 2006). This dissertation focuses on both the basic molecular biology of VSV and SeV, more specifically 5' cap methylation of viral mRNAs, and additionally, potential applications of these viruses as an anticancer therapy.

Mononegavirales and eukaryotes share a similar 5' mRNA cap structure.

Viruses of *Mononegavirales* encode only 5-10 proteins and utilize the host cell machinery for a successful replication cycle to occur. Therefore, similar to eukaryotic mRNA, viral mRNA requires a 5' cap structure that is methylated for efficient translation and mRNA stability (Abraham et al. 1975). Viral mRNA mimicks the host's mRNA thereby utilizing all the necessary components of the translation machinery for the efficient production of viral proteins. This viral mimicry may also play a role in evading host antiviral responses (Daffis et al. 2010; Zust et al. 2011). While this dissertation focuses on the methylation of viral mRNA 5' cap structures, it is important to describe the different mechanisms of 5' cap addition between *Mononegavirales* and eukaryotes, both ending up with identical mRNA 5' cap structures which are required for successful translation (Fig. 1).

The process of mammalian transcription centers around RNA polymerase II and requires a multitude of transcription factors to aid in all aspects of this important cellular process. RNA polymerase II consists of 12 subunits and is responsible for catalyzing mRNA synthesis of all genes that code for proteins (Alberts et al. 2002). As the mRNA molecule is being synthesized, other mRNA processing reactions are occurring co-transcriptionally (Cowling 2010). These reactions include RNA splicing to remove intron sequences from the RNA transcript, the addition of a 5' cap structure, and 3' polyadenylation (Cowling 2010). The enzymes that catalyze these modifications interact with the RNA polymerase II tail known as the C-terminal domain (CTD) (Alberts et al. 2002; Cowling 2010). The CTD is highly phosphorylated during transcription elongation which allows for a high amount of protein association (Alberts et al. 2002; Cowling

2010). Four enzymes are involved in creating the 5' cap structure of all eukaryotic mRNAs and these enzymes all associate with CTD during transcription elongation and are transferred at certain time points to the nascent RNA molecule for the addition of the 5' cap (Alberts et al. 2002; Cowling 2010). First, a triphosphatase removes a phosphate from the 5' end of the nascent RNA molecule (Cowling 2010). Secondly, a guanylyltransferase transfers a GMP from GTP in an unusual 5' to 5' linkage (instead of 5' to 3') (Cowling 2010). For mammals, the phosphatase and guanylyltransferase activity is catalyzed by a single polypeptide known as capping enzyme (CE) or also known as RNA guanylyltransferase and 5' triphosphatase (RNGTT) (Pillutla et al. 1998; Tsukamoto et al. 1998; Yamada-Okabe et al. 1998). Lastly, methyltransferases (MTases) add methyl groups to the guanine-*N7* (G-*N7*) position (Cap0) and the 2'*O*-ribose of the 5' penultimate nucleotide residue (Cap1) (Cowling 2010). The G-*N7* (RNA guanine-7 MTase, RNMT) and 2'*O*-ribose MTases are distinct proteins (Pillutla et al. 1998; Tsukamoto et al. 1998; Cowling 2010). It has been well established that methylation of the 5' cap at the G-*N7* position is absolutely required for efficient translation, but significance of methylation at the 2'*O*-ribose has remained unclear (Daffis et al. 2010; Züst et al. 2011). Recent studies have demonstrated that the presence or absence of 2'*O*-ribose methylation has an evolutionary basis and plays a role in distinguishing self from non-self mRNA (Daffis et al. 2010; Züst et al. 2011).

The 5' cap structure of mammalian mRNA plays several important roles in the cell cycle and because viruses hijack the cell's translational machinery, it is important for viruses to mimic cellular mRNA structure. The 5' cap structure of the newly synthesized mRNA is bound by a cap-binding complex (CBC) in the nucleus which aids in further

RNA processing and transport to the cytoplasm (Alberts et al. 2002). In the cytoplasm, eukaryotic initiation factor 4E (eIF4E) directly binds to the 5' cap and then associates with eIF4G (Alberts et al. 2002). The small ribosomal subunit recognizes eIF4E/eIF4G and then moves along the mRNA until it identifies the first AUG start codon (Alberts et al. 2002). The initiation factors dissociate from the small ribosomal subunit which allows the large ribosomal subunit to assemble and translation proceeds (Alberts et al. 2002). The 5' cap structure plays an important role in exit from the nucleus and entry into the cytoplasm in addition to efficient translation initiation (Alberts et al. 2002; Cowling 2010), but it also has other important functions. Fully methylated 5' caps provide mRNA stability by protecting mRNA from degradation by exonucleases (Murthy et al. 1991). The guanylyltransferase reaction is reversible, and uncapped mRNA created by the reverse reaction is rapidly degraded. There is evidence that the methylation reaction is irreversible and therefore the guanylyltransferase cannot use methylated cap structures as substrate for the reverse reaction, and this allows for stabilization of mRNA (Furuichi et al. 1977; Murthy et al. 1991). The mRNA 5' cap structure in eukaryotes and *Mononegavirales* are identical so that viral mRNAs can be recognized and utilize the host cell translational machinery however the mechanisms of 5' cap addition differ greatly.

The unusual mechanism of *Mononegavirales* 5' mRNA capping and cap methylation.

All members of *Mononegavirales* share a similar genome organization and common mechanisms of genome replication and gene expression (Lamb and Parks 2007; Lyles 2007). The L protein, whose large size (more than 2,000 amino acids in a single polypeptide chain) reflects its multifunctional nature, plays a central role in virus RNA replication and transcription. This protein has six sequence regions ("domains") with a

high degree of homology among all *Mononegavirales*. Although there is no protein structure data available for any part of the L protein, these domains have been postulated to constitute the specific enzymatic activities of the viral RNA polymerase involved in transcription, mRNA 5' capping, cap methylation, mRNA 3' polyadenylation, and replication of viral RNA (Whelan et al. 2004; Lamb and Parks 2007; Lyles 2007).

The mRNA 5'-cap structures of *Mononegavirales* are methylated by the virally encoded L protein at the guanine-*N*7 and 2'-*O*-adenosine positions (Abraham et al. 1975; Moyer et al. 1975; Rhodes and Banerjee 1975; Gupta et al. 1979; Barik 1993; Takagi et al. 1995). The single multifunctional L polypeptide is responsible for all enzymatic capping reactions because this process takes place in the cytoplasm of host cells whose capping enzymes are localized to the nucleus. The viral capping reaction is different from the eukaryotic capping mechanism (described above); however, both reactions lead to identical mRNA 5' cap structures (Ogino and Banerjee 2011). The capping mechanism of *Mononegavirales* is beyond the scope of this dissertation; however, it is a required precursor to the methylation reactions and will be briefly described (Fig. 1). The first step requires a GTPase activity of the L protein (to date this activity has not been mapped to a specific region of L) to remove the γ -phosphate group of GTP to generate GDP (Ogino and Banerjee 2007; Ogino and Banerjee 2008). The α and β phosphates of the nascent mRNA are therefore derived from a GDP donor instead of a GMP (as seen in eukaryotes) and the enzymatic activity responsible for this reaction is a RNA:GDP polyribonucleotidyltransferase (PRNTase) activity (Ogino and Banerjee 2007; Li et al. 2008). The PRNTase activity has been mapped to a specific motif (GxxT[n]HR) in domain V of the VSV and Chandipura virus (also Family *Rhabdoviridae*) L proteins (Li

et al. 2008; Ogino and Banerjee 2010). The PRNTase domain of L interacts with the triphosphate of the newly synthesized mRNA which has a specific start sequence ($L + \text{pppAACAG} \rightarrow L\text{-pAACAG} + \text{PP}_i$) (Rhodes and Banerjee 1976). More recently, Ogino et al. has described an alternative mechanism for the addition of guanosine to the 5' ends of viral mRNA (Ogino and Banerjee 2008). In this mechanism, the PRNTase domain of L interacts with the triphosphate of the newly synthesized mRNA which has a specific start sequence ($L + \text{pppAACAG} \rightarrow L\text{-pAACAG} + \text{PP}_i$). GTP (GDP is not efficiently generated from GTP using their experimental conditions) is then transferred to the L-pA intermediate to form a guanosine-tetraphospho-adenosine cap structure (GppppAACAG). This process occurs at a much lower efficiency than the originally described VSV mechanism of 5' cap addition; however, both of these mechanisms differ greatly from eukaryotic and other viral capping reactions (Ogino and Banerjee 2008).

Currently there is no structural data available for any portion of L, however independent computational analyses (Bujnicki and Rychlewski 2002; Ferron et al. 2002) propose that, while L proteins share a very low degree of homology with other known S-adenosylmethionine (AdoMet) dependent MTases at the aa level, their domain VI has a prototypical MTase fold; a glycine-rich motif shared by all members of the AdoMet-dependent MTase superfamily and directly involved in AdoMet binding (Ingrosso et al. 1989; Martin and McMillan 2002); and several potential catalytic residues. Although all these studies suggest that a conserved domain VI is the MTase domain of L, many important questions remain including the MTase specificity of domain VI (G-N7, 2'-O-adenosine, or both?), and there have been no reports for the L protein in VSV or any

other *Mononegavirales* that directly demonstrate the location of the L protein region physically binding AdoMet.

The MTase function of L was originally shown by Sue Moyer and coworkers through the characterization of two host-range (*hr*) mutants of VSV. It was shown that these mutants were defective in viral mRNA cap methylation (Horikami and Moyer 1982; Horikami et al. 1984), and that purified wild-type (wt) L protein was able to complement their defect during transcription *in vitro*, demonstrating that the VSV L protein possesses cap MTase activities (Hercyk et al. 1988). In addition to defective cap methylation, a link was documented between L protein MTase activities and the phenotype of the VSV mutants. Specifically, VSV mutants defective in cap methylation were temperature sensitive (*ts*) and, more interestingly, *hr* restricted as manifested by their inability to grow in certain nonpermissive cell lines (e.g., HEp-2 cells) while retaining their ability to grow to high titers in permissive cells (e.g. BHK-21) (Horikami and Moyer 1982; Horikami et al. 1984; Grdzlishvili et al. 2005; Grdzlishvili et al. 2006). Previous studies linked the inability of VSV cap methylation defective mutants to grow in HEp-2 cells to nontranslatability of primary VSV transcripts (Horikami and Moyer 1982; Horikami et al. 1984) and showed that host cells methylate viral mRNA in permissive cell lines through an unknown mechanism (Horikami et al. 1984).

A more recent analysis of the VSV *hr1* mutant showed that a single aa substitution (D1671V) in this putative AdoMet-binding glycine-rich motif, completely eliminated viral mRNA cap methylation at both the guanine-*N7* and 2'-*O*-adenosine positions (Grdzlishvili et al. 2005), thus experimentally supporting the above computational predictions (Bujnicki and Rychlewski 2002; Ferron et al. 2002). In

addition, it has been demonstrated that substitutions at other positions within the VSV L protein domain VI (including an invariant lysine 1651 and aa 1670 and 1672 within the glycine-rich motif) also resulted in various defects in mRNA cap methylation (Grdzlishvili et al. 2005; Li et al. 2005; Grdzlishvili et al. 2006; Li et al. 2006; Galloway et al. 2008). These data suggest that domain VI catalyzes both G-N7 and 2'-O-ribose methylation and uses a single AdoMet binding site (order of methylation is discussed below) (Li et al. 2006). The exact mechanism of these two methylation reactions is unclear; however, it is possible that other regions of L have varying effects on these two activities through allosteric interactions (Li et al. 2007). For example, Li et al. demonstrated that aa substitutions in domain II and III of the VSV L protein can affect cap methylation (Li et al. 2007). Both MTase activities do require specific *cis* acting signals in the viral RNA (Wang et al. 2007). As transcription proceeds, the viral mRNA has a conserved 5' sequence (pppAACAGNNAUC) that is thought to be the substrate for the capping and cap methylation enzymatic activities of the L protein (Rhodes and Banerjee 1976; Wang et al. 2007). Substitutions at aa positions 1, 2, 3, and 5 inhibit cap addition and it is thought that the conserved residues at positions 8, 9, and 10 are required for cap methylation (Ogino and Banerjee 2007). Therefore the length of the mRNA substrate for capping and cap methylation differs (Ogino and Banerjee 2007). To further analyze the cap methylation function of the VSV L protein, Zhang et al. identified two highly conserved aromatic aa residues in domain VI of the VSV L protein that play a role in mRNA substrate recognition (Zhang et al. 2010). Together, these data confirm and support the role of domain VI of the L protein in many of the aspects of cap methylation in VSV and potentially other *Mononegavirales*.

Studies with VSV also identified a region upstream of domain VI important for cap methylation (Grdzlishvili et al. 2006). Interestingly, it has been shown that VSV tolerates an insertion of the GFP gene between domain VI and this upstream region, and a recombinant virus with such insertion showed a normal growth in cell culture but no virion-associated activity in vitro (Ruedas 2009). The upstream region has not been studied in SeV as there is no homology in this variable region between rhabdoviruses and paramyxoviruses, although the L protein of measles virus (a paramyxovirus) was also reported to tolerate GFP insertion in a region just upstream of domain VI (Duprex et al. 2002).

The cap methylation order for *Mononegavirales* is controversial with some evidence pointing to the conventional order $GpppA \rightarrow m7GpppA \rightarrow m7GpppAm$ and some evidence pointing to $GpppA \rightarrow GpppAm \rightarrow m7GpppAm$. The in vitro results using detergent-activated VSV (Indiana strain) virions proposed the following order of MTase reactions: $GpppA + AdoMet$ (low concentration) $\rightarrow GpppAm + AdoMet$ (high concentration) $\rightarrow 7mGpppAm$ (Testa and Banerjee 1977; Li et al. 2006). Rahmeh et al. demonstrated that aa substitutions in the positions of the KDKE catalytic tetrad inhibit methylation at both positions most likely because efficient G-N7 methylation requires 2'-O-ribose methylation to occur first (Rahmeh et al. 2009). They also speculate that KDKE residues, in addition to catalyzing 2'-O-ribose methylation, play a role in positioning the RNA substrate for G-N7 methylation to occur (Rahmeh et al. 2009). However, the previous in vitro data on VSV (Indiana strain) mRNA synthesis in the presence of the methylation inhibitor cycloleucine (Moyer 1981) and in vitro transcription data on VSV New Jersey serotype (Hammond and Lesnaw 1987) suggest

that the reverse order of VSV mRNA methylation (GpppA→7mGpppA →7mGpppAm) can also occur.

While most of the cap methylation studies were conducted using VSV, limited studies using SeV and other *Mononegavirales* demonstrated similarities as well as differences in the cap methylation function of L between these distantly related viruses. SeV produces mRNA that is capped and methylated at both the G-N7 and 2'-O positions (Takagi et al. 1995), but interestingly, purified SeV L protein or just its C-terminal portion retaining domain VI, catalyzed only G-N7, but not the 2'-O cap methylation (Ogino et al. 2005). Also, a previous study showed that Newcastle disease virus (NDV), another paramyxovirus, produces viral mRNAs that are not 2'-O-methylated at all (Colonna and Stone 1976). While much is known about VSV cap methylation, there are very few studies with other members of *Mononegavirales*; therefore, we chose to analyze cap methylation function in the SeV L protein, which is distantly related to VSV, to determine if cap methylation function is similar across different families of this order.

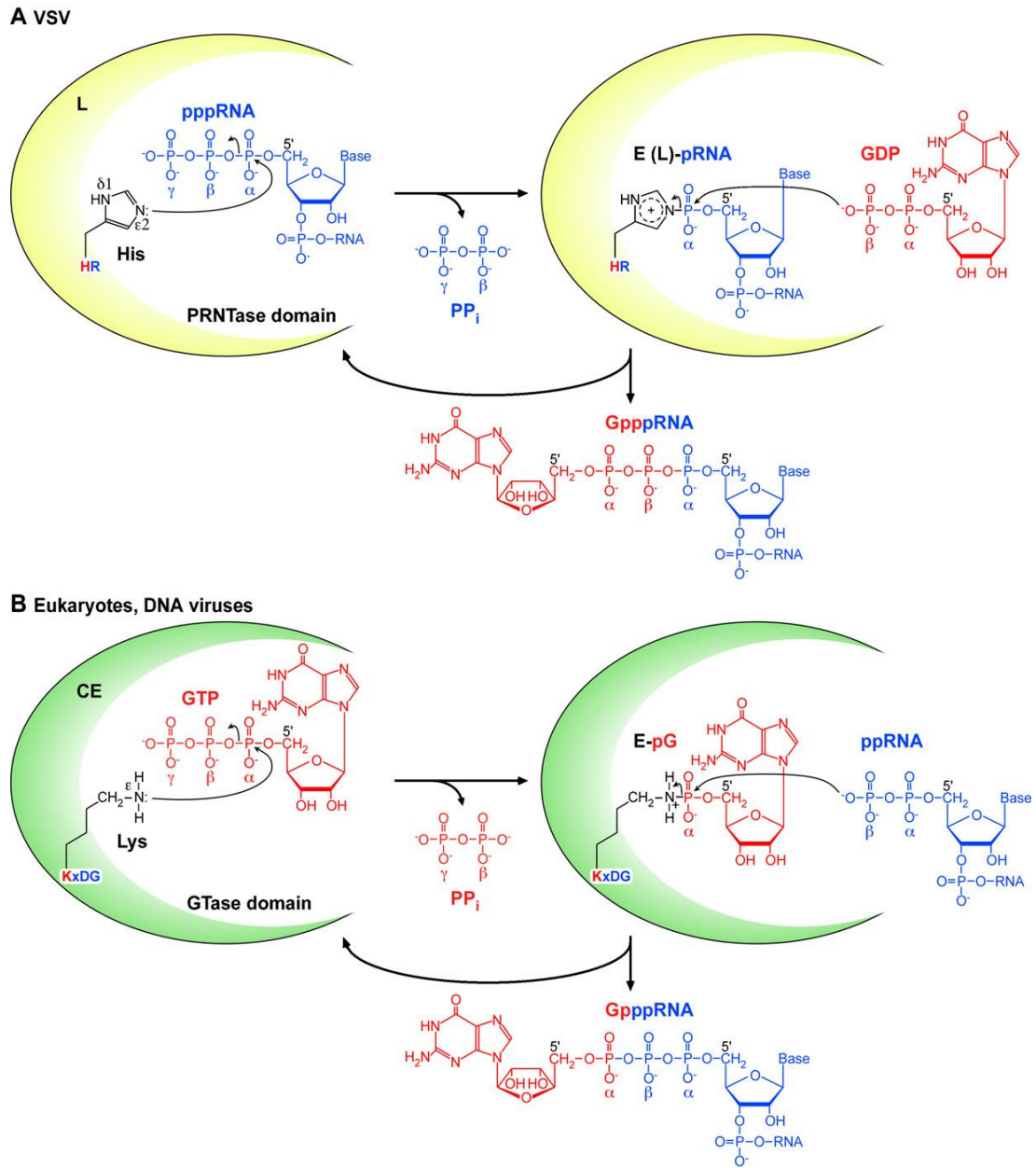


Figure 1. Proposed 5' capping mechanisms for viruses of *Mononegavirales* (A) and eukaryotes (B). Adapted from Ogino and Banerjee (2011).

The role of viral mRNA cap methylation in a successful replication cycle.

In general, the viruses of *Mononegavirales* have similar strategies when it comes to a successful infection/replication cycle. Viral mRNA 5' capping and cap methylation is an important part of replication because of the utilization of host cell translational machinery and the necessity of production of viral proteins. Virus infection begins with attachment and entry into host cells. Protruding from the host-derived viral envelope, are varying proteins that recognize certain aspects of the cell membrane. For members of *Mononegavirales*, viruses are recognized by specific cellular receptors, sugar moieties or interactions with certain cell membrane properties. Sialic acid moieties serve as receptors for SeV and are found on both membrane glycoproteins and lipids (Markwell et al. 1984; Markwell et al. 1985). Anchored in the SeV envelope are hemagglutinin/neuraminidase (HN) proteins that interact with sialic acid residues and fusion (F) proteins that facilitate envelope-membrane fusion (Scheid and Chopin 1974; Lamb and Parks 2007). Upon recognition and attachment of SeV, the viral envelope fuses with the cell membrane at neutral pH and ribonucleoprotein (RNP) complexes are released into the cytoplasm (Scheid and Chopin 1974; Lamb and Parks 2007). RNP structures consist of the viral RNA genome tightly surrounded and protected by virally encoded nucleocapsid (N) proteins. The single VSV envelope glycoprotein (G) is not recognized by a known receptor and because VSV has a wide host range, it is thought that VSV can enter host cells through electrostatic interactions at the host cell membrane (Schlegel et al. 1983; Bailey et al. 1984; Coil and Miller 2004). To date it is unclear the actual mechanism of VSV attachment. Following attachment, VSV enters host cells via clathrin-dependent endocytosis and passes through the stages of early to late endosomes in the cytoplasm

(Matlin et al. 1982; Cureton et al. 2009). As the endocytic pathway progresses, the pH drops within the endosome, triggering fusion of the viral envelope with the endosome membrane and the release of the viral RNP complexes into the cytoplasm (Matlin et al. 1982). Following attachment and entry into host cells, VSV and SeV have very similar strategies for a successful replication cycle. Because all aspects of the *Mononegavirales* life cycle take place in the cytoplasm of host cells, the RNA-dependent RNA polymerase (RdRp), consisting of two viral subunits (the cofactor phosphoprotein (P) and the enzymatic large (L) polymerase protein) is packaged into mature virions (Whelan et al. 2004). The RdRp is associated with N, and the matrix (M) protein initially surrounds all components beneath the viral envelope (Whelan et al. 2004). Upon entry into the cytoplasm, the M protein spontaneously dissociates from the RNP structure, allowing for primary transcription to proceed (Rigaut et al. 1991). Primary transcription is defined as transcription from the original RNA templates that have entered the cell. The RdRp always initiates transcription at the 3' leader sequence and proceeds down the genome, in what is known as the start-stop model, to transcribe the mRNAs encoded by VSV and SeV (Whelan et al. 2004). The RdRp will pause at intergenic regions and either dissociate or continue on to transcribe the next gene (Abraham and Banerjee 1976). Transcripts are co-transcriptionally modified (capped, methylated and polyadenylated) and created in a gradient fashion with genes encoding proteins that are needed at higher levels located closer to the 3' end of the genome and genes that encode for proteins that are needed in lesser amounts located closer to the 5' end (5'-N-P-M-G-L-3' for VSV and 5'-N-P/V/C-M-F-HN-L-3' for SeV) (Abraham et al. 1975; Abraham and Banerjee 1976; Ball and White 1976; Ball 1977; Whelan et al. 2004). In addition to mRNAs, a leader RNA is

always synthesized prior to N mRNA; however, this RNA is neither capped nor polyadenylated and is thought to play a role in evading antiviral responses (the exact functions remain unclear) (McGowan et al. 1982; Grinnell and Wagner 1985; Whelan and Wertz 1999). For most *Mononegavirales* the N protein is the first gene to be transcribed because a large quantity of N is needed for genome and antigenome encapsidation throughout the replication cycle (Bishop and Roy 1971; Emerson and Wagner 1972). The genomes and antigenomes of these viruses never exist without being tightly associated with N and therefore a sufficient amount of N must be synthesized prior to viral replication and secondary transcription (Bishop and Roy 1971; Emerson and Wagner 1972; Patton et al. 1984). SeV primarily transcribes monocistronic mRNAs similarly to VSV; however, the SeV P gene also undergoes mRNA editing to produce accessory (V and C) proteins that play roles in inhibiting host antiviral responses (Garcia-Sastre 2004; Conzelmann 2005; Lamb and Parks 2007). Once sufficient amounts of N have been synthesized, the RdRp switches from transcriptase to replicase, catalyzing synthesis of antigenomes and negative strand genomes from antigenomes (Wertz 1983; Lyles 2007). Accumulation of progeny genomes triggers the RdRp to proceed with secondary transcription (Whelan et al. 2004; Lyles 2007). RdRp can now transcribe from the progeny genomes and virion assembly most likely takes place at the same time (Whelan et al. 2004; Lyles 2007). Viral proteins associated with the envelope are localized to (Bergmann et al. 1981) and inserted into the host cell membrane in microdomains known as lipid rafts (Brown and Lyles 2003). The M protein is also localized to the cell membrane (Knipe et al. 1977; Ohno and Ohtake 1987; Flood and Lyles 1999) and interacts with the progeny RNPs (Odenwald et al. 1986; Flood and Lyles

1999). Infectious virus particles, with all viral protein components and RNA genomes, bud through the host cell membrane and can go on to infect adjacent host cells (Harty et al. 1999; Jayakar et al. 2000; Harty et al. 2001; Irie et al. 2004).

Virus infection results in recognition by host cell innate immune molecules, an adaptive response, and viral clearance. VSV and SeV are recognized by cytoplasmic sensors, RIG-I and MDA5, which signal the production of Type I IFN and other antiviral cytokines (Fig. 2) (Kato et al. 2006; Onoguchi et al. 2011). Recognition of viral RNA by RIG-I and MDA5 results in a cascade of signaling molecules that ultimately lead to the activation of the IFN- β promoter and production of IFN- β (Fig. 2) (Gerlier and Lyles 2011). IFN- β is then secreted and acts in a paracrine manner by binding to IFN- $\alpha\beta$ receptors on neighboring cells (Fig. 3). Binding of IFN- β to its receptor leads to a signaling cascade of adapter molecules and the production of IFN-stimulated genes (ISG, Fig. 3) (Gerlier and Lyles 2011). ISGs play an important role in creating an 'antiviral state' in cells surrounding uninfected cells, and this state allows them to resist further virus infection. While host cells are equipped with virus recognition tools, VSV and SeV have evolved strategies to evade host antiviral responses. These viruses inhibit host gene expression and translation as evasion mechanisms (Lamb and Parks 2007; Lyles 2007). The leader RNA and M protein both play a role in inhibition of host antiviral responses. There is evidence that the leader RNA inhibits host RNA synthesis (McGowan et al. 1982; Grinnell and Wagner 1985) and the M protein, in addition to its role in virus assembly and budding, inhibits the transport of host mRNA from the nucleus to the cytoplasm thus downregulating production of Type I IFN and interferon-stimulated genes

(ISGs) (Black and Lyles 1992; Lyles et al. 1996; Ferran and Lucas-Lenard 1997; Ahmed and Lyles 1998). As mentioned earlier, SeV encodes additional accessory proteins (V and

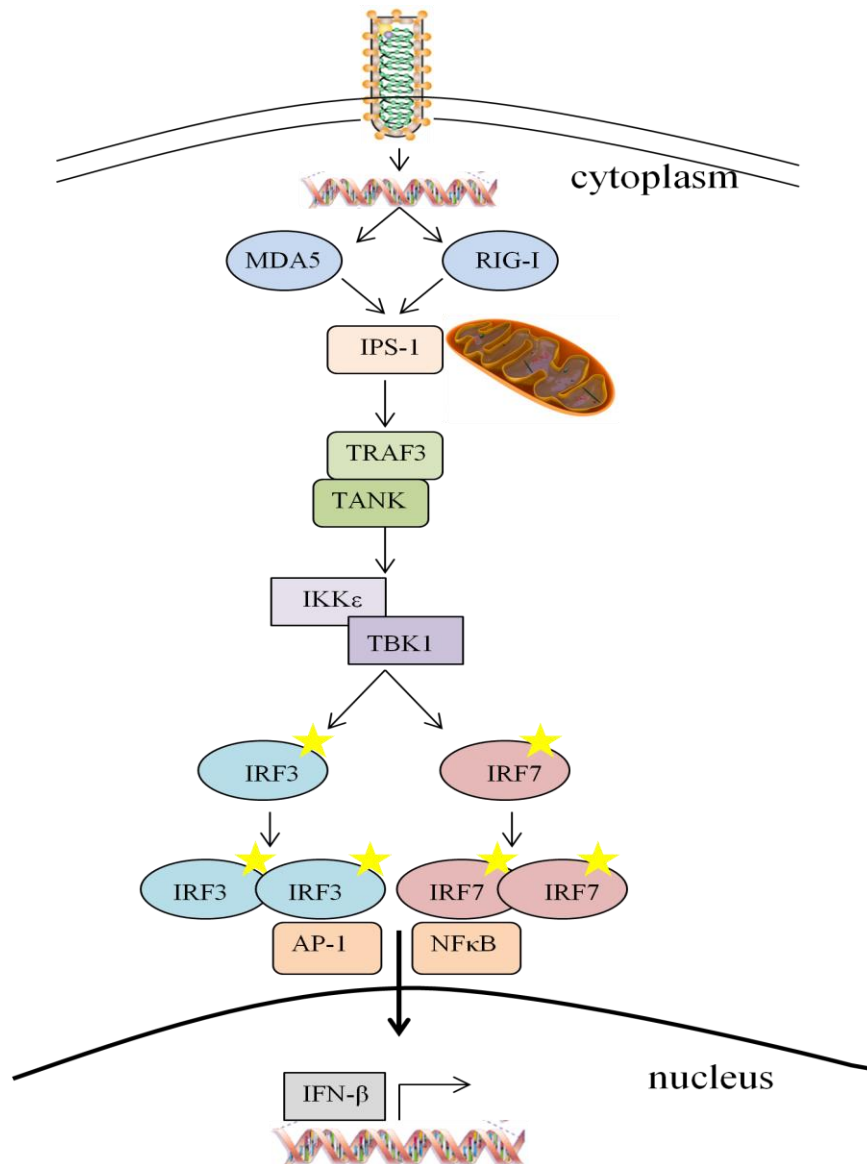


Figure 2. Recognition of viral RNA by RIG-I and MDA5 results in production of IFN- β . Adapted from Gerlier and Lyles (2011).

C) that antagonize host IFN production. The V protein has been shown to bind directly to MDA5 and block IFN- β production (Andrejeva et al. 2004). The C protein interferes with

STAT (signal transducers and activators of transcription) phosphorylation which obstructs IFN signaling (Gotoh et al. 2003). There is new evidence that cytoplasmic innate immune receptors recognize viral RNA that lack cap methylation at the 2' *O*-ribose position (Daffis et al. 2010; Zust et al. 2011). This was shown for positive strand RNA viruses and has not been investigated in any NNS RNA viruses. We performed some preliminary experiments to explore whether SeV cap methylation defective mutants induced greater immune responses in primary mouse cells.

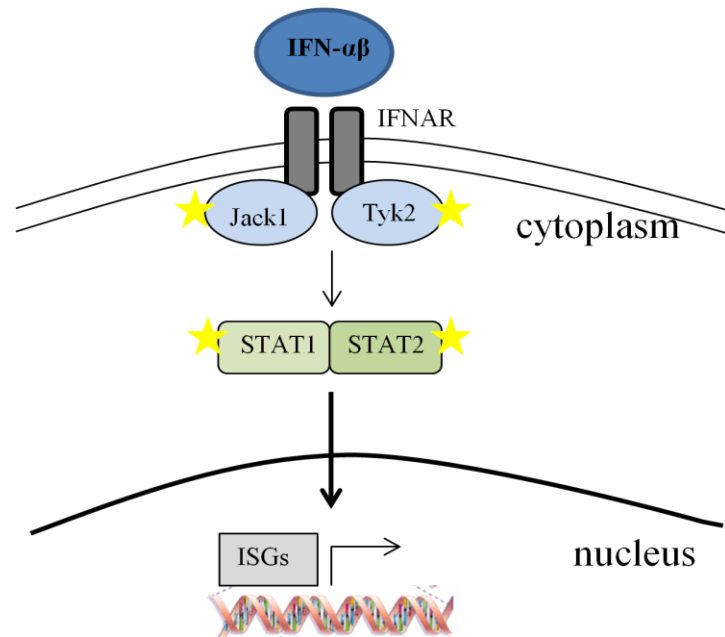


Figure 3. IFN- α/β is recognized by IFNAR and a subsequent signaling cascade leads to the production of ISGs. Adapted from Gerlier and Lyles (2011).

Practical implications of Mononegavirales cap methylation studies.

A better understanding of the biology of the viruses of *Mononegavirales* can lead to the development of new effective antiviral therapies and the rational design of live-attenuated viruses for their use as vaccine (von Messling and Cattaneo 2004; Finke and

Conzelmann 2005; Bukreyev et al. 2006), oncolytic (von Messling and Cattaneo 2004) and gene therapy (Finke and Conzelmann 2005) vectors. The cap methylation function of L, while important in a successful virus replication cycle, is not essential and is therefore thought to be a promising target for drug development and rational attenuation.

Adenosine analogues that inhibit the host cell enzyme, S-adenosylhomocysteine (SAH) hydrolase, and thereby inhibit cap methylation have shown success against

paramyxoviruses, rhabdoviruses, and filoviruses (De Clercq 1998; Bray et al. 2000).

SAH is the byproduct of AdoMet-dependent MTase reactions and the SAH hydrolase eliminates the buildup of SAH allowing for further methylation to proceed (De Clercq 1998; Bray et al. 2000). Blockage of SAH hydrolase causes increased concentration of SAH which competes with AdoMet binding to MTases and interferes with 5' cap methylation ultimately leading to decreased efficiency in translation (Bray et al. 2000).

Similarly, sinefungin, a natural AdoMet analogue generated by *Streptomyces griseolus* inhibits MTase activity and successfully interferes with VSV replication (Li et al. 2007).

Remarkably, cap methylation defective viruses (VSV, SeV or any other

Mononegavirales) have never been tested in any animal system. It is possible that cap

methylation defective viruses will be attenuated in vivo; however, it is unclear if

infectious viruses carrying these specific mutations will exhibit any unusual tissue

specificity as compared to their wild type counterpart. Further studies of cap methylation

defective viruses can lead to the rational design of vectors for vaccine, gene therapy and

oncolytic virotherapy development.

VSV as an oncolytic agent against pancreatic ductal adenocarcinoma.

It was first observed in the early 1900s that some cancer patients suffering from viral infections exhibited tumor regression or stabilization (Sinkovics and Horvath 2008). With this observation came the development of oncolytic virus (OV) therapy which utilizes replication-competent viruses to specifically target and kill tumor cells (Russell and Peng 2007; Vähä-Koskela et al. 2007; Breitbach et al. 2010). Such selectivity is possible because many tumors are characterized by defective innate immune responses or tumor-related abnormalities in regulation of mRNA translation or certain cellular signaling pathways, facilitating selective replication of viruses in cancer cells. For example, many cancer cells have defective Type I IFN responses, which provides growth advantages to tumor cells; however, it also makes them more susceptible to viral infections (Stojdl et al. 2000; Naik and Russell 2009). As a result, OV can infect, replicate within and kill tumor cells. Successful virus replication in cancer cells leads to the release of newly formed infectious virus particles that go on to infect neighboring tumor cells.

In the field of OV therapy, several members of *Mononegavirales* have shown preclinical success with VSV being the most successful against a variety of malignancies, including prostate (Ahmed et al. 2004; Chang et al. 2010; Moussavi et al. 2010), breast (Fernandez et al. 2002; Obuchi et al. 2003; Shi et al. 2009; Ahmed et al. 2010), melanoma (Fernandez et al. 2002; Galivo et al. 2010), colorectal (Huang et al. 2003; Shinozaki et al. 2005; Edge et al. 2008), liver (Wu 2008; Altomonte et al. 2009; Ausubel et al. 2011), glioblastoma (Ozduman et al. 2008; Wollmann 2010; Cary et al. 2011) and

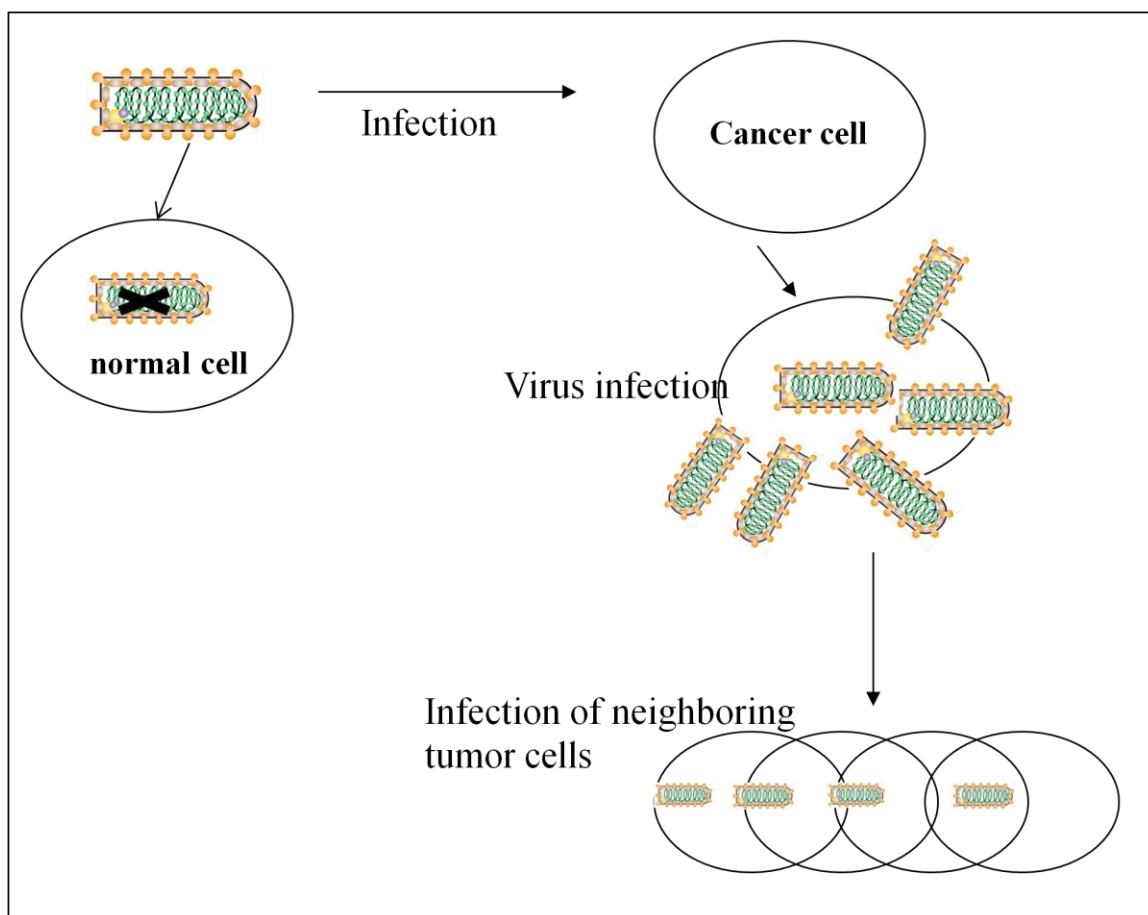


Figure 4. Schematic of oncolytic virus (OV) therapy.

other cancers (Barber 2004). There are several advantages of using VSV as an anticancer therapy. VSV is the prototypic NNS RNA virus (order *Mononegavirales*, family *Rhabdoviridae*), and its basic biology and interactions with host immune responses have been extensively studied (Lyles 2007). While VSV is very sensitive to IFN-mediated antiviral responses (and therefore unable to productively infect healthy cells), it can specifically infect and kill tumor cells, the majority of which are believed to be defective in Type I IFN production and responses (Barber 2004; Lichty et al. 2004). Also, the mechanisms of VSV-mediated killing by apoptosis have been established (Gaddy and Lyles 2007). In addition to tumor specificity, VSV has several important advantages

as an OV: (i) replication occurs in the cytoplasm of host cells with no risk of host cell transformation, (ii) cellular uptake in many mammalian cell types occurs rapidly and there is no cell cycle dependency, (iii) the genome is easily manipulated with the possibility for strong and adjustable levels of foreign gene expression to enhance oncolysis and specificity, and (iv) there is no preexisting immunity against VSV in humans (Barber 2004). While VSV is not considered a significant human pathogen, it can cause neurotoxicity in mice, nonhuman primates and even humans (Quiroz et al. 1988). However, several VSV mutants have been generated which are not neurotropic but retain their oncolytic activity (Ahmed 2008; Kelly et al. 2010; Wollmann 2010). In addition to improving the safety of VSV, several groups have engineered VSV to enhance specificity and oncolysis by introducing specific mutations to the viral genome, or by arming the virus with cytotoxic genes or cytokines that can elicit a more robust immune response.

Because of its preclinical success, at least two VSV OV have been considered for clinical trials by the NIH Recombinant-DNA Advisory Committee (Cary et al. 2011). However, VSV oncolytic potential has never been studied in any pancreatic cancer models. OV therapy with several viruses, including adenoviruses (Kuhlmann et al. 2008; He et al. 2009; Huch 2009), herpesviruses (Sarinella et al. 2006; Kasuya et al. 2007; Nakao et al. 2007; Watanabe et al. 2008; Eisenberg et al. 2010), measles virus (Carlson 2009; Penheiter et al. 2010; Bossow et al. 2011) and reoviruses (Etoh et al. 2003; Himeno et al. 2005; Hirano et al. 2009), has recently shown promise in several PDA tumor models. About 95% of pancreatic cancers are pancreatic ductal adenocarcinomas (PDA) which are highly invasive with aggressive local growth and rapid metastases to surrounding tissues (Stathis and Moore 2010). PDA is considered one of the most lethal

abdominal malignancies with annual deaths closely matching the annual incidence of the disease (Lindsay et al. 2005; Farrow et al. 2008), resulting in a 5-year survival rate of merely 8-20%. PDA begins with mutations in oncogenes and tumor suppressor genes. These alterations progress through a series of pre-invasive stages known as pancreatic intraepithelial neoplasias (PanINs) ultimately resulting in invasive and metastatic PDA (Farrow et al. 2008). These PanIN lesions secrete numerous soluble factors that result in a local inflammatory response and the recruitment of immune cells (Farrow et al. 2008). Unfortunately, the locally secreted factors recruit regulatory T cells (T_{reg}), myloid-derived suppressor cells (MDSCs) and tumor-associated macrophages (TAM) all of which play a role in immunosuppression (Ben-Baruch 2006; Farrow et al. 2008). Therefore the site of the PanIN lesions becomes a site of immune-privilege and the progression to the devastating PDA disease (Ben-Baruch 2006). Several cancer therapies proven successful in other tumor types have shown little efficacy in treating PDA. Chemotherapy is the primary treatment available; however, patients exhibit little improvement or develop chemoresistance (Stathis and Moore 2010). Therefore, development of new treatment strategies for patients suffering from PDA is of utmost importance and OV therapy using VSV has great potential (Kasuya et al. 2005).

Hypotheses and Present Study

In the present study we have focused on the cap methylation function of SeV, the prototypic member of the *Paramyxoviridae* family of the order *Mononegavirales*; and evaluating VSV as an oncolytic agent against pancreatic ductal adenocarcinoma.

The large (about 2200 amino acids) L polymerase protein of *Mononegavirales* has six conserved sequence regions (“domains”) postulated to constitute the specific

enzymatic activities involved in viral mRNA synthesis, 5' capping, cap methylation, 3' polyadenylation, and genomic RNA replication (Whelan et al. 2004; Lamb and Parks 2007; Lyles 2007). Similar to eukaryotic mRNA, viral mRNA requires a methylated 5' cap structure for mRNA stability and efficient translation of viral proteins (Abraham et al. 1975). Virus-encoded cap methylation function, which is distinct from host cells, can be a target for drug development and rational attenuation. The majority of previous cap methylation studies were done with VSV and identified aa residues within the L protein domain VI required for mRNA cap methylation (Grzelishvili et al. 2005; Li et al. 2005; Grzelishvili et al. 2006; Li et al. 2006; Galloway et al. 2008). While most cap methylation studies have been done using a VSV experimental system, we wanted to determine if the aa residues required for VSV cap methylation had similar importance in other members of *Mononegavirales*. Therefore we chose to study SeV (distantly related to VSV) to investigate the importance of the L protein domain VI in paramyxovirus cap methylation function. We hypothesized that domain VI of paramyxoviruses has similar cap methylation function as rhabdoviruses. Initially, four aa residues within domain VI of the SeV L protein were analyzed and our data indicated that there could be differences in L protein sequence requirements for cap methylation in two different families of *Mononegavirales* - rhabdoviruses and paramyxoviruses. To further analyze domain VI of the SeV L protein, we conducted a more comprehensive mutational analysis by targeting the entire SeV L protein domain VI, creating twenty-four L mutants, and testing these mutations for their effects on viral mRNA synthesis, cap methylation, viral genome replication and virus growth kinetics. Our analysis identified several residues required for successful cap methylation and virus replication and clearly showed the importance of a

putative catalytic tetrad and methyl donor binding site in SeV cap methylation. This study is the first extensive sequence analysis of the L protein domain VI in the family *Paramyxoviridae*, and it confirms structural and functional similarity of this domain across different families of the order *Mononegavirales*.

VSV is also one of the most promising oncolytic viruses against a variety of malignancies and we have analyzed for the first time the oncolytic potential of VSV against pancreatic ductal adenocarcinoma (PDA). PDA is the most common form of pancreatic cancer with highly aggressive local growth and rapid metastases to surrounding tissues. Currently there are few treatments options available to patients suffering from this disease therefore there is a great need to develop alternative therapies. VSV has shown preclinical success in several cancer models, however VSV has never been studied in any form of pancreatic cancer. We hypothesized that VSV can be an effective oncolytic virus against PDA and set out to determine the ability of VSV to infect and cause cell death in pancreatic cancer cell lines in a nude mouse model of tumorigenesis. The oncolytic potential of several recombinant VSVs were analyzed in a panel of 13 clinically relevant human PDA cell lines and compared to conditionally replicative adenoviruses (CRAds), SeV and respiratory syncytial virus (RSV). VSV variants showed superior oncolytic abilities compared to other viruses, however, PDA cells were highly heterogeneous in their susceptibility to virus-induced oncolysis and several cell lines were resistant to all tested viruses. For resistant cells we demonstrated low levels of very early VSV RNA synthesis, indicating possible defects at initial stages of infection. In addition, most of the resistant cell lines were able to both produce and respond to Type I interferon (IFN), suggesting that intact IFN responses contributed to

their resistance phenotype. We selected certain cell lines that varied in their permissiveness to VSV and tested them in nude mice, and in vivo results closely mimicked those in vitro. Our results demonstrate VSV is a promising oncolytic agent against PDA, and further studies are needed to better understand the molecular mechanisms of resistance to oncolytic virotherapy.

CHAPTER 2: SEQUENCE-FUNCTION ANALYSIS OF THE L PROTEIN DOMAIN VI OF SENDAI VIRUS

2.1 Objective of the study

Viruses of the order *Mononegavirales* include diverse human, animal and plant pathogens that share structurally similar NNS RNA genomes with similar strategies for viral RNA genome replication, transcription and posttranscriptional modifications of viral mRNAs (Whelan et al. 2004; Lamb and Parks 2007; Lyles 2007). All members of this order encode the large (L) polymerase protein which has six highly conserved regions (“domains”) postulated to be responsible for the specific enzymatic activities of the viral polymerase complex which include viral genome replication, transcription, mRNA 5’ capping, cap methylation and 3’ polyadenylation. Currently, there is no structural data available for the entire L or any region of L. However, site-directed mutagenesis and computational analyses support the multifunctional nature of the L protein as targeted amino acid substitutions in the different L domains were able to inactivate individual functions of viral polymerase (Poch et al. 1990; Sidhu et al. 1993; Sleat and Banerjee 1993; Schnell and Conzelmann 1995; Cortese et al. 2000; Smallwood et al. 2002; Cartee et al. 2003; Grdzlishvili et al. 2005; Li et al. 2005; Li et al. 2008; Ogino and Banerjee 2010; Ogino et al. 2010).

Similarly to eukaryotic mRNA, most of *Mononegavirales* synthesize mRNA containing a 5’ cap structure methylated at the G-N7 and 2’-O-ribose positions. The 5’

cap is required for mRNA stability, and cap methylation, especially at G-N7 position, is required for efficient mRNA translation (Horikami and Moyer 1982; Horikami et al. 1984; Gingras et al. 1999). The MTase activity was originally mapped to the L protein following the characterization of two vesicular stomatitis virus (VSV, family *Rhabdoviridae*) hr mutants. These mutants exhibited severe defects in cap methylation (Horikami and Moyer 1982; Horikami et al. 1984), but this function was successfully complemented with purified wt L protein in vitro, demonstrating that L possesses the viral mRNA MTase activities (Hercyk et al. 1988). More recently, computational analyses predicted that the L protein domain VI has a typical 2'-O-ribose MTase fold and identified a putative KDKE catalytic tetrad and a glycine-rich motif (GxGxG) as the putative AdoMet binding site (Bujnicki and Rychlewski 2002; Ferron et al. 2002; Martin and McMillan 2002). These predictions were experimentally confirmed by several studies with the VSV L protein leading to the identification of the aa residues important for cap methylation within domain VI (Grzelishvili et al. 2005; Li et al. 2005; Li et al. 2006; Galloway et al. 2008). Grzelishvili et al. (2005) showed that one of the VSV hr mutants, *hr1*, had a single substitution D to V within the glycine-rich motif (GDGSG in VSV) and was completely defective in cap methylation. Further site-directed mutagenesis of the glycine-rich motif and putative KDKE catalytic tetrad by Li et al. (2005, 2006) showed that they are important for mRNA cap methylation at both the G-N7 and 2'-O positions. Most of previous studies suggest that the L protein uses a single AdoMet binding site for both G-N7 and 2'-O MTase activity, and that, at least in VSV, 2'-O methylation precedes G-N7 methylation (Testa and Banerjee 1977; Rahmeh et al. 2009).

While most of the cap methylation studies were conducted using VSV, limited studies using Sendai virus (SeV, family *Paramyxoviridae*) demonstrated similarities as well as differences in the cap methylation between these two distantly related viruses. SeV produces mRNA that is capped and methylated at both the G-N7 and 2'-O-ribose positions (Takagi et al. 1995), but interestingly, purified SeV L protein or just its C-terminal portion retaining domain VI, catalyzed only G-N7, but not the 2'-O-ribose cap methylation (Ogino et al. 2005).

To dissect the L protein sequence requirements for cap methylation in SeV in more detail, we conducted a more comprehensive analysis by targeting the entire SeV L protein domain VI and created twenty-four L mutants by site-directed mutagenesis at highly conserved positions within this domain, using sequence conservation between L proteins in *Mononegavirales* as a guide (Bujnicki and Rychlewski 2002). The L mutations were analyzed in the context of infectious mutant viruses for their effect on viral mRNA cap methylation and virus growth in vitro, and we found a good correlation between attenuation in cell culture and defects in MTase activity for most of SeV mutants. Our analysis experimentally confirms previous computational predictions suggesting the importance of the glycine-rich motif and KDKE catalytic tetrad in cap methylation across different families of the order *Mononegavirales*. In addition, the majority of L mutants were tested for their ability to synthesize viral mRNA and replicate viral genomic RNA. This study is the first detailed analysis of the L protein domain VI in the family *Paramyxoviridae*.

2.2 Materials and Methods

Cell lines and viruses.

African green monkey (Vero, ATCC# CCL-81), human epidermal carcinoma (HEp-2, ATCC# CCL-23), human lung carcinoma (A549, ATCC# CCL-185) and BSR-T7/5 cells [derived from baby hamster kidney (BHK-21) cells and constitutively expressing bacteriophage T7 polymerase (Buchholz et al. 1999)] were used for virus infections and plasmid transfections. Monolayer cultures of these cell lines were maintained in Dulbecco's modified Eagle's medium (DMEM, Cellgro) supplemented with 9% fetal bovine serum (FBS, Gibco). Mouse embryonic fibroblasts (MEFs) were kindly provided by Dr. Takemasa Sakaguchi (Hiroshima University, Japan) and were maintained in DMEM supplemented with 9% FBS. Wild-type C57BL/6 MEFs and RIG-I knock-out (KO) MEFs, MDA5 KO MEFs, IRF-3 KO MEFs, and IRF-7 KO MEFs (C57BL/6 background) were used in immune response studies.

Recombinant wt (rWT) SeV (Fushimi strain) (Leyrer et al. 1998) and SeV-GFP- F_{mut} (rWT-GFP) with an enhanced green fluorescent protein (eGFP) upstream of the NP gene (Wiegand et al. 2007) were kindly provided by Dr. Wolfgang J. Neubert (Max-Planck-Institute of Biochemistry, Germany). All viruses were approved by the IBC at UNCC. To grow and purify SeV wt or mutants, Vero or BSR-T7 cells were infected with wt or mutant viruses at a multiplicity of infection (MOI) of 0.1 CIU/ml in MegaVir HyQSFM4 (SFM) serum-free medium (Hyclone) and in the presence of 4 μ g/ml acetylated trypsin (Leyrer et al. 1998), and incubated for 48-120 hours (h) at 34°C. Cleavage by a cellular protease is necessary for the SeV fusion (F) protein to be biologically active in vivo, making the viral particle infectious and allowing for multiple

rounds of virus replication. SeV-GFP viruses were grown similarly but without acetylated trypsin in the medium, as they have a wt monobasic trypsin-dependent cleavage site in the F protein mutated to an oligobasic cleavage site, allowing F activation in any cell type through an ubiquitous furin-like protease (Wiegand et al. 2007). The released viruses were purified from the medium as described previously (Grzelishvili et al. 2005), suspended at about 5 mg/ml in 1 mM Tris-HCl, pH 7.4, 1 mM EDTA, 10% DMSO, and stored at -80°C. Recombinant VSV wt (Indiana serotype) and its derivative VSV rHR1-1 (referred to as *hr1*) with a single aa substitution D1671V in the L protein were described in (Grzelishvili et al. 2005).

For the immune response studies, SeV wt and the following SeV mutants - K1782A, E1805A, and G1806A were propagated in eggs as described in (Kiyotani et al. 1990) and titered on LLC-MK2 (ATCC CCL-7) cells.

Plasmids and mutagenesis.

The pGEM plasmids containing wt genes for SeV NP, L, and Pstop (expressing P but not C due to a stop codon in the C open reading frames, and referred to here as wt P), under the control of the T7 promoter have been described previously (Curran et al. 1991). The pGEM-L plasmid and mutagenic primers were used for the L protein domain VI deletion and for site-directed mutagenesis (Table 1). Primers also contained silent restriction sites (Table 1) for screening and confirmation purposes. Using an overlapping PCR approach (Higuchi et al. 1988), two rounds of PCR were done using wt pGEM-L plasmid as a template, common flanking primers VG19 and VG20, and two specific primers designed for aa substitutions (Table 1). The final PCR products were digested with *XhoI* and *MfeI* and cloned into *XhoI-MfeI* digested pGEM-Lwt plasmid. All L

plasmids were tested for the presence of silent sites by digestion with the appropriate silent site enzymes, followed by sequence analysis to confirm the presence of the desired mutations and absence of any spontaneous secondary mutations. The SeV pTM-NP, pTM-P and pTM-L plasmids, the pRS3Gg (Leyrer et al. 1998) full length SeV antigenomic plasmid and the SeV pRSIdeF_{mut} plasmid (a full length SeV antigenomic plasmid with the GFP gene inserted upstream of the NP gene) used for the rescue of recombinant SeV viruses were kindly provided by Dr. Wolfgang J. Neubert (Max-Planck-Institute of Biochemistry, Germany).

Recovery of recombinant SeV.

The recombinant virus rescue was done using the reverse genetics system for SeV described by Leyrer *et al.* (Leyrer et al. 1998) using plasmids with SeV wt NP, P, and L genes and SeV full-length genomic cDNA (wt or mutant L gene) all under the control of the T7 promoter. For this study we used the BSR-T7 cell line stably expressing the T7 RNA polymerase (Buchholz et al. 1999) for initial plasmid transfections and Vero cells for consequent virus passages. All mutations were introduced into the full length genomic SeV plasmid, pRS3Gg. To obtain a mutant plasmid, pGEM-Lmut was digested with *KpnI* and *NheI* and the fragment containing the L mutation was cloned into *KpnI-NheI* cut pRS3Gg. Similarly, K1782A, E1805A and G1806A mutations were introduced into the pRSIdeF_{mut} plasmid to generate recombinant SeV-GFP viruses. To rescue recombinant viruses, 10 µg of full length pRS3Gg or pRSIdeF_{mut} plasmid containing wt or a mutant L gene along with 1 µg of pTM-L, 3 µg of pTM-P and 5 µg of pTM-NP plasmids were transfected into BSR-T7 cells in 35-mm dishes using Opti-MEM medium (Gibco) and Lipofectamine (Invitrogen) in a total of 2 ml according to the manufacturer's protocol.

All transfection reactions were incubated for 24 h at 34°C. After 24 h, the transfection medium was aspirated and 1.5 ml of SFM medium and 4 µg/ml acetylated trypsin were added to each well (SeV-GFP viruses were grown without trypsin). The cells were then incubated at 34°C for 2 days. On day 3 post transfection (p.t.), 500 µl of BSR-T7 supernatant was collected and passed (Pass1) onto a fresh monolayer of Vero cells in 1 ml of fresh SFM with 4 µg/ml acetylated trypsin. Between 2-5 days following Pass1, there were noticeable cytopathic effects (CPE) and cellular debris was pelleted and the medium harvested. The recombinant SeV mutants were titered on Vero cells with an agar overlay with 4 µg/ml acetylated trypsin, and individual infectious foci were picked and grown on Vero cells. Recombinant viruses were purified as in (Grdzlishvili et al. 2005) and all mutations were confirmed by RT-PCR and digestion with the appropriate silent restriction enzymes, and by sequence analysis for the presence of the desired mutations and absence of any spontaneous secondary mutations in the L gene.

Virus growth analysis.

SeV infectivity, expressed as cell infectious units/ml (CIU/ml), was measured by virus titration on Vero cells and counting infectious foci visually using light microscopy and/or immunofluorescence (IF) assay for SeV mutants, or by GFP-based fluorescence for SeV-GFP viruses. For IF, SFM media from 6-well plates was aspirated 2 or 3 days post infection, cells were washed with PBS, fixed with 3% paraformaldehyde (Sigma) for 10 minutes, and permeabilized for 2 minutes on ice with 20 mM HEPES pH 7.5, 300 mM sucrose, 50 mM NaCl, 3 mM MgCl₂, and 0.5% Triton-X-100. Cells were then blocked in PBS with 5% bovine serum albumin (BSA, Sigma) for 20 minutes and incubated with anti-SeV primary antibodies (1:100) for 1 h. Cells were washed, incubated with goat

anti-rabbit IgG-FITC antibodies (Santa Cruz) for 1 h in the dark, and viewed under a fluorescent microscope to determine virus titer.

For multistep growth analysis, Vero or HEp-2 cells in 6-well plates were infected at an MOI of 0.001 CIU/cell in 1.5 ml SFM per well. One h post infection (h p.i.), media was aspirated, cells were washed with PBS and 1.5 ml SFM with 1 µg/ml acetylated trypsin was added to each well. Supernatants were harvested at 12 h (for Vero) or 24 h (for HEp-2) intervals and flash frozen at -80°C. Virus titers were determined using a 96-well plate format by infecting Vero cells with the serial dilutions (1:8) of wt or mutant SeV (collected at various time points) and incubating at 37°C with shaking. At 1 h p.i., viruses were aspirated, and cells were overlaid with 100 µl SFM with 2 µg/ml of acetylated trypsin, and cells were analyzed at 48 h p.i.

For one-step growth kinetics, Vero cells were incubated for 1 h with SeV wt or mutants at an MOI of 3 CIU/cell in 24 well plates. At 1 h p.i., unabsorbed viruses were aspirated, cells were washed two times with PBS and SFM with 4 µg/ml acetylated trypsin was added to each well. Plaque assays were performed on Vero cells using supernatants collected at different time points.

For superinfection experiments, virus infectious foci were detected by IF as described above or by 4 CN Peroxidase Substrate colorimetric staining (KPL). Briefly, cells were fixed in 3% paraformaldehyde for 10 min and permeabilized for 2 min on ice. Cells were blocked in PBS with 5% BSA for 20 min and incubated with anti-SeV primary antibodies (1:100) for 1 h. Cells were then washed, incubated with goat anti-rabbit IgG-HRP (Jackson ImmunoResearch) secondary antibodies (1:500) for 1 h. To

visualize infectious foci, cells were washed and incubated with equal volumes 4 CN Peroxidase Substrate and Peroxidase Substrate Solution B (KPL).

In vitro transcription with T7-expressed L proteins.

For virus-driven expression of the bacteriophage T7 RNA polymerase, Vero or A549 cells were infected with T7-expressing vaccinia virus (VV-T7) (Fuerst et al. 1986). To express SeV wt P and wt or mutant L proteins, 60-mm dishes of A549 or Vero cells were infected with VV-T7 at MOI of 2.5 PFU/cell for 1h at 37°C, washed with Opti-MEM (Gibco), transfected with 1.5 µg of SeV pGEM-Pstop and 1 µg of pGEM-L (wt L or one of the mutant L genes) plasmids using Lipofectamine, and incubated at 34°C in Opti-MEM. At 18 h p.t., cytoplasmic extracts were prepared exactly as described previously (Chandrika et al. 1995; Grdzlishvili et al. 2005). To assay for SeV mRNA synthesis, 1 µg of wt SeV polymerase-free RNA-N template and 20 µCi of [α^{32} P]CTP were added to each extract, and reactions were incubated for 2 h at 30°C. Total RNA was purified using RNeasy columns (Qiagen) or Quick RNA Miniprep (Zymo Research) and analyzed by 1.5% agarose/6 M urea gel electrophoresis. The gels were fixed in 7% acetic acid, dried, and exposed to Kodak X-OMat film for 18 h at -80°C, and quantitated using a Typhoon 8600 PhosphorImager and ImageQuant software (Molecular Dynamics).

DI RNA replication with T7-expressed L proteins.

To produce cell lysates containing SeV wt NP, wt P and wt or mutant L proteins for in vitro replication of SeV defective interfering (DI) RNA, 60-mm dishes of A549 cells were infected and transfected as above using 5 µg of SeV pGEM-Pstop, 2 µg SeV pGEM-NP and 0.5 µg of pGEM-L (wt L or one of the mutant L genes). At 18 h p.t., cytoplasmic extracts were prepared as for in vitro transcription. To assay for SeV genome

synthesis, 2 µg of detergent disrupted DI-H (Carlsen et al. 1985) and 18 µCi of [α - 32 P]CTP were added to each extract, and reactions were incubated for 2 h at 30°C and then treated with micrococcal nuclease to digest unpackaged RNA (mRNA). Total RNA was purified and analyzed as described above for in vitro transcription.

In vitro transcription using purified SeV virions.

SeV in vitro transcription by detergent-activated purified virions was conducted essentially as described in (Mizumoto et al. 1995). For [α - 32 P]UTP-labeled RNA, 10 µg of purified virus was incubated at 30°C for 6 h in a 50 µl reaction containing: 30 mM HEPES-KOH (pH 7.9), 75 mM NaCl, 50 mM KCl, 6 mM MgCl₂, 2 mM dithiothreitol, 2 mM spermine, 0.1% NP-40, 500 µM each of ATP, CTP and GTP, 50 µM UTP, 50 U of RNasin (Promega), 12 µg of purified tubulin (>99% pure) from bovine brain (Cytoskeleton Inc.) and 20 µCi of [α - 32 P]UTP. Total RNA was purified using RNeasy columns (Qiagen) and analyzed by 1.5% agarose/6 M urea gel electrophoresis. The gels were fixed in 7% acetic acid, dried, and exposed to Kodak X-OMat film for 4-18 h at -80°C, and quantitated using a PhosphorImager. To test for viral mRNA cap methylation, in vitro transcription by detergent-activated purified SeV wt or mutants was conducted as described above, but RNA was synthesized in a 200 µl reaction with cold NTPs (1 mM each) and 11 µCi of [3 H]AdoMet (55 Ci/mmol, 1 µM AdoMet final concentration) in the presence or absence of 100 µM of the methylation inhibitor S-adenosylhomocysteine (AdoHcy). Total RNA was purified using RNeasy columns (Qiagen), diluted in 25 µl of H₂O, and used for measurement of [3 H]Met incorporation by scintillation counting (20 µl) or analyzed by Northern blot to measure mRNA levels (5 µl).

Cap methylation analysis of purified SeV virions.

To generate viral mRNA for cap analysis using tobacco acid pyrophosphatase (TAP), SeV rWT and VSV rWT in vitro transcription by detergent-activated purified virions was performed as described above using [³H]AdoMet and the same reaction conditions for SeV and VSV. VSV mRNA was synthesized in a 100 µl reaction. To obtain sufficient amounts of SeV mRNA for this analysis, ten 200-µl transcription reactions were used for SeV rWT, and viral mRNA products were isolated and pooled together for TAP treatments. For preparation of synthetic mRNA controls, uncapped SeV NP mRNA was synthesized in vitro with the MAXI-Script T7 kit (Ambion) using SeV pGEM3-NP plasmid digested at the BamHI restriction site located immediately after the stop codon for the NP gene as a template. This RNA was divided to generate: i) Cap 0 containing mRNA (m⁷GpppA...) labeled with [³H] only at the G-N7 position, or ii) Cap 1 containing mRNA (m⁷Gppp[m^{2'-O}]A...) labeled with [³H] only at the 2'-O position. To make synthetic mRNA containing Cap 0, uncapped mRNA transcripts were capped and G-N7 methylated in the presence of 1.75µM [³H]AdoMet using the ScriptCap m⁷G Capping System (Epicentre Biotechnologies) based upon the tri-functional vaccinia virus capping enzyme, and purified using Spin-50 Sephadex G-50 mini-columns (USA Scientific). To make synthetic mRNA with Cap 1 but [³H]-labeled only at the 2'-O position, uncapped mRNA transcripts were first capped in the presence of 100µM cold AdoMet using the ScriptCap m⁷G Capping System to make mRNA with the unlabeled Cap 0 structure (which is the template for 2'-O methylation by the vaccinia virus 2'-O MTase). After purification using Spin-50 Sephadex G-50 mini-columns, the unlabeled Cap 0 mRNA was 2'-O methylated in the presence of 1.75µM [³H]AdoMet using

ScriptCap 2'-*O*-MTase (Epicentre Biotechnologies) based upon the vaccinia virus 2'-*O*-MTase, and purified again using Spin-50 Sephadex G-50 mini-columns.

For TAP analysis, virion-produced viral mRNA (SeV or VSV) and synthetic (G-*N7* or 2'-*O* labeled) mRNAs were normalized by [³H] counts and digested by TAP (Epicentre Biotechnologies) in 10 µl reactions in the presence or absence of 5 units of TAP for 1 h at 37°C. All reactions were then adjusted to 25 µl and passed through Spin-50 Sephadex G-50 mini-columns. Spin columns were then placed in new microfuge tubes and 25 µl diH₂O was passed each column to retrieve the residual column-bound RNA. Separate optimization experiments demonstrated effective separation of RNA from nucleotides using this procedure (data not shown). [³H]AdoMet incorporation into the G-*N7* or 2'-*O* cap position was measured by scintillation counting of the entire flow through (contained mRNA) and the Sephadex G-50 column material removed from mini-columns after separation (contained removed G).

Northern blot analysis.

For Northern blot analysis, mRNA products of in vitro transcription reactions with [³H]AdoMet were separated in a 1.2% agarose/formaldehyde gel system, transferred to a Hybond-N+ nylon membrane (GE Healthcare) and incubated with an RNA probe complementary to the SeV NP gene. The probe was synthesized by digestion of the SeV pGEM3-NP plasmid at the EcoRV restriction site and transcribed in vitro in the presence of [α -³²P]-CTP using the MAXI-Script SP6 kit (Ambion). Radioactive signals were measured using a PhosphorImager and ImageQuant software.

For analysis of RNA synthesized during superinfection, both supernatants and cells were collected at 48 h p.i. Virus particles in the supernatant were pelleted by

centrifugation at 50,000 rpm for 1 h using a Beckman TLA 100.2 rotor and total RNA was extracted from both cells and pelleted virions using the Zymo Research Quick-RNA MiniPrep kit. Total RNA (0.7 µg or 7 µg) from the supernatant or cells respectively was separated on a 1.5% agarose formaldehyde gel and transferred to a nylon membrane. Membranes were originally probed for full length and DI genomic RNA using an oligonucleotide [5'-

ACAAGAAGACAAGAAAATTTAAAAGAATAAATATCTCTTAAACTCTTGTCTG
GT-3' (Integrated DNA Technologies)] complimentary to the first 54 5'-nucleotides of the SeV genomic RNA. The primer was labeled with [γ -³²P]-ATP using bacteriophage T4 polynucleotide kinase (New England Biolabs). Membranes were then reprobed for NP mRNA using the riboprobe described above. Radioactive signals were measured using a Typhoon 8600 Phosphorimager and ImageQuant software (Molecular Dynamics).

Western blot analysis.

To compare the amounts of P and L proteins in cell lysates used for in vitro transcription, total protein samples from transfected cytoplasmic lysates (5 µl of a total of 100 µl of lysate) were separated by 7.5% SDS-PAGE and electroblotted onto a PVDF membrane (Sigma). Membranes were blocked with 5% non-fat dry milk in TBST [0.5 M NaCl, 20 mM Tris pH (7.5), 0.1% Tween 20] and antibodies were diluted in the same buffer. The blots were initially incubated with a mixture of rabbit antibodies against SeV L protein [a-TrpE-SeV-L #5 (“1-19-90”) and a-TrpE-SeV-L #1 (“10-23-89”)] (Horikami et al. 1992) and developed with a horseradish peroxidase conjugated secondary antibody using the Enhanced Chemiluminescence Plus (ECL+) protein detection system (GE Healthcare) according to the manufacturer’s protocol. Blots were then reprobed with a

rabbit anti-SeV antibody (“1-4-83”) (Carlsen et al. 1985) and developed in the same manner. Protein bands were quantified using VisionWorksLS software (UVP).

For immune response studies, 6 well plates of MEFs were infected at an MOI of 10 CIU/cell and cells were harvested for lysates at 24 h p.i. Lysates were prepared directly in the 6 well plates in 1X SDS sample buffer and 5 μ l (of a total of 150 μ l) of each sample was separated by 10% SDS-PAGE and electroblotted onto PVDF membranes. Membranes were blocked with 5% non-fat dry milk in TBST and membranes were incubated with rabbit anti-SeV antibodies (1:5000) followed by incubation with goat anti-rabbit IgG-HRP secondary antibodies (1:5000). Membranes were developed as described above. Lysates were also probed for IFIT-1 (ISG56, Santa Cruz, Cat. # sc-134949, 1:500) and membranes were developed as described above.

2.3 Results

Site-directed mutagenesis of the SeV L protein domain VI and recovery of infectious SeV mutants.

To date, all the domain VI mutagenesis studies have been carried out using the VSV (Family *Rhabdoviridae*) experimental system (Grzelishvili et al. 2005; Li et al. 2005; Grzelishvili et al. 2006; Li et al. 2006). Based on these studies and computational predictions (Bujnicki and Rychlewski 2002; Ferron et al. 2002), it has been postulated that the glycine-rich motif (L aa positions 1670-1674 in VSV, 1804-1808 in SeV) constitutes an AdoMet-binding site of L, while a KDKE motif (aa position K1651, D1762, K1795, and E1833 in VSV; K1782, D1901, K1938, and E1975 in SeV) is the putative active MTase site (Bujnicki and Rychlewski 2002; Ferron et al. 2002; Li et al. 2006). Because the L proteins of *Mononegavirales* are conserved and all have a glycine-rich motif and KDKE motif at the same positions as VSV (Fig. 5), it has been suggested that these aa residues are likely to have similar importance in all *Mononegavirales* (Bujnicki and Rychlewski 2002; Ferron et al. 2002; Li et al. 2006). To test this hypothesis experimentally, we initially targeted by site-directed mutagenesis the SeV L protein aa residues homologous to those that are important for cap methylation in VSV. Figure 5 shows sequence alignments comparing domain VI of the L protein (including the glycine-rich motif and KDKE motif) between various paramyxoviruses and other *Mononegavirales*. Using the SeV pGEM-L_{wt} plasmid (SeV L wt gene under control of the T7 promoter), in addition to targeting the glycine-rich motif (the putative AdoMet binding site) and the putative catalytic tetrad KDKE, which also is conserved in other known 2'-O MTases including NS5 protein of flaviviruses (Fig. 5), we also targeted

residues D1799 and Y1802 located just upstream of the glycine-rich motif and conserved only in some paramyxoviruses (Fig. 5). Many classes of MTases of known structure contain either a conserved aspartate or glutamate, or a tyrosine residue within the beta strand that precedes the conserved glycine-rich motif, but rarely do they contain both these residues. A polar residue in this position has been implicated in reaction mechanism as the fifth catalytic entity (Kozbial and Mushegian 2005), and we were interested in determining whether one or both of these aa may play a functional role in SeV MTase. We also targeted the DKDKD sequence located immediately upstream of the residue D1799. Although this DKDKD sequence is present only in some paramyxoviruses, we wanted to determine whether such high concentration of aspartates and lysines and its close proximity to the glycine-rich motif may play some role in cap methylation catalysis. In addition to single aa substitutions, several double and triple alanine substitutions were created, and the glycines within the glycine-rich motif were changed to leucines to address a possibility that this motif is possibly more tolerant to single glycine-to-alanine substitutions as compared to VSV. Also, additional mutants were generated: i) E1805V, based on an analogous D1671V mutation in the VSV *hr1* mutant (Grzelishvili et al. 2005) and ii) L- Δ VI with a deletion of the entire domain VI to confirm that the presence of this region is critical for L transcriptional activity as it was previously shown for a VSV L protein mutant (Canter and Perrault 1996). All together, twenty-nine SeV L mutant genes were generated.

To examine the abilities of L mutants to synthesize viral genomic negative-stranded, as well as viral mRNA, we used a VV-T7-based (vaccinia virus expressing T7 polymerase) mammalian expression system previously described in (Chandrika et al.

1995; Grdzlishvili et al. 2005). These assays do not depend on the viability of SeV mutant viruses and are based on the exogenously provided polymerase-free wt genomic (for transcription) or DI (for replication) RNA-N template and cell extracts containing T7 RNA polymerase-expressed SeV L (wt or mutant), P and NP (for DI replication only) proteins as described in Materials and Methods. Briefly, A549 cells were infected with vaccinia virus (VV) expressing T7 polymerase (VV-T7), transfected with SeV P wt and L (wt or mutant) and NP wt (only for DI replication), and incubated at 34°C. At 18 h post transfection, cytoplasmic extracts, containing P-L or NP-P-L complexes, were prepared and supplied with the exogenous wt SeV polymerase-free RNA-N template (genomic or DI, isolated from wt SeV virions) and [α^{32} P]CTP to assay for mRNA or DI RNA synthesis. The transcription and replication products were analyzed by 1.5% agarose/6M urea gel electrophoresis, visualized by autoradiography and quantitated using a PhosphorImager. As shown in Figure 6 for A549 cells (similar results were obtained with Vero cells, data not shown), most tested proteins were transcriptionally active except for the L- Δ VI deletion mutant and L-E1805V where mutations completely inactivated L. The L-E1805V result is rather unexpected as a similar substitution in the VSV L protein (D1671), while abolishing cap methylation, had little effect on VSV transcription (Grdzlishvili, Smallwood et al. 2005). Additionally, two L mutations - E1805L and G1808L, produced no detectable mRNA and were also defective in genomic RNA replication (<5% of rWT) (Fig. 6). The E1975A mutant L protein, had wt-like levels of transcription in the VV-mediated system, but replication levels were 10% of rWT. Several other mutant L proteins had transcription levels higher than 50% of rWT but lower levels of replication (<40% of rWT) including D1901A, E1903A, and

K1938A/I1938L (but not K1938S), all of which are members of the KDKE catalytic tetrad. G1804L, E1805A, G1806L, and G1804A/G1806A/G1808A, all members of the glycine-rich motif, had similar levels of transcription and replication ranging from 30 to 60% of rWT. This indicates that the intactness of the primary AdoMet-binding site and the majority of the catalytic residues are required for multiple functions of L protein, most likely including synthesis of the negative-strand genomic RNA and its transcription into mRNAs. Only two mutant L proteins, S1777A and K1782A, had rWT levels of transcription and replication, indicating a more limited role of the predicted first helix in the Rossmann fold in SeV RNA synthesis.

Interestingly, we observed that many aa substitutions negatively affected L protein accumulation in the plasmid based expression assays. Some of these mutations could potentially affect L gene expression or L protein stability of the protein, which could impact viral RNA synthesis. However, we did not see any clear correlation between L protein levels and transcriptional activities for most mutant proteins (Fig. 6). The lowest protein accumulation (26% of wt) was shown for the K1938A/I1939L mutation; however, it had 107% transcriptional activity. At the same time, this mutant showed only 14% DI replication activity suggesting a possibility that L protein accumulation may specifically affect replication (but not transcription) activity of viral polymerase. However, two other mutations, E1903A and E1975A, which had disproportionately low DI replication activities (relative to transcription), did not show any dramatic decreases in protein accumulation (Fig. 6).

Nevertheless, as most mutations passed the *in vitro* transcription/replication test (Fig. 6), they were cloned into the SeV full-length infectious cDNA plasmid to generate

mutant viruses using the BSR-T7 cell line stably expressing the T7 RNA polymerase (Buchholz et al. 1999) for initial plasmid transfections and Vero cells for consequent virus passages. Although BSR-T7 cells are derived from BHK-21 cells (Buchholz et al. 1999) which support replication of cap methylation defective VSV mutants (Horikami et al. 1984; Grdzlishvili et al. 2005), we wanted to confirm that BSR-T7 were suitable for recovery of SeV mutants potentially defective in cap methylation. Similarly, we wanted to verify that potential cap methylation defective viruses can be passed on Vero cells which support robust replication of wt SeV. Therefore, prior to the rescue attempts, we tested VSV wt and the cap methylation defective mutant VSV *hr1* (Grdzlishvili et al. 2005) for their ability to grow on BSR-T7 and Vero cells and compared it to their growth on HEp-2 cells which do not support replication of VSV *hr1* or any other tested cap methylation defective VSV mutants (Grdzlishvili et al. 2005; Grdzlishvili et al. 2006). VSV *hr1* was unable to grow in HEp-2 cells as expected (Table 2) but was only moderately attenuated in Vero cells (2.4×10^9 PFU/ml for VSV wt and 6.0×10^7 PFU/ml for VSV *hr1*) (Table 2) and grew normally in BSR-T7 (2.4×10^9 PFU/ml for VSV wt and 1.1×10^9 PFU/ml for VSV *hr1*). Therefore, we concluded that a BSR-T7/Vero recovery system could be successfully used to rescue SeV mutants even if they are defective in cap methylation. Using this approach, we successfully recovered 24 infectious SeV mutants using a reverse genetics system (Table 3). Infectious virus particles could not be recovered for the remaining five mutant L genes (indicated as NR in Table 3). All viruses were confirmed for the presence of the desired mutations and absence of any spontaneous secondary mutations by virus purification followed by RT-PCR amplification of the L gene and sequence analysis using primers VG19 and VG20 (Table 1).

Growth analysis of SeV L mutants in cell culture.

Previously studied VSV cap methylation mutants exhibited host range (*hr*) and temperature sensitivity (*ts*) (Grzelishvili et al. 2005; Grzelishvili et al. 2006), therefore we tested our initially recovered recombinant SeV mutants (r1782A, r1804A, r1805A, r1806A, r1804A/1806A) for their possible *hr* and *ts* phenotypes. The wt and mutant SeV were titered on Vero and HEp-2 cells at 34°C and 40°C (Table 2). In addition, we used rVSV wt and rVSV *hr1* viruses as convenient controls for the conditions used in these studies. rVSV *hr1* grew to high titers on Vero cells (permissive cells) at 34°C (permissive temperature) but, unlike rVSV wt, displayed more than 60,000-fold reduction in growth in HEp-2 cells at 34°C (nonpermissive cells) and in Vero cells at 40°C (nonpermissive temperature). Therefore, we predicted that SeV mutants defective in cap methylation would be moderately attenuated in Vero cells (as VSV *hr1* compared to wt), but be severely attenuated in HEp2 cells. As shown in Table 2 and Figure 7A, SeV r1782A mutant showed a *hr* phenotype with a Vero/HEp-2 titer ratio of 100 (compare to 2.3 for rWT), which supported a possible role of the SeV L protein lysine 1782 at the active MTase site. This ratio was much smaller than in VSV *hr1* (Table 2) because rK1782A was also attenuated in Vero cells reaching a maximum titer of only 4.0×10^5 CIU/ml at 120 h p. i. compared to 2.0×10^8 CIU/ml for rWT at 48-72 h p. i. (Table 2). Also, infectious foci counted for r1782A in HEp-2 cells were noticeably smaller than in rWT (Fig. 7A).

Unexpectedly, all tested SeV mutants with aa substitutions in the glycine-rich motif produced similar numbers of infectious foci in Vero and HEp-2 cells with a Vero/HEp-2 titer ratio of about 2.5. However, r1805A displayed slow growth in both

Vero and HEp-2 cells with about a 24 h delay in infectious foci formation and noticeably smaller foci on both Vero and HEp-2 cells.

To independently confirm these observations, we cloned three representative mutations, K1782A, E1805A and G1806A, into a plasmid with the full-length SeV genome additionally encoding the GFP gene, and successfully rescued two of the three recombinant viruses (r1805A-GFP and r1806A-GFP) containing the appropriate L mutations (Fig. 7B). Ten separate attempts were made to rescue r1782A-GFP, but no infectious virus was ever recovered and no GFP signal was visible during these attempts. We think that the combination of negative factors, the K1782A mutation and GFP insertion, made this virus too attenuated for recovery, at least using our standard rescue conditions. For successfully rescued GFP viruses, virus titrations were conducted on Vero and HEp-2 cells and virus infection sites were compared between rWT-GFP, r1805A-GFP and r1806A-GFP using fluorescent microscopy. As shown in Figure 7B for both Vero and HEp-2 cells, rWT-GFP and r1806A-GFP viruses had similarly sized foci with similar GFP signal at 48 h p.i. The r1805A-GFP virus at 48 h p.i. had smaller infectious sites on both Vero and HEp-2 cells. However, we did not observe differences in the relative ability of r1805A-GFP to grow on HEp-2 cells versus Vero cells (by CIU counts). Together, these data using SeV-GFP viruses confirmed that the G1806A mutation had no effect on SeV growth in Vero or HEp-2 cells, while the E1805A mutation similarly attenuated virus replication in Vero and HEp-2 cells.

In addition, virus titration experiments were performed with the wt or mutant SeV (and SeV-GFP) viruses on Vero cells at 34°C and 40°C to determine possible *ts* phenotypes of these viruses as previously shown for VSV *hr1* and other cap methylation

defective mutants (Grzelishvili et al. 2005; Grzelishvili et al. 2006). As shown in Table 2, rVSV *hr1* was clearly *ts* with a 34°C/40°C titer ratio in Vero cells of more than 60,000 compared to 75 for rVSV wt. However, only two SeV mutants displayed a *ts* phenotype, r1782A and r1805A. In agreement with this result, the GFP signal was present in Vero cells at 40°C for the rWT-GFP and r1806A-GFP viruses as early as 48 h p.i. (Fig. 7B). However, there was no GFP signal in cells infected with r1805A-GFP virus at 40°C at any time point (Fig. 7B).

Our titration experiments demonstrated that, unlike the r1782A mutant, all recombinant SeV with the aa substitutions in the glycine-rich motif did not display *hr* phenotypes. We wanted to confirm this result using a separate assay testing for the ability of these mutants to generate infectious particles in HEp-2 versus Vero cells (rather than their ability to form infectious foci as in our titration experiments). Therefore, we conducted a multistep growth kinetics assay for these viruses by infecting Vero cells at low MOI, harvesting cell supernatants at various time points, and assaying them on Vero cells to determine viral titers for each time point. As shown in Figure 8, most recombinant viruses, except for SeV r1782A, displayed similar growth kinetics in Vero cells with all titers peaking at 60 h p.i. The r1782A mutant grew very slowly in Vero cells producing about 2.5×10^2 CIU/ml at 72 h p.i. (Fig. 8) and reaching only 4.0×10^5 CIU/ml at 120 h p. i. While r1804A, r1806A and r1804A/1806A viruses all behaved similarly to rWT, r1805A had about 12 h delay in virus production. In HEp-2 cells, r1782A could be detected only at 96 and 120 h p. i. (maximum titer 2×10^3 CIU/ml at 96 h p. i.) and the r1805A infection of HEp-2 cells was clearly delayed with viral titers beginning to increase after 72 h p.i. In addition, two SeV mutants, r1804A and r1806A, behaved very

unusually in HEp-2 cells with r1804A growing considerably faster than rWT and r1806A slower than rWT. The presence of both mutations in r1804A/1806A produced an intermediate growth phenotype suggesting that these mutations had a reciprocal effect when present together. Despite these differences in growth kinetics, all initially rescued recombinant viruses, except for r1782A, were able to grow in HEp-2 cells to relatively high titer, which was consistent with our titration experiments (Table 2) and suggested that the aa substitutions in the glycine-rich motif did not abolish the L protein MTase function.

Our *hr* studies with our initially rescued SeV mutants did not result in large Vero/HEp-2 ratios and we observed that the r1782A virus was attenuated in Vero cells. Therefore all infectious SeV mutants generated at a later date than our initial study, were tested for their ability to infect and produce CPE in Vero cells only. Infectious foci were visualized by crystal violet staining or IF at 48 or 72 h p.i. Several mutants behaved similarly to rWT, while some mutants had obvious defects in growth based on their inability to form visible infectious foci (Fig. 9A). All of the mutants with the substitutions between positions 1795 and 1800 (DKDKDR) were capable of forming visible infectious foci and grew to rWT-like titers (Fig. 9A and Table 3). The rG1804A, rE1805A, rG1806A mutants and the double-mutant rG1804A/G1806A behaved as described above, i.e., they showed similar growth to rWT. Even the rE1805A mutant, which had a slight delay in growth, still grew to high titers. Additional alanine mutants in or around the glycine-rich motif behaved with minor variations: the rG1808A and especially the triple mutant rG1804A/G1806A/G1808A had infectious foci smaller than rWT, but grew to a high titer (1.4×10^8 CIU/ml), and the rY1802A mutant had small infectious foci 48 h p.i

but at 72 h p.i. had foci size and titer similar to rWT (Fig. 9B). In contrast to these mutants, leucine substitutions had dramatic effect on virus growth: E1805L and G1808L could not be recovered despite all efforts; rG1804L was dramatically attenuated in Vero cells and infectious foci could only be detected by IF (Fig. 9C); and rG1806L was severely attenuated in cell culture, and even after several passages on Vero cells, titers remained extremely low ($<10^2$ CIU/ml) (Fig. 9C and Table 3). Thus, the GxGxG motif, which in the cases of homologous MTases with the known structure is invariably located in the loop between the first beta strand and the alpha helix of the Rossmann fold, tolerates substitutions to small side chain residue such as alanine, but the bulkier aliphatic side chain of leucine appears incompatible with the structure or function of this region. The rules for E1805 were similar: negative charge turned out to be unimportant for virus viability, even though this residue is conserved in all *Mononegavirales*, but a bulky aliphatic leucine residue was not tolerated.

In our initial studies (described above), we observed that the SeV L mutant with an alanine substitution at the first position of the putative KDKE catalytic tetrad, rK1782A, was attenuated in cell culture. We went on to create alanine substitutions at the other positions of this motif and rescued viruses with substitutions at the D1901 and K1938 positions; however, we were not able to rescue a virus with a mutation at E1975. Interestingly, after sequencing, the K1938 position mutant had a substitution to serine and not alanine. This serine substitution apparently has been selected in vivo, as the input plasmids used for virus recovery were confirmed by sequencing to have the alanine substitution. In addition to targeting the KDKE tetrad, we created alanine mutants of two other positions invariant in *Mononegavirales*, S1777 and E1903, and a double mutant,

rK1938A/I1939L. All SeV L mutants with substitutions in and around this putative KDKE catalytic tetrad were attenuated when grown on Vero cells (Fig. 9A). rK1782A, rE1903A, and rK1938A/I1939L produced infectious foci detectable only by IF (Fig 9C).

The aa of the KDKE tetrad are widely spaced in the sequence of virus MTase, but are brought into close proximity in the homologous MTases of the known structure and in the predicted spatial structures of the L domain VI proteins (Bujnicki and Rychlewski 2002; Galloway et al. 2008). They form a semi-circle on the outer rim of the AdoMet binding pocket and are thought to work together in transferring the methyl group from that donor to the 5' nucleotides of virus mRNA, though exact role of each residue, as well as the details of the reaction mechanism (and indeed, the native three-dimensional structures of MTases of *Mononegavirales*), remain to be investigated. Residues S1777 and E1903 are predicted to be further outwards from the AdoMet-binding pocket, and may be expected not to interact with the methyl donor, but rather perhaps play a role in recognition of the RNA substrate. Our results indicate that single alanine mutations in most of these residues result in attenuation of virus infection.

We also recovered several mutants with alanine substitutions at other invariant positions of domain VI, i.e., W1876A, S1969A, and Y1977A. These mutant viruses behaved similarly to rWT in Vero cells and grew to high titers (Fig. 5 and Table 3). The corresponding residues are predicted to be located outside of the ligand-binding pocket and may not be involved in any intramolecular interactions. We, however, were unable to recover virus progeny in the mutants that had multiple alanine substitutions in these patches of amino acids predicted to face outwards, i.e., a triple substitution Y1825A/N1826A/S1827A or a double substitution T1875A/W1876A. These highly

conserved regions might be necessary for interactions of SeV MTase with other regions within the L protein or with other proteins.

To further examine the growth characteristics of all rescued mutant viruses, a one-step growth kinetics analysis was performed as described in Materials and Methods (Fig. 10). rWT reached its highest titer at 48 h p.i. and then declined at 72 and 96 h p.i. Mutants with substitutions within the DKDKD sequence upstream of the glycine-rich motif had slightly lower titers than rWT overall, but still reached their highest titers at 48 h p.i. (Fig. 10A). For mutants with substitutions in the glycine-rich motif, the majority behaved similarly to rWT with slightly lower titers overall and maximum titers (10^7 - 10^8 CIU/ml) reached at 48 h p.i. (Fig. 10C). rG1804L was severely attenuated with infectious particles detected only after 24 h p.i. and maximum titers reaching only 10^5 CIU/ml at 96 h p.i. L mutants with substitutions in and around the putative KDKE catalytic tetrad were delayed in growth and had dramatically lower maximum titers (10^4 - 10^5 CIU/ml) as compared to rWT.

Correlation between virus attenuation in cell culture and defects in cap methylation.

In addition to a phenotypic analysis of SeV mutants, we directly tested mutants for their ability to methylate viral mRNAs in vitro. The limitation of the described VV-T7-based in vitro transcription assay with plasmid-expressed P and L proteins is its dependence on the vaccinia virus vector, which provides trans-active viral MTases (Horikami et al. 1984), thus making these systems unusable for our studies on the SeV MTase function. Therefore, the effects of the SeV L protein mutations on viral mRNA cap methylation were studied using detergent-activated purified viruses, naturally carrying active virion-bound polymerase, as was conducted previously for VSV

(Grdzlishvili et al. 2005; Grdzlishvili et al. 2006). In addition to rSeV, we used rVSV wt and rVSV *hr1* viruses as positive and negative controls for cap methylation throughout all these assays. It is important to note that in contrast to the VSV system, the reactions with detergent-activated purified SeV (and many other *Mononegavirales*) virions require the addition of cytoplasmic extracts to each reaction (Moyer et al. 1986; Moyer et al. 1990; De et al. 1991; Mizumoto et al. 1995). However, such addition would be undesirable for our experiments as these extracts might contain *trans*-active cellular cap MTases which could complement L protein defects in cap methylation and thus prevent discrimination between mutants based on their ability to methylate mRNA caps. Therefore, we optimized the SeV *in vitro* transcription conditions using purified tubulin which has been shown to stimulate SeV virion transcription even when other cellular components are absent (Moyer et al. 1986; Mizumoto et al. 1995). Interestingly, our optimal reaction condition, producing similar amounts of viral mRNA to reactions with cell lysate from Vero cells (data not shown), generated about 200-fold less viral mRNA compared to VSV virions transcribed using the same conditions (Fig. 11A). Nevertheless, despite these big differences in the efficiency of mRNA synthesis, [$\alpha^{32}\text{P}$]UTP-labeled SeV mRNA was easily detectable (Fig. 11A) and we proceeded to compare all our SeV mutants for their ability to i) synthesize and ii) methylate viral mRNAs *in vitro*.

For our initially rescued infectious SeV mutants, Figure 11B shows a representative gel with [$\alpha^{32}\text{P}$]UTP-labeled viral mRNA produced by detergent-activated purified SeV wt and mutant virions (all purified viruses were tested by SDS-PAGE analysis confirming that similar amounts of virus were used in each reaction, data not shown). We did not observe any dramatic reduction in mRNA synthesis for most

mutants, although r1782A produced about 60% less mRNA than rWT. Interestingly, the L-1782A protein produced viral mRNA levels similar to L-WT in the VV-T7-based in vitro transcription system. The decrease in mRNA synthesis by purified r1782A virions could be a result of a partial loss of virion activity as r1782A virus was collected for purification 5 days p.i. due to its slow growth (compare to 2-3 days p.i. for rWT and other mutants). Interestingly, r1804A, r1806A and r1804A/1806A showed a slight increase (10-20%) in viral mRNA synthesis compared to rWT (Fig. 11B). Next, we tested all our mutants for their ability to methylate cap structures using rVSV wt and rVSV *hr1* viruses as positive and negative controls for mRNA cap methylation. For this assay, in vitro transcription by detergent-activated purified virions was conducted with cold NTPs and [³H]AdoMet (methyl group donor) in the presence or absence of S-adenosylhomocysteine (AdoHcy), a competitive inhibitor of AdoMet-dependent MTases. The total RNA was purified and used for measurement of [³H]AdoMet incorporation into mRNA as assayed by binding to DEAE-cellulose paper and scintillation counting. As shown in Figure 11C, most tested SeV virions produced a similar mRNA methylation pattern with cap methylation completely abolished in the presence of AdoHcy, as in the case of VSV wt. The only SeV mutant that showed no detectable methylation in the absence of AdoHcy (as for the VSV *hr1* mutant) was SeV r1782A, which is consistent with its *hr* phenotype. Interestingly, the SeV r1805A mutant always showed an intermediate level of cap methylation (Fig. 11C) with about 60% reduction in [³H]AdoMet incorporation into viral mRNA. To test whether no mRNA methylation in r1782A and a decrease in cap methylation in r1805A were results of the inhibition of MTase activity rather than decreased mRNA synthesis, a portion of the total mRNA

produced with [^3H]AdoMet (Figure 11C) was examined by Northern blot analysis using a specific riboprobe against the SeV NP gene. As shown in Fig. 11D, most SeV mutants produced mRNA levels similar to those of rWT (with about 40% for r1782A) further indicating that K1782A and E1805A mutations specifically affected mRNA cap methylation rather than viral mRNA synthesis.

We performed similar experiments with all other rescued infectious SeV mutants to determine whether the L mutations affected the ability of viruses to methylate mRNA 5' cap structures. In vitro transcription was performed using detergent-activated purified virions in the presence of [^3H]-AdoMet with or without AdoHcy, and RNA products were isolated and analyzed by scintillation counting for [^3H]-AdoMet incorporation and by Northern blot for total mRNA levels (Table 3). Cap methylation activity of each L mutant protein was expressed as a ratio of [^3H]-AdoMet incorporation into viral mRNA to the NP + P mRNA products (Table 3, columns 5 and 6). This normalization was done to account for variability in overall transcription levels between different viruses (Table 3, columns 3 and 4). This variability could be due to mutations specifically effecting viral mRNA synthesis or due to variability in the transcriptional activity of individual virion preparations (see below).

Unfortunately, a high-resolution analysis of cap structure in SeV mRNA is beyond our reach due to the more than 200-fold lower abundance of mRNA produced by SeV virion-associated L protein as compared to VSV. However, to confirm that [^3H]-labeled SeV mRNA (Table 3) had methylated cap structures, we analyzed [^3H]-AdoMet labeled mRNA generated as described above, using tobacco acid pyrophosphatase (TAP) (Fig. 12). TAP is commonly used to specifically remove the 5'-terminal guanosine

monophosphate from the cap of mRNA, while uncapped mRNA cannot serve as a substrate for the TAP (Shinshi et al. 1976). In addition to SeV mRNA, we used three different control mRNAs (described in detail in Materials and Methods): i) [^3H]-AdoMet labeled VSV mRNA generated using detergent-activated wt VSV virions using in vitro transcription conditions identical to SeV; ii) synthetic SeV NP mRNA containing Cap 0 ($\text{m}^7\text{GpppA}\dots$) structure labeled with [^3H] at the G-N7 position, and iii) synthetic SeV NP mRNA containing Cap 1 structure ($\text{m}^7\text{Gppp}[\text{m}^{2'-\text{O}}]\text{A}\dots$) labeled with [^3H]-AdoMet only at the 2'-O position (2'-O methylated by the vaccinia virus enzyme). For TAP analysis, all these mRNAs were normalized by [^3H] counts and digested by TAP (or mock-treated using the same conditions without TAP). Figure 12 shows [^3H] counts associated with the released 5'-terminal G (“ m^7G ”) or with mRNA after TAP treatment and separation using Sephadex G-50 columns. As expected, TAP treatment did not affect an association of [^3H] with the synthetic mRNA having Cap 1 structure ($\text{m}^7\text{Gppp}[\text{m}^{2'-\text{O}}]\text{A}\dots$) labeled only at the 2'-O position, but resulted in the release of [^3H]- m^7G from the synthetic Cap 0 mRNA labeled at the G-N7 position (Fig. 12), confirming that TAP specifically hydrolyzed the phosphoric acid anhydride bonds in the triphosphate bridge of the cap structure. Importantly, TAP treatment clearly resulted in the release of [^3H]- m^7G from SeV mRNA produced by detergent-activated virions in vitro, indicating that SeV mRNA was at least partially methylated at the G-N7 position. A similar result was obtained for VSV virion-produced mRNA, which is consistent with the previous studies demonstrating that the fully-methylated VSV mRNA has Cap 1 structure (Abraham et al. 1975; Testa and Banerjee 1977; Rahmeh et al. 2009).

Although our data (Fig. 12) demonstrate that SeV methylates its mRNA at least partially at the G-N7 position, at this point we cannot make any conclusions about cap structure of SeV mRNA produced under our experimental conditions. Figure 8 shows that TAP released more [³H]-m⁷G from SeV mRNA than from VSV mRNA, and similar amounts of [³H]-m⁷G were released from SeV mRNA and the synthetic Cap 0 mRNA, which could indicate that SeV was methylated exclusively at the G-N7 position. However, it would be premature to make this conclusion based solely on the TAP experiments. Thus, we did not observe a complete removal of [³H]-m⁷G from the synthetic Cap 0 mRNA labeled only at G-N7 position, indicating that under our experimental conditions TAP was only about 50% effective in hydrolyzing triphosphate bridges. Furthermore, mRNA products analyzed in Figure 12 were normalized by [³H] counts. However, it is likely that the efficiency of cap methylation is different for SeV, VSV and vaccinia virus MTases and, therefore, different molar amounts of capped mRNA were likely present in these reactions further complicating conclusions about cap structure. Further studies using alternative biochemical assays are needed to determine cap structure of SeV mRNA produced under our experimental conditions, although a dramatic improvement in our in vitro transcription conditions is needed to obtain sufficient amounts of viral mRNA for cap analysis. Most of the SeV L mutants of the DKDKD sequence had methylation levels similar to rWT, while rD1795A and rR1800A had about a 50% decrease in cap methylation compared to rWT. Consistent with our previous results, the SeV L mutant rG1804A/G1806A had only slightly decreased methylation compared to rWT and the rE1805A mutant had methylation levels about 23% of rWT. The other SeV L mutants of the glycine-rich motif all had lower levels of

methylation as compared to rWT ranging from about 10% for rY1802A and rG1804L to about 40% for rG1808A and rG1804A/G1806A/G1808A. Except for rS1777A, all SeV L mutants with substitutions in and around the KDKE tetrad (rK1782A, rD1901A, rE1903A, rK1938S, and rK1938A/I1939L) were severely defective in cap methylation (2-8% of rWT). In general, most of the SeV mutants defective in cap methylation were attenuated in Vero cells, indicating the importance of this function in the SeV life cycle. Interestingly, while rWT and most of our mutants showed only residual mRNA methylation in the presence of AdoHcy, this value was surprisingly high (12.5%) for rG1804A/G1806A. At this point, we do not have an explanation for this result, but it was consistently reproduced in several independent experiments. We cannot exclude an interesting possibility that this mutation improves the preference of L towards AdoMet over AdoHcy, making it less sensitive to the excess of this product. Further studies are needed to address this possibility.

Superinfection analysis.

To test whether SeV mutants with substitutions at different positions within domain VI could potentially complement each other when grown together, we infected Vero cells with various combinations of defective mutants at an MOI of 1 CIU/cell per virus (total MOI of 2). Under these conditions, most of the cells are co-infected with both viruses. In addition to viruses with the phenotypes described above, we included rWT and other mutants that behaved similarly to rWT as controls (rS1777A, rR1800A, rE1805A, rG1804A/G1806A/G1808A, and rY1977A). We did not see any increase in CPE when defective mutants were combined with other defective mutants (data not shown). Instead, when two of the defective mutants (rK1938S and rK1938A/I1939L)

were combined with rWT, we observed an inhibition of CPE with less cell rounding and cells remaining attached to the plastic (data not shown), suggesting they interfered with rWT replication. To investigate this observation further, we repeated the experiment looking at all SeV L methylation defective mutants in combination with rWT only (Fig. 13A). All combinations grew to titers comparable to supernatant collected from Vero cells infected with rWT only with the exception of K1938S and K1938A/I1939L which had 99% lower titers for rWT (rWT foci can be easily discriminated from those generated by mutants due to their significantly larger size and earlier appearance). We then compared growth kinetics of two mutants, K1938S and K1782A in combination with rWT by infecting Vero cells and collecting supernatants at 18-72 h p.i. Similar to our titration experiments (Fig. 13A), K1782A when combined with rWT had similar growth kinetics to rWT alone while K1938S in combination with rWT had delayed growth and lower maximal titers (Fig. 13B), indicating that cap methylation defect alone is not sufficient for the interference of rK1938S and rK1938A/I1939L with rWT replication and that some additional factors are involved in the dominant negative phenotype of these SeV mutants. At this time, we cannot explain why viruses containing aa substitution at the L position 1938 interfere with rWT replication. One possibility is that such inhibition may simply reflect elevated levels of DI particles generated by these mutants. To test this hypothesis, we infected Vero cells again (as in Fig. 13A), collected cells and the medium at 48 h p.i. Consistent with Figure 10A, both rK1938S and rK1938A/I1939L inhibited production of rWT as was determined by titration of the collected medium on fresh Vero cells (Fig. 13B). For analysis of RNA synthesized during superinfection, both collected supernatants and cells were analyzed by Northern blot as described in Materials and

Methods. To detect DI genomes, a probe complimentary to the first 54 5'-nucleotides of the SeV genomic RNA was used, which should be able to detect full-length genomic RNA of SeV as well as DI genomes independent on the mechanism of their generation. As shown in Figure 13D, we were unable to detect any DI genomes in Vero cells under our experimental conditions. Interestingly, despite clear inhibition of SeV rWT virion production (Fig. 13A-C), we did not see any statistically significant decrease in SeV NP mRNA accumulation in the superinfected cells (Fig. 13E) using a probe against coding NP gene sequences, although a modest decrease in the full-length genomic RNA (wt plus mutant) levels was observed (Fig. 13D, FL gRNA band). A similar lack of DI genomes and a very modest reduction in full-length genomic RNA levels was observed when virus particles from the medium were pelleted by ultracentrifugation, and RNA from these particles was analyzed by Northern blot as above (data not shown). Together, our data suggest that rK1938S and rK1938A/I1939L are able to over-compete rWT during superinfection and, while the mechanism is unclear, this effect is apparently DI-independent.

Role of SeV mRNA cap methylation in antiviral responses in primary cell cultures.

Cap methylation defective viruses (VSV, SeV, or any other *Mononegavirales*) have never been tested in any animal system or primary cells. It has been well established that methylation of the 5' cap at the G-N7 position is absolutely required for efficient translation, but significance of methylation at the 2' *O*-ribose has remained unclear (Daffis et al. 2010; Zust et al. 2011). Recent studies have demonstrated that the presence or absence of 2' *O*-ribose methylation has an evolutionary basis and plays a role in distinguishing self from non-self mRNA (Daffis et al. 2010; Zust et al. 2011). Therefore

several viruses have evolved strategies for ensuring that their viral mRNAs are capped and methylated, mimicking host mRNAs and evading antiviral responses (Daffis et al. 2010; Züst et al. 2011). Two separate research groups demonstrated that lack of 2' *O*-ribose methylation in positive strand RNA viruses led to increased immune responses in host cells thus indicating the importance of methylation at this position of the mRNA cap structure (Daffis et al. 2010; Züst et al. 2011). The relationship between 2' *O*-ribose cap methylation and host immune responses in negative strand RNA viruses has not been explored. We analyzed the ability of infectious recombinant SeV mutants with varying defects in viral cap methylation to infect and replicate in primary mouse fibroblasts (MEFs). It is important to note that our SeV mutants have been characterized for their ability to produce cap structures with or without methylation however due to limitations in our assays we have not been able to characterize whether defects occur at the 2' *O*-ribose, G-*N7* or both positions of the cap structure. To evaluate the significance of general cap methylation in SeV infection, MEFs, wt as well as several cell types that are deficient in immune components important for antiviral responses against RNA viruses (RIG-I KO, MDA5 KO, IRF3 KO, IRF7 KO), were used. Three SeV mutants were selected based on our described cap methylation studies: (i) the rK1782A virus which is completely defective in viral mRNA cap methylation (a single K to A substitution in the putative *KDKE* catalytic tetrad of the L protein), (ii) the rE1805A virus with intermediate levels of cap methylation (a single E to A substitution in the glycine-rich motif *GEGAG* of the L protein), or (iii) the rG1806A virus with wt levels of cap methylation (a single G to A substitution in the glycine-rich motif *GEGAG* of the L protein).

Monolayer cultures were infected with SeV wt and mutants at an MOI of 10 CIU/cell. Twenty-four h p.i. supernatant was collected, cell lysates were prepared and RNA was isolated. Supernatant was analyzed for infectious virus particles budding from the cells by standard plaque assay on Vero cells (Fig 14). In general, rK1782A and rE1805A were more attenuated in all cell types compared to wt and rG1806A. Interestingly, all viruses were able to replicate to higher titers in the RIG-I KO MEFs compared to all other cell types. Western blots were performed to analyze viral protein expression levels and induction of ISGs as a downstream indicator of recognition of SeV. In wt MEFs and IRF7 KO MEFs, rE1805A had lower viral protein expression than the other SeV. In MDA5 KO MEFs, rK1782A had lower viral protein expression than the other SeV. And in RIG-I KO and IRF3 KO MEFs, viral protein expression for all SeV mutants was comparable (Fig 15A). We also analyzed lysates for expression of the interferon-stimulated gene ISG56/IFIT-1 to examine if certain cell types have increased expression following infection with cap methylation defective SeV. As expected, ISG56/IFIT-1 was not expressed in RIG-I and IRF3 KO MEFs and for the other cell types there was no difference in expression when infected with any of the tested SeV (Fig 15B). Overall, in our preliminary experiments we did not observe any increased immune responses to SeV mutants lacking cap methylation in wt MEFs. However, in MEFs lacking the viral RNA sensor, RIG-I, viral protein expression was equivalent for all mutant viruses and the wt virus which indicates that RIG-I possibly plays a role in detecting viral RNA lacking specific cap methylation. Future experiments are needed to further investigate the importance of RIG-I in the recognition of SeV mRNA lacking 2'-O-ribose methylation.

2.4 Conclusions

In this study, we conducted site-directed mutagenesis of the SeV L polymerase protein by targeting several aa residues within the L domain VI, homologous to those previously shown to be important for mRNA cap methylation in VSV (Grzelishvili et al. 2005; Li et al. 2005; Grzelishvili et al. 2006; Li et al. 2006). The present study is the first mutagenic analysis of the L protein domain VI conducted for any *Mononegavirales* other than VSV. In addition to the VSV L protein domain VI, a previous study identified a new region between VSV L aa 1450-1481 which was critical for mRNA cap methylation (Grzelishvili et al. 2005; Grzelishvili et al. 2006). However, we did not find any significant homology between rhabdo- and paramyxoviruses in this variable region between conserved domains V and VI, and in this study we targeted only those aa that were homologous between VSV and SeV. Therefore, we initially set out to generate six mutant SeV L genes: K1782A, G1804A, E1805A, E1805V, G1806A, and a double mutant G1804A/G1806A; in addition, we made the L- Δ VI mutant with a deletion of the entire domain VI to confirm that the SeV L protein has similar sensitivity to a loss of this region as previously shown for the VSV L protein (Canter and Perrault 1996).

When these mutant proteins were tested for their ability to synthesize mRNA using a VV-T7 expression system, we found that, while most mutants retained normal RNA polymerase activity, two mutants, L-E1805V (but not L-E1805A) and L- Δ VI, were completely inactive. The loss of activity in L- Δ VI was not surprising as an even smaller deletion within domain VI abolished RNA synthesis by the VSV L protein as a result of an inability of this mutant to form the P-L complex required for normal L RNA polymerase activity (Canter and Perrault 1996). Unlike mRNA capping, which is tightly

coupled with mRNA transcription, viral mRNA synthesis proceeds with a similar efficiency in the absence or presence of the methyl group donor, AdoMet (Abraham et al. 1975), and, therefore, cap methylation is not required for mRNA synthesis in *Mononegavirales*. Thus, we think that the inactivation of L- Δ VI transcription had no relation to the cap methylation function of this protein but that the deletion negatively affected the overall conformation of the L protein resulting in a defect in P protein binding (Canter and Perrault 1996) or other functions important for normal L protein RNA polymerization activity. The inactivation of the L-E1805V protein was more surprising as a similar substitution in the VSV *hr1* mutant (D1671V), while abolishing cap methylation, had no effect on VSV mRNA synthesis (Grzelishvili et al. 2005). It is likely that the aa substitution in the L-E1805V protein negatively affected L protein folding resulting in a complete inactivation of this protein.

All mutations that passed the *in vitro* transcription test were cloned into the SeV full-length infectious cDNA plasmid, and initially, recombinant infectious viruses r1782A, r1804A, r1805A, r1806A, and a double mutant rG1804A/G1806A were successfully recovered and characterized. We conducted a phenotypic and biochemical analysis of these mutants using VSV *wt* and *hr1* recombinant viruses as convenient positive and negative controls, respectively, for the *hr* and *ts* virus growth phenotypes and mRNA cap methylation activities.

First, we conducted the phenotypic analysis of SeV mutants by testing their relative growth at 34°C in Vero against HEp-2 cells by virus titration or by multistep growth kinetics analysis using these cell lines. Previous studies linked the inability of VSV cap methylation defective mutants to grow in HEp-2 cells to a viral defect in

mRNA cap guanine-*N7* methylation and consequent nontranslatability of primary VSV transcripts (Horikami and Moyer 1982; Horikami et al. 1984; Grdzlishvili et al. 2005; Grdzlishvili et al. 2006). It was also suggested that host cells methylate viral mRNA in permissive cell lines through an unknown mechanism (Horikami et al. 1984). It should be noted that VSV *hr1*, while unable to grow in HEp-2 cells, was also attenuated in Vero cells (titer on Vero cells: 2.4×10^9 CIU/ml for VSV wt against 6.0×10^7 for VSV *hr1*). Therefore, while a Vero/HEp-2 titer ratio could serve as a good indicator of a possible defect in cap methylation (e.g., for VSV *hr1*), we expected an attenuation of cap methylation defective SeV mutants in both, Vero and HEp-2, cells. In agreement with a possible role of the lysine 1782 as an active site of the L protein MTase domain, the SeV r1782A mutant was attenuated in both, Vero and HEp-2 cells and showed a *hr* phenotype with a Vero/HEp-2 titer ratio of 100 (compared to 2.3 for rWT). Given the importance of the glycine-rich motif in VSV and other MTases and the homology of the substituted aa in SeV to those shown to be critical for guanine-*N7* methylation in VSV (Grdzlishvili et al. 2005; Li et al. 2005; Grdzlishvili et al. 2006; Li et al. 2006), we expected that all other tested SeV mutants would also be *hr* restricted. To our surprise, most of the mutant viruses with aa substitutions in the glycine-rich motif grew normally not only in Vero but also in HEp-2 cells indicating that they were not defective in cap methylation. r1805A displayed slow growth in both Vero and HEp-2 cells with about a 24 h delay in infectious foci formation and noticeably smaller foci on both Vero and HEp2 cells. However, we did not observe differences in the relative ability of r1805A (or r1805A-GFP) to grow on HEp-2 cells versus Vero cells by CIU counts indicating that r1805A retained at least some MTase activity.

We also tested SeV mutants for their temperature sensitivity in Vero cells at 34°C against Vero cells at 40°C. Although *ts* phenotype alone could not indicate whether SeV mutations affected viral MTase activities, our previously tested VSV mutants defective in cap methylation were also *ts* (Grzelishvili et al. 2005; Grzelishvili et al. 2006). Again, most of the initially tested SeV mutants were not *ts* with the exception of r1782A and r1805A displaying a clear *ts* phenotype similar to that of VSV *hr1*. Together, our phenotypic analysis of recombinant SeV mutants identified only one mutant, r1782A, that behaved similarly to VSV *hr1* (*hr* and *ts*) indicating that all other tested SeV L mutants retain at least some cap methylation function.

To directly test SeV mutants for their MTase function, we conducted mRNA cap methylation analyses using an in vitro transcription assay with detergent-activated SeV virions and tested viral mRNA products for the presence of methyl groups. Unfortunately, in contrast to our previous VSV studies (Grzelishvili et al. 2005; Grzelishvili et al. 2006), we were unable to conduct a very detailed analysis of the SeV cap structure because of very low levels of viral mRNA produced in vitro (about 200-fold less viral mRNA compared to VSV in vitro transcription system). Nevertheless, our assays (supported by the described virus growth analysis) allowed us to make general conclusions about cap methylation function in all tested SeV mutants. Thus, consistent with the described phenotypic analyses, the r1782A mutant was completely defective in cap methylation, while r1805A displayed about a 60% decrease in cap methylation. Our data is the first study experimentally supporting the previous computational predictions (Bujnicki and Rychlewski 2002; Ferron et al. 2002) suggesting the importance of the

invariant lysine (position 1782 in the SeV L protein) and the glycine-rich motif in different *Mononegavirales*.

The invariant lysine (L position 1782 in the SeV, 1651 in VSV) is conserved in most *Mononegavirales*, is also present in the known 2'-*O* cap MTases including NS5 protein of flaviviruses (Fig. 5) and nonstructural protein 16 of coronaviruses (Decroly et al. 2008), and was predicted to be the first lysine within so called KDKE tetrad catalyzing an S_N2-reaction-mediated 2'-*O* methyl transfer in 2'-*O* MTases (Hodel et al. 1998; Egloff et al. 2002; Hager et al. 2002). In West Nile virus (WNV, a flavivirus), a similar substitution of K61A (K61 is a putative functional analog of K1782 in SeV L) in the NS5 protein, which also carries both guanine-*N*7 and ribose 2'-*O* MTase activities, specifically inhibited 2'-*O* cap methylation (Ray et al. 2006; Zhou et al. 2007). In contrast, the K1782A mutation in SeV L (this study) and the previously analyzed VSV K1651A (homologous to SeV K1782A) substitutions abolished both G-*N*7 and 2'-*O* methylation (Li et al. 2005). This discrepancy between WNV and *Mononegavirales* can be explained by the different order of cap methylation previously shown for flaviviruses (GpppA → m7GpppA → m7GpppAm) (Zhou et al. 2007) and proposed for VSV (GpppA → GpppAm → m7GpppAm) (Testa and Banerjee 1977; Li et al. 2006). While the inactivation of 2'-*O* methylation by substitution of the catalytic lysine (K61) could not affect G-*N*7 methylation in WNV due to the order of cap methylation (Ray et al. 2006; Zhou et al. 2007), it prevented G-*N*7 methylation in VSV (Li et al. 2006) and in SeV (K1782A mutation in this study), suggesting that paramyxoviruses may use the same order of cap methylation as VSV. It is important to note that that the cap methylation order for *Mononegavirales* is still controversial with some evidence pointing to both

orders. The *in vitro* results using detergent-activated VSV (Indiana strain) virions proposed the following order of MTase reactions: GpppA + AdoMet (low concentration) → GpppAm + AdoMet (high concentration) → 7mGpppAm (Testa and Banerjee 1977; Li et al. 2006). However, the previous *in vivo* data on VSV (Indiana strain) mRNA synthesis in the presence of the methylation inhibitor cycloleucine (Moyer 1981) and *in vitro* transcription data on VSV New Jersey serotype (Hammond and Lesnaw 1987) suggest that the reverse order of VSV mRNA methylation (GpppA → 7mGpppA → 7mGpppAm) can also occur. Moreover, a previous study showed that SeV produces mRNAs methylated at both the G-N7 and 2'-*O*-adenosine positions or at G-N7 only (7mGpppA), but did not detect any mRNAs methylated only at the 2'-*O*-adenosine position (Takagi et al. 1995). Finally, a previous study showed that Newcastle disease virus (NDV), another paramyxovirus, produces viral mRNAs that are not 2'-*O*-methylated at all (Colonno and Stone 1976).

While our results show clear similarities between VSV K1651A and SeV K1782A mutants (both completely defective in cap methylation), the aa substitutions in the L protein glycine-rich motif had milder (E1805A) or non-significant effects (G1804A and G1806A) on viral mRNA cap methylation. Generally, this region, especially the second glycine residue (G1806 in the SeV L), is sensitive to aa substitutions as demonstrated in VSV and many other known AdoMet-dependent MTases (Martin and McMillan 2002), including cap mRNA MTases of vaccinia virus (Mao and Shuman 1996; Saha et al. 2003), reovirus (Luongo et al. 1998) and eukaryotic cells (Wang and Shuman 1997; Yamada-Okabe et al. 1999). The previously characterized VSV mutants with homologous changes in the glycine-rich motif showed the following cap

methylation phenotypes: 1) VSV G1670A (homologous to SeV G1804A): <1 to 20% for guanine-*N7* (depending on in vitro conditions) and about 40% overall methylation compared to wt VSV (Li et al. 2006); 2) VSV D1671V [similar to E1805V (not rescued) and E1805A]: <1% for G-*N7* and 2'-*O* methylation compared to wt VSV (Grdzlishvili et al. 2005; Li et al. 2006); 3) VSV G1672A [similar to SeV G1806A]: <1 to 20% for G-*N7* (depending on in vitro conditions) and about 40% overall compared to wt VSV (Grdzlishvili, Smallwood et al. 2006; Li, Wang et al. 2006). Although VSV G1670A and G1672A mutants retained a substantial 2'-*O* MTase activity, they were severely inhibited for their G-*N7* MTase activity (Li et al. 2006). Importantly, under the in vitro conditions similar to those utilized in this study, these VSV mutants showed no detectable G-*N7* methylation, while SeV G1804A and G1806A did not significantly affect G-*N7* or 2'-*O* cap methylation. The tolerance of SeV L protein to aa substitutions G1804A and G1806A is also supported by the fact that double substitution G1804A/G1806A had little effect on virus growth or mRNA methylation in vitro. Interestingly, we found that, while both r1804A and r1806A had normal mRNA synthesis and cap methylation, they behaved very unusually during multistep growth in HEp-2 cells with r1804A growing considerably faster than rWT and r1806A slower than rWT. The presence of both mutations in r1804A/1806A produced an intermediate growth phenotype suggesting that these mutations had a reciprocal effect when present together. Further experiments are needed to elucidate molecular basis for the differences between r1804A and r1806A in HEp-2 cells.

While we still do not understand the exact mechanism of *hr* restriction of cap methylation mutants of VSV, the *hr* analysis of SeV mutants justifies future use of this

approach as a supporting assay to determine cap methylation status of SeV mutants in addition to the direct cap methylation analysis. Thus, although none of the tested SeV mutants showed Vero/HEp-2 titer ratio as dramatic as in VSV *hr1* (more than 60,000), the only SeV mutant with asymmetric attenuation in HEp-2 was the rK1782A virus (with Vero/HEp-2 ratio of 100), and this mutant was also completely defective in cap methylation. The only other SeV mutant attenuated in HEp-2 cells (although equally in Vero cells) was r1805A, which also showed 60% reduction in cap methylation. Therefore, while the ability of a mutant (VSV or SeV) to grow in HEp-2 cells may not be sufficient by itself to determine methylation status of viral mutants, our data on SeV r1782A and r1805A mutants show that this assay can be successfully used to complement an *in vitro* cap methylation analysis of the SeV mutants.

Although we did not find dramatic differences between SeV r1804A, r1806A, r1804A/1806A and rWT using our experimental conditions, the wt glycine-rich motif sequence may be beneficial during normal viral infection, and we believe that there must be some evolutionary basis for sequence conservation of this motif among paramyxoviruses and *Mononegavirales* in general. To further analyze the importance of L protein domain VI of paramyxoviruses we performed a more detailed sequence-function analysis.

We conducted site-directed mutagenesis targeting the residues highly conserved among *Mononegavirales*, including the KDKE tetrad and glycine-rich motif. Similar to VSV, alanine substitutions in the putative KDKE catalytic tetrad of SeV generated mutant viruses defective in cap methylation. Our data also confirms the importance of the glycine-rich motif (putative AdoMet binding site of domain VI) in SeV cap methylation

but with different effect of mutations in the glycine-rich motif in SeV as compared to VSV. For VSV, it was shown that virions with alanine substitutions at the first two glycines had decreased cap methylation, while alanine substitution at the third glycine did not affect MTase activity (Li et al. 2006). Here, we determined that the third glycine of the glycine-rich motif seems to play a more significant role in cap methylation in SeV than VSV, decreasing cap methylation by about 70% (compared to rWT). As further confirmation of the importance of this position, a triple mutant with all three glycines substituted to alanines also had low methylation levels (37% of rWT) while a double mutant with only the first two glycines substituted to alanines had rWT-like levels of growth and higher methylation. Our initial results described above, showed so much tolerance to substitution in the first two glycines in the glycine-rich motif as to even doubt that this is a functional AdoMet-binding site. Our further analysis of the glycine-rich motif, including the role of the third glycine in the SeV cap methylation and dramatic effect of glycine to leucine substitutions in this motif restore a more conventional view of the role of this conserved sequence motif.

Another mutation resulting in defective cap methylation (10% of wt SeV) and virus attenuation was Y1802A. This residue has never been studied before in any *Mononegavirales* and is highly conserved in most paramyxoviruses. It possesses a hydroxyl group and may substitute for the aspartic or glutamic acid residues frequently found in the middle of the first beta-strand of the Rossmann fold. It has been proposed (Kozbial and Mushegian 2005) that the side chain of this residue makes either direct or water molecule-mediated contact with the methionine portion of AdoMet and may be directly involved in catalysis. In several paramyxoviruses, just next to this residue there is

a motif DKDKD1799 with potential importance in catalysis due to the high concentration of aspartates and lysines and its close proximity to the glycine-rich motif. We targeted these positions for substitution to alanines, but all these SeV L mutants were easily recovered, grew to high titers with similar kinetics to rWT in Vero cells and had high levels of cap methylation.

Consistent with the role of cap methylation in the translatability of mRNA, SeV mutants with decreased methylation (<10%) were attenuated in Vero cells. The majority of these mutants had substitutions in and around the putative KDKE catalytic tetrad. In agreement with our initial study, we observed that alanine substitutions at positions in and around the glycine-rich motif were well tolerated; however, a triple mutant with all three glycines replaced with alanines did show slight attenuation, confirming the importance of this motif for SeV L function and virus replication. We also observed that two cap methylation defective mutants, rK1938S and rK1938A/I1939L, had strong interfering effect on replication of wt SeV during superinfection. Interestingly, another cap methylation defective mutant, rK1782A, did not interfere with rWT replication indicating that cap methylation defect alone is not sufficient for this dominant-negative mutant phenotype and that some additional factors are involved. Currently, we cannot explain how K1938S mutation could inhibit the growth of rWT and further studies are warranted to explore this interesting observation.

Interestingly, a single alanine substitution at the putative catalytic K1938 position was successfully introduced into plasmids containing the SeV L gene and the full-length antigenome of SeV. However, when infectious virus particles, recovered using a reverse genetics system, were sequenced, the substitution was to serine rather than alanine. Based

on the importance of this position in the catalytic tetrad, we speculate that the change to the polar serine residue led to a more favorable configuration of hydrogen bond network linking catalytic residues to AdoMet and perhaps additionally supporting proper conformation of the L protein, which may be important for its function. When tested in a VV-T7 in vitro transcription or replication systems, the K1938A mutant L had slightly lower transcription (~80%) and lower replication levels (~60%) as compared to rWT. Mutant virions with the K1938S substitution were defective in cap methylation (8% of rWT), but had high transcription levels (91% of rWT): apparently, a serine substitution is more favorable for the overall activity of the L protein (although not necessarily for cap methylation).

We propose two main theories explaining the tolerance of the SeV L protein to the G1804A, G1806A and double G1804A/1806A substitutions. First, it is possible that, despite a homology between VSV and SeV at the glycine-rich motif, this region is not an AdoMet-binding site in SeV and possibly other paramyxoviruses, and that an actual AdoMet-binding site could be located at a different position in the SeV L protein. Importantly, even in VSV, a putative role of this motif as an AdoMet-binding site was postulated based on computational predictions and site-directed mutagenesis studies, but no experimental biochemical data are available to date for the L protein of any *Mononegavirales* directly demonstrating that this or any other L region actually binds AdoMet. While a different AdoMet-binding site location in SeV and VSV is a possibility, the complete inactivation of L cap methylation by K1782A (the first lysine of the catalytic KDKE tetrad in 2'-O MTases is generally positioned upstream and in a close proximity to the AdoMet-binding site) and about 60% decrease in methylation by

E1805A support another hypothesis that, while the glycine-rich motif is likely to be the SeV L protein AdoMet-binding site, SeV and possibly other paramyxoviruses are far more flexible than VSV to the aa substitutions in this motif. Such tolerance may explain why, while most *Mononegavirales*, including VSV and SeV, have the motif G(D/E)G(S/A)G (glycines important for VSV cap methylation are underlined; Fig. 1), more variation in this motif can be found in the members of the family *Paramyxoviridae*, especially in the genera *Rubulavirus* (subfamily *Paramyxovirinae*) and *Avulavirus* (subfamily *Pneumovirinae*), which have the motif AEG(S/A)G very similar to the sequence in our mutant SeV r1804A (AEGAG). Interestingly, the avian pneumovirus L protein has a motif AEASG which is similar to our double mutant SeV r1804A/1806A (AEAAG), which had a wt growth phenotype and normal mRNA cap methylation pattern. Previously, Li *et al.* (Li, Wang et al. 2006) speculated that these differences at the glycine-rich motif between NDV (genus *Avulavirus*) and VSV may account for the differences of these viruses in cap methylation pattern [the NDV caps are not 2'-O-methylated at all (Colonno and Stone 1976)]. However, our data suggest that these sequence variations among paramyxoviruses reflect their tolerance to aa substitutions and are not functionally important as r1804A, r1806A and r1804A/1806A mutants displayed a normal cap methylation pattern.

Despite some observed differences between VSV and SeV (more tolerance of SeV to aa substitutions in the glycine-rich motif), our results do clearly show the importance of the putative KDKE catalytic tetrad and glycine-rich motif, thus confirming previous computational predictions that these regions are important for MTase function

across different families of the order *Mononegavirales* (Bujnicki and Rychlewski 2002; Ferron et al. 2002; Martin and McMillan 2002).

Cap methylation defective viruses (VSV, SeV, or any other *Mononegavirales*) have never been tested in any animal system or primary cells. Our preliminary analysis of select SeV mutants in primary MEFs demonstrate attenuation in wt MEFs which could indicate that these mutants lack 2'*O*-ribose methylation. Recent studies have demonstrated that the presence or absence of 2'*O*-ribose methylation plays a role in distinguishing self from non-self mRNA (Daffis et al. 2010; Zust et al. 2011). Therefore several viruses have evolved strategies for ensuring that their viral mRNAs are capped and methylated, mimicking host mRNAs and evading antiviral responses (Daffis et al. 2010; Zust et al. 2011). Two separate research groups demonstrated that lack of 2'*O*-ribose methylation in positive strand RNA viruses led to increased immune responses in host cells thus indicating the importance of methylation at this position of the mRNA cap structure (Daffis et al. 2010; Zust et al. 2011). Our SeV mutants have been characterized for their ability to produce cap structures with or without methylation however due to limitations in our assays we have not been able to characterize whether defects occur at the 2'*O*-ribose, G-N7 or both positions of the cap structure. Interestingly, although the r1782A mutant was attenuated in wt MEFs, protein expression levels in these cells was similar to rWT and r1806A while r1805A had lower protein levels. This could indicate that r1805A, which exhibits intermediate levels of cap methylation, could be defective in 2'*O*-ribose methylation and the cells are recognizing this defect and mounting a robust antiviral response against this mutant. It is unclear at this time why r1782A which is completely defective in cap methylation did not have lower viral protein levels than the

rWT and r1806A viruses that have normal cap methylation function. When cells infected with these viruses were analyzed for ISG56/IFIT-1 expression, an IFN-stimulated gene and a downstream indicator of an antiviral response, there was no difference in protein levels at the 24 h p.i. time point in wt MEFs. SeV cap methylation defective mutants grew to higher titers in RIG-I KO primary MEFs (but still lower than rWT in RIG I KO MEFs). Analysis of viral protein expression in RIG-I KO MEFs showed similar protein levels for all viruses which could indicate a role for RIG-I in detecting cap methylation defective mutants. Future experiments are needed to further investigate the importance of RIG-I in the recognition of SeV mRNA lacking 2' *O*-ribose methylation.

Future experiments will include a comparative pathogenesis study in mice (the natural host for SeV) to determine the role of the mutated aa residues during normal infection and thus to understand why the glycine-rich motif is conserved in paramyxoviruses (and other *Mononegavirales*) if it can be mutated without serious consequences to virus fitness. Mutants defective in cap methylation could possibly be attenuated in vivo, however it is unclear if infectious viruses carrying these specific mutations will exhibit any unusual tissue specificity as compared to their wt counterpart. In addition to better understanding the biology of these viruses, these experiments would have important practical implications because targeting aa residues critical for cap MTase function in VSV, SeV and other *Mononegavirales* could be used to rationally attenuate these viruses (or manipulate their *hr*) for development of live attenuated viruses and their use as vaccine (Bukreyev et al. 2006), oncolytic (von Messling and Cattaneo 2004) and gene therapy (Finke and Conzelmann 2005) vectors.

Figure 5 continued. SeV L protein mutants generated and analyzed in this study. Multiple alignment of the L protein domain VI for members of the order *Mononegavirales* in comparison to the MTase domain of NS5 protein in flaviviruses. Multiple alignment was conducted using AliBee Multiple Alignment program from the GeneBee website (www.genebee.msu.su/genebee.html) [25]. The K-D-K-E and glycine-rich motif mutated positions are highlighted in black, while gray shadows indicate other amino acid substitutions generated in this study. “SeV”: Sendai virus L protein [NCBI gene ID (gi):297180]; “HPIV1 or 3”: human parainfluenza virus 1 [gi:19718373] or 3 [gi:3510306]; “CDV”: canine distemper virus [gi:39938470]; “Nipah”: Nipah virus [gi:253559849] “MV”: measles virus [gi:1041625] “RV”: Rinderpest virus [gi:56410436] “NDV”: Newcastle disease virus [gi:11545725]; “HPIV2”: human parainfluenza virus 2 [gi:19525727]; “Mumps”: mumps virus [gi:50404170] “SV41”: Simian virus 41 [gi:55770827]; “HMPV”: human metapneumovirus [gi:46852141]; “RSV”: human respiratory syncytial virus [gi:1695266]; “VSV”: vesicular stomatitis virus [gi:336028] “Rabies”: rabies virus [gi:237688385] “Ebola”: Ebola virus [gi:10313999] “Marburg”: Marburg virus [gi:158539115]; 2NYU – ortholog of RNA MTase FtsJ [gi:119390696]; “WNV”: West Nile virus [gi:27735310] “JEV”: Japanese encephalitis virus [gi:189086643] “Dengue”: Dengue virus 2 [gi:158851624].

2.5 Figure 6

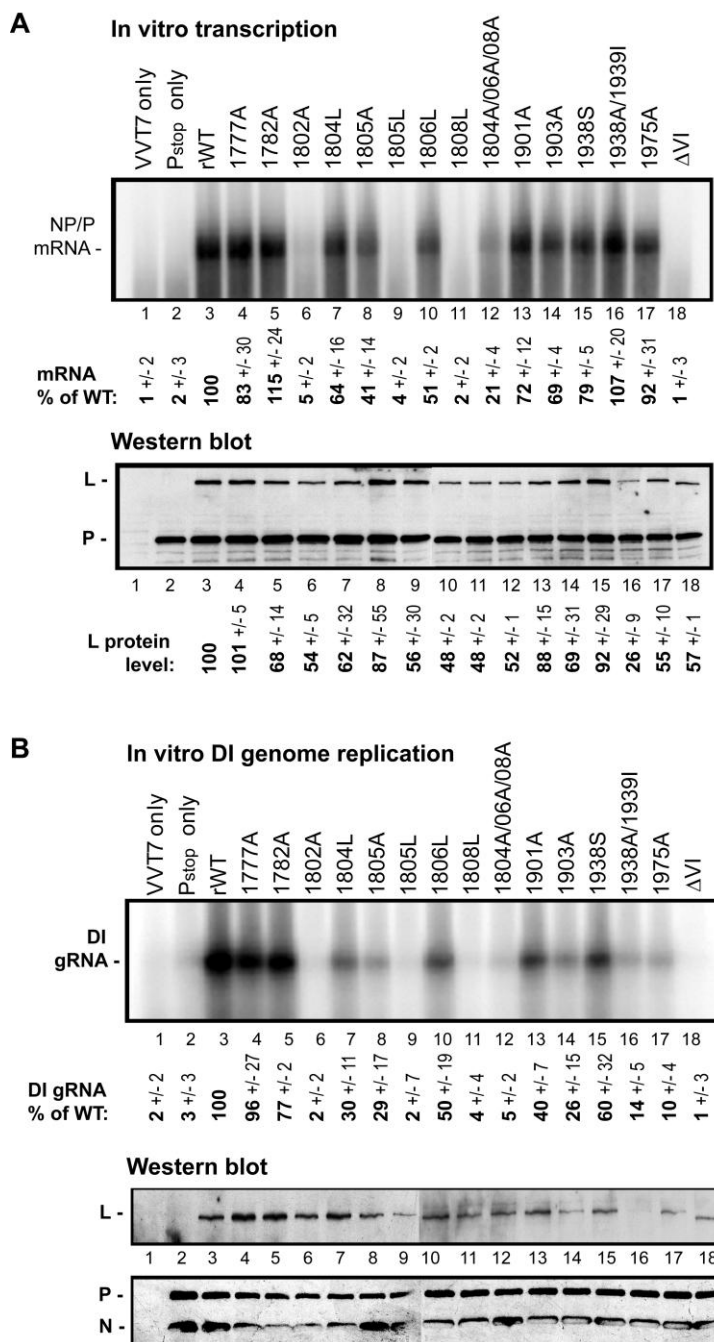


Figure 6. In vitro mRNA synthesis and genome replication with SeV mutant L proteins using a VVT7 expression system. Plasmids expressing P and wt or mutant L proteins were transfected into VV-T7 infected A549 cells. N protein was also expressed for DI replication. Total RNA was isolated from cell lysates and in vitro transcription (A) or DI replication (B) reactions were performed in the presence of [α^{32} P]-CTP. Western blot analyses of cell lysates used in (A) or (B) demonstrate relative expression of the SeV L, P and N (for DI replication) proteins in A549 cells. Transcription and DI replication data represent the mean \pm standard deviation of two independent experiments.

2.5 Figure 7

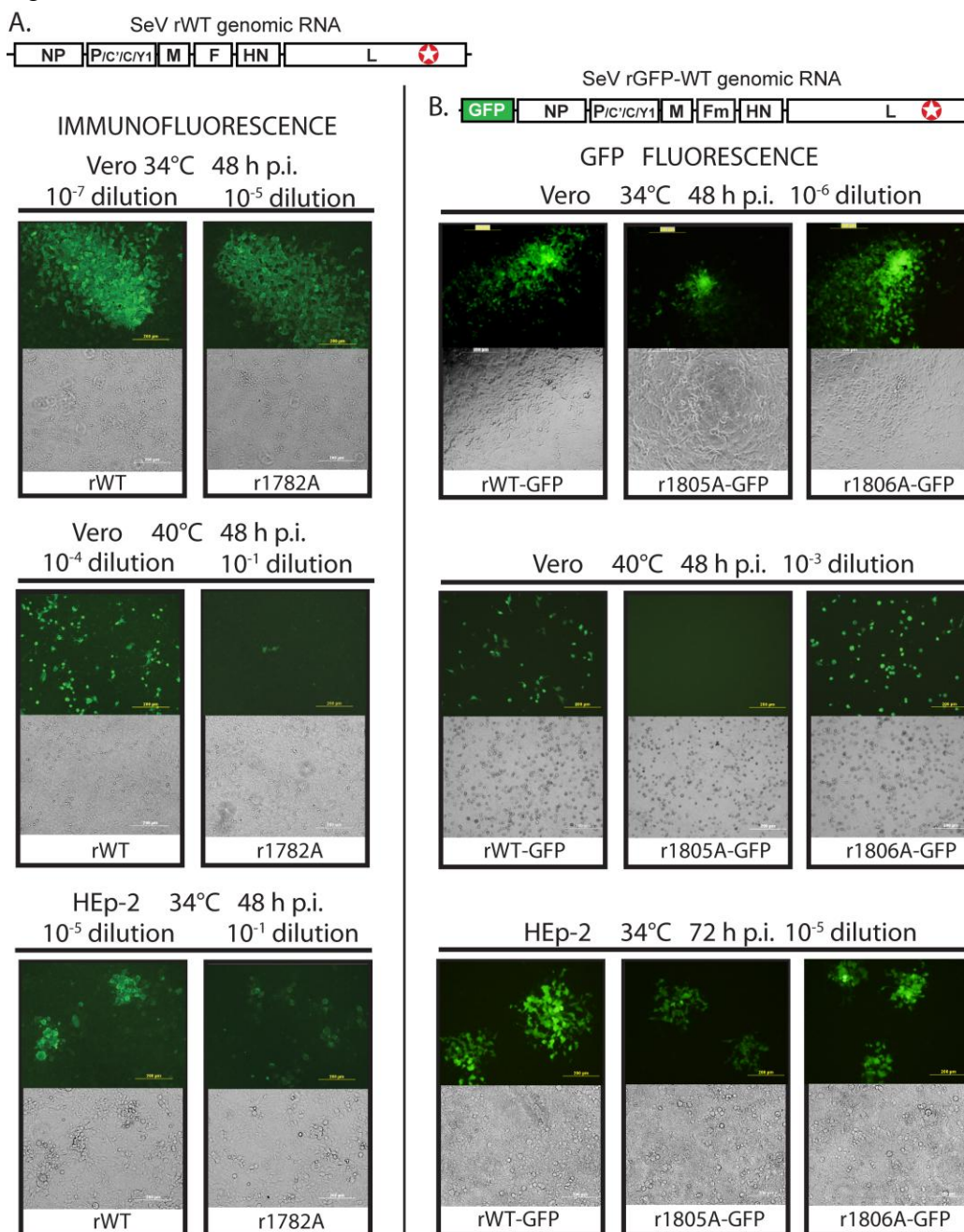


Figure 7. Host range and temperature sensitivity analysis of SeV mutants. (A) IF infectious focus assay to analyze SeV r1782A (compare to SeV rWT) for *hr* and *ts* phenotypes. Virus infectious foci were visualized by IF using anti-SeV antibodies and IgG-FITC secondary antibodies on fixed and permeabilized Vero or HEp-2 cells infected with SeV r1782A or rWT at 34°C or 40°C. (B) GFP fluorescence focus assay to analyze SeV rWT-GFP, r1805A-GFP and r1806A-GFP viruses encoding the GFP gene upstream of the NP gene for *hr* and *ts* phenotypes. Assays were done on Vero or HEp-2 cells at 34°C or 40°C. Virus infectious foci were visualized by microscopy at 48 or 72 h p.i. as indicated using fluorescence (upper panels) or bright-field (lower panels) channels.

2.5 Figure 8

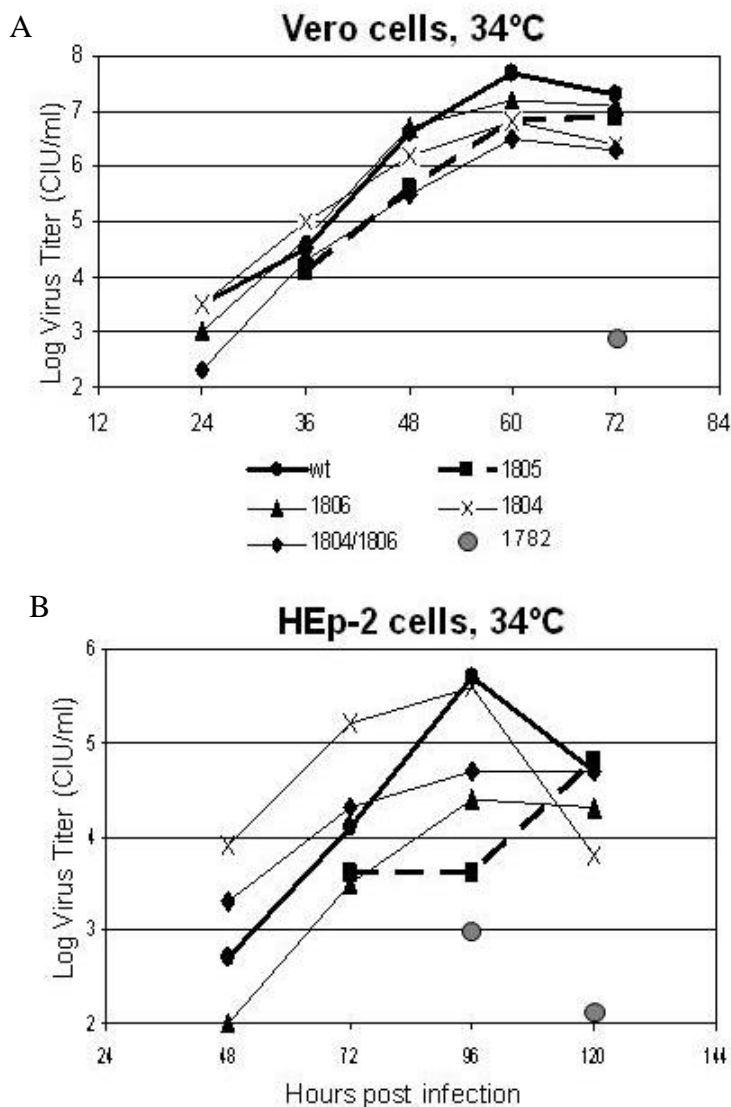


Figure 8. Multistep growth kinetics of wt and recombinant SeV in Vero and HEp-2 cells at 34°C. SeV wt or recombinant viruses were used to infect (A) Vero or (B) HEp2 cells at MOI 0.001 CIU/cell. Supernatants were harvested at 12 h (A) or 24 h (B) intervals and flash frozen. Supernatants were assayed on Vero cells and virus titers were determined for each time interval.

2.5 Figure 9

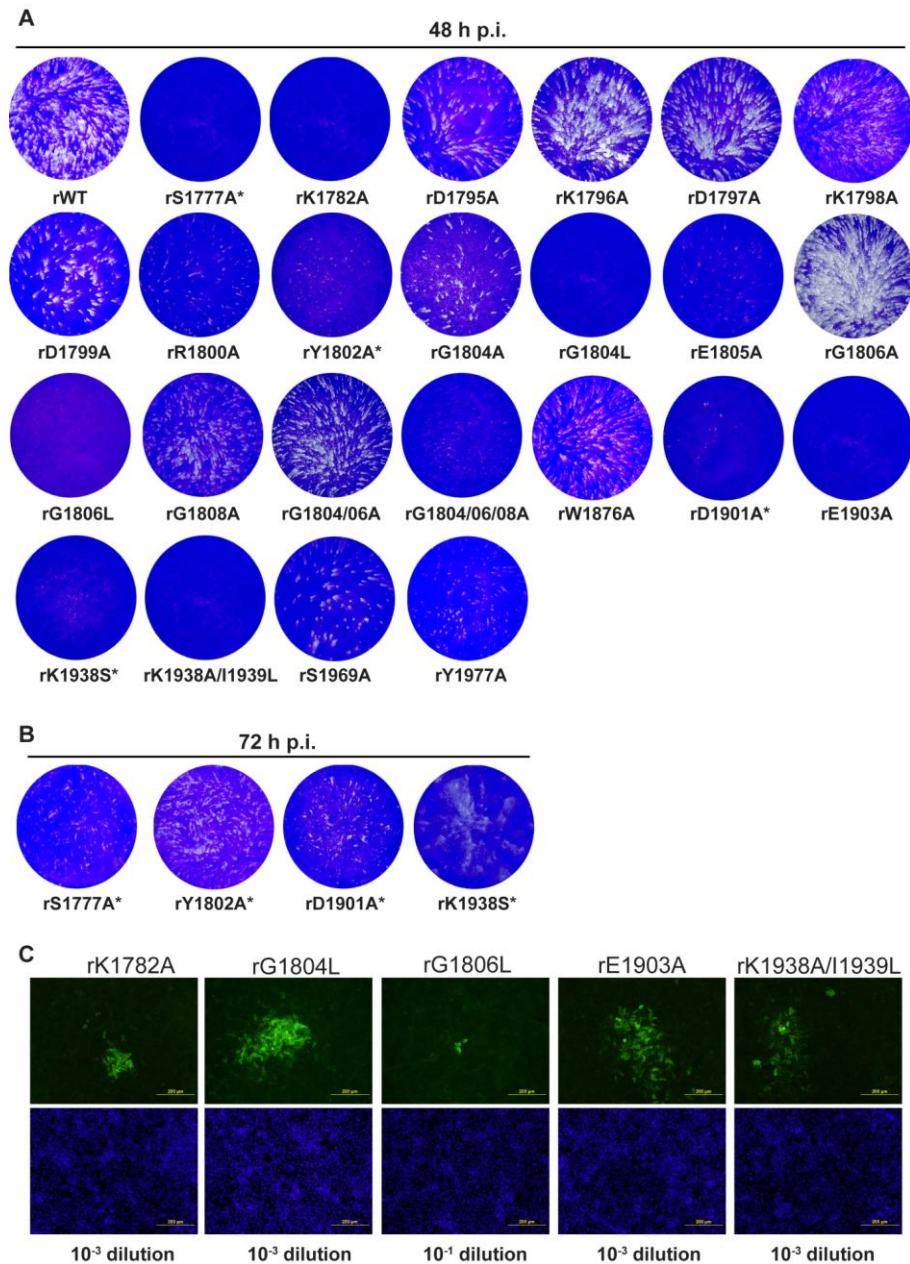


Figure 9. Growth analysis of recombinant SeV mutants in Vero cells. (A) Crystal violet staining of infectious foci of all rescued SeV L mutants. Plaque assays were performed on Vero cells and infectious foci from the lowest dilution displaying infectious foci were stained 48 h p.i. Wells with no visual infectious foci at 48 h p.i. were analyzed at 72 h p.i. or by IF. (B) For delayed mutants (indicated by *), plaque assays were again performed and crystal violet staining of infectious foci was done at 72 h p.i. (C) For severely attenuated mutants that had no visible infectious foci at 48 or 72 h p.i. an IF assay was performed at 72 h p.i. Upper panels represent cells stained with an anti-SeV primary antibody and an IgG secondary antibody conjugated to FITC. Lower panels represent Hoeschst staining of nuclei from the same fields shown in upper panels.

2.5 Figure 10

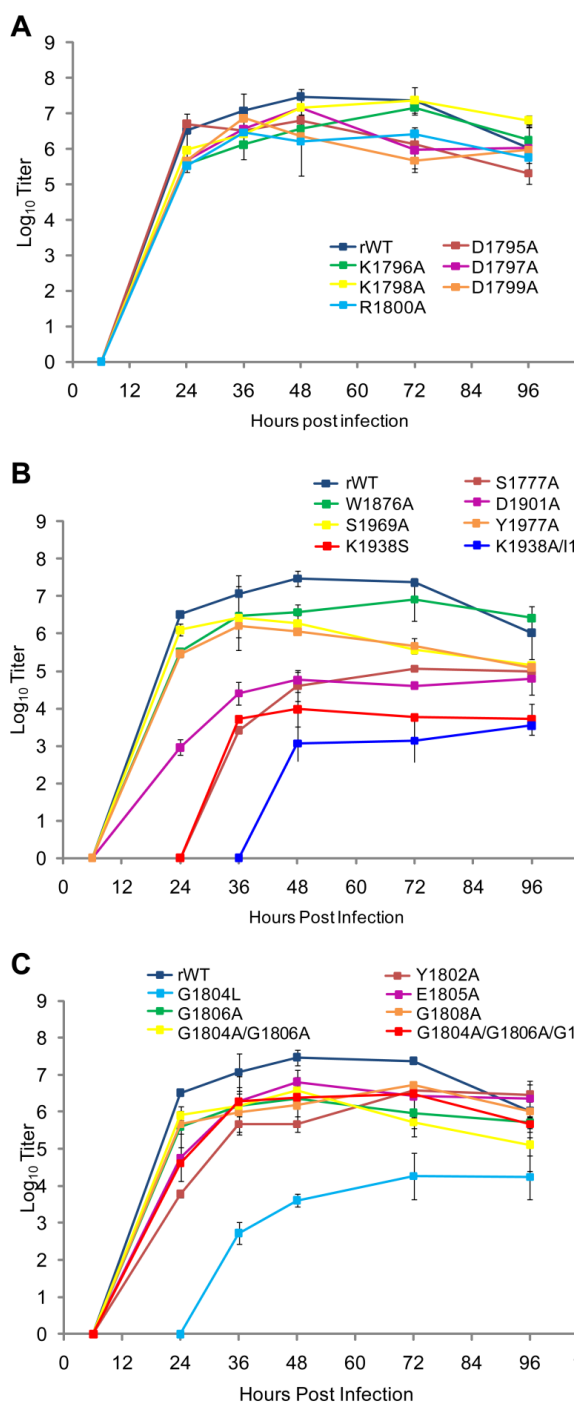


Figure 10. One-step growth kinetics of SeV mutants in Vero cells. Monolayer cultures of Vero cells were infected at an MOI of 3 CIU/cell with each mutant SeV. Vero cells were incubated with viruses for 1 h, then unabsorbed viruses were aspirated, cells were washed two times with PBS and fresh was added to each well. Supernatants were collected at 6, 24, 36, 48, 72, and 96 h p.i. and flash frozen. Plaque assays were performed on Vero cells and virus titers were determined for each time interval. * Zero titer indicates that virus titer at the indicated time point was below our detection threshold (50 CIU/ml). (A) SeV mutants with alanine substitutions in a DKDKD motif upstream of the glycine-rich motif. (B) SeV mutants that showed delayed growth in Vero cells or lower titers as compared to rWT. (C) SeV mutants with substitutions in and around the glycine-rich motif. The data represent the mean \pm standard deviation of two independent experiments.

2.5 Figure 11

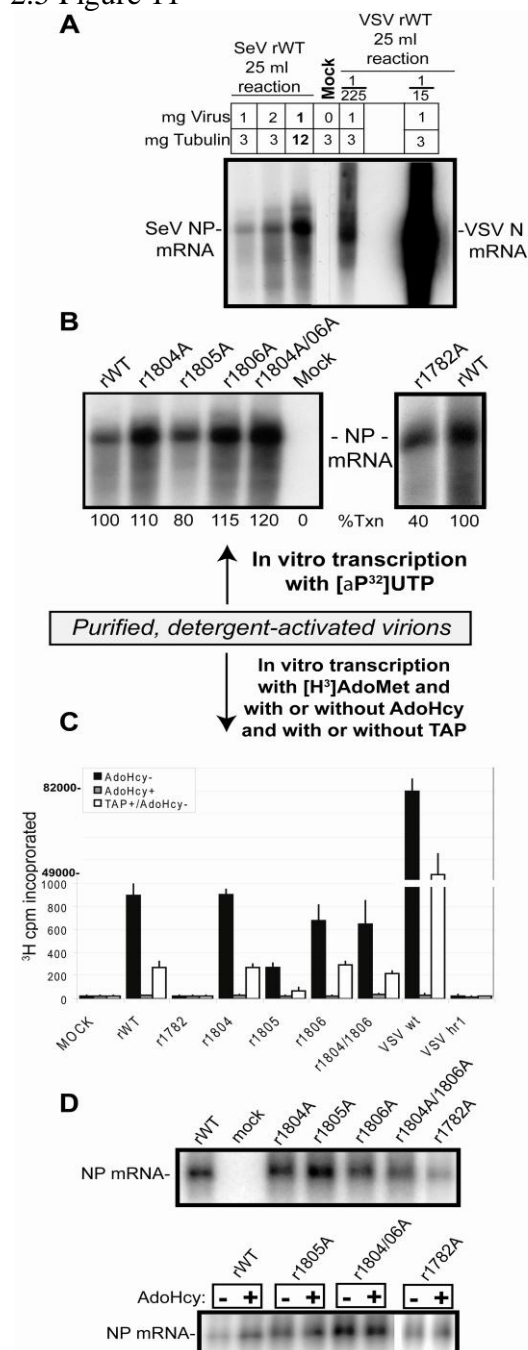


Figure 11. In vitro mRNA synthesis with purified mutant SeV. (A) Optimization of SeV virion transcription. In vitro transcription by detergent-activated purified SeV and VSV virions was performed using the same conditions in the presence of [α^{32} P]UTP and varying amounts of virus and purified tubulin. 1/225 or 1/15 of a 25 μ l transcription

reaction was loaded for wt VSV, while the entire product of a 25 μ l transcription reaction was loaded for SeV. The mock sample had all reaction components except for virus. The positions of the SeV NP and VSV N mRNAs are indicated. For all reactions total RNA was purified and analyzed by urea-agarose gel electrophoresis and visualized by autoradiography. (B) 10 μ g of purified wt or mutant SeV were detergent activated and used for in vitro mRNA synthesis in a 50 μ l transcription reaction in the presence of [α^{32} P]UTP. The mRNA products were purified, separated by urea-agarose gel electrophoresis and visualized by autoradiography. The position of the SeV NP mRNA is indicated. “% Txn” shows mRNA levels relative to wt SeV (100%) using PhosphorImager and represents the average of two or three experiments where variation was less than 15%. (C) 80 μ g of purified wt SeV (lane 1) or mutant SeV (lanes 2-5) were detergent activated and used for in vitro mRNA synthesis in a 200 μ l transcription reaction in the presence of [3 H]AdoMet with (gray bars) or without (black bars) addition of AdoHcy. For all conditions, RNA was purified, separated from nucleotides using gel filtration columns and used for the measurement of [3 H]AdoMet incorporation into mRNA by scintillation counting. (D). Northern blot analysis to compare viral mRNA levels produced by SeV mutants in the absence of AdoHcy (upper panel) or to compare mRNA levels produced with and without AdoHcy (lower panel). For Northern blotting, 1/10 of the mRNA produced in (C) was separated in a 1.2% agarose formaldehyde gel system, transferred to a nylon membrane and incubated with an RNA probe complementary to the SeV NP gene.

2.5 Figure 12

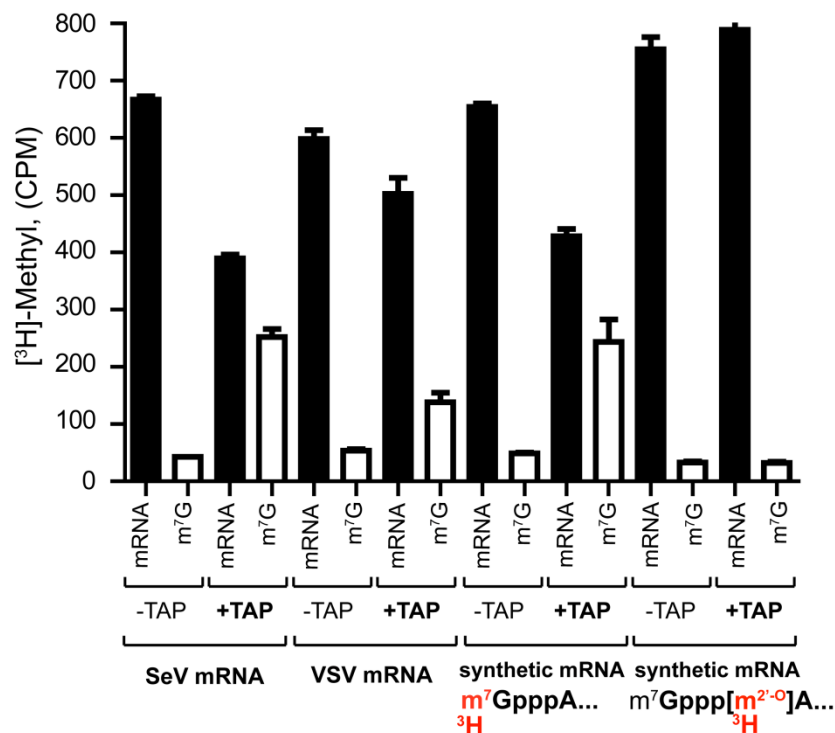


Figure 12. Cap methylation analysis using tobacco acid pyrophosphatase. SeV rWT (“SeV mRNA”) and VSV rWT (“VSV mRNA”) were produced in vitro transcription by detergent-activated purified virions in the presence of [³H]AdoMet. Synthetic SeV NP mRNA controls were synthesized in vitro using T7 RNA polymerase and then used to make mRNA containing Cap 0 (m⁷GpppA...) labeled with [³H]AdoMet at the G-N-7 position, or mRNA containing Cap 1 (m⁷Gppp[m^{2'-O}]^{3H}A...) labeled with [³H]AdoMet only at the 2'-O position using vaccinia virus enzymes as described in Materials and methods. For TAP analysis, all RNAs were normalized by [³H] counts and digested by TAP (“+TAP”) or mock-treated using the same reactions but without TAP (“-TAP”). mRNA was then separated from [³H]m⁷G using Sephadex G-50 mini-columns. [³H]Met incorporation into the G-N-7 or 2'-O cap positions was measured by scintillation counting of the entire flow through (for mRNA containing [³H-m^{2'-O}]^{3H}A) and columns (for removed [³H]m⁷G). The data represent the mean ± standard deviation of two independent experiments.

2.5 Figure 13

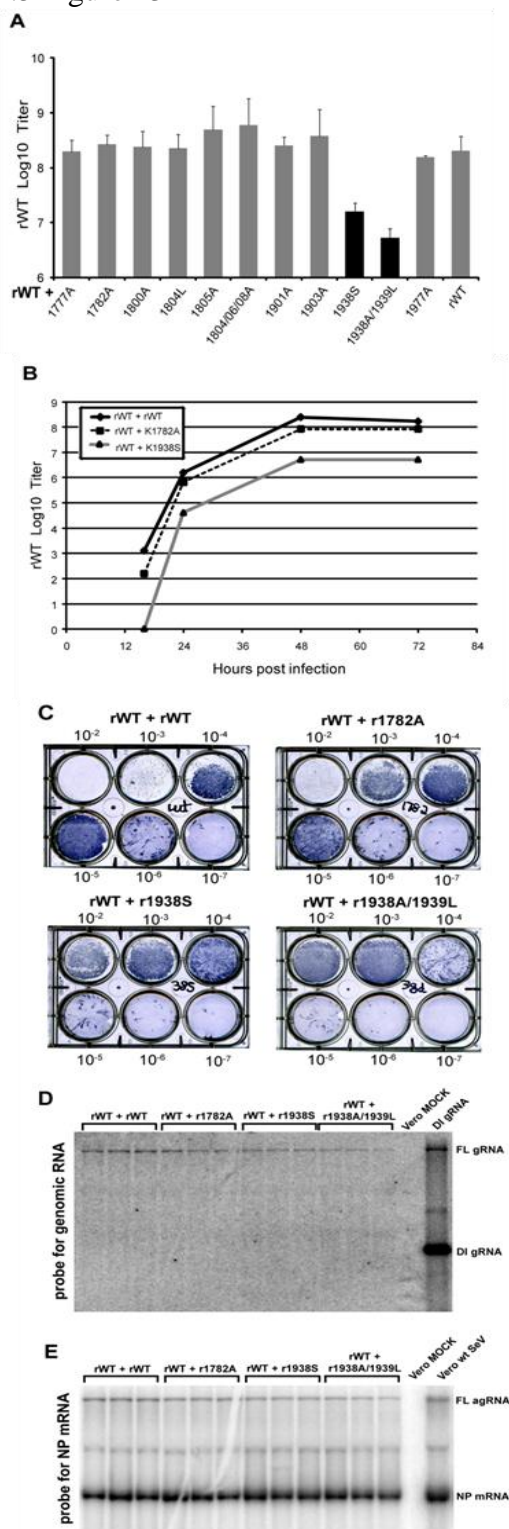


Figure 13. Superinfection of Vero cells with SeV mutants. (A) Vero cells were infected with combinations of SeV mutants and rWT at an MOI of 1

CIU/cell (total MOI of 2). Cells were observed and CPE was visualized by light microscopy at 24, 48, and 72 h p.i. The supernatant was collected at the same time points and each sample was further analyzed by plaque assays performed on Vero cells. Data represent the mean of three independent infections \pm standard deviation. (B) One-step growth kinetics for rWT grown in combination with K1782A and K1938S mutant viruses. Vero cells were infected at MOI 1 CIU/cell (total MOI of 2), supernatants collected at 18, 24, 48, and 72 h p.i. and titered on Vero cells. (C-E) Vero cells were infected with combinations of SeV mutant viruses plus rWT at an MOI of 1 CIU/cell for each virus (total MOI of 2). 48 h p.i., cells were analyzed by Northern blot (D-E) and the medium was titered on fresh Vero cells (C). Titration was done on 6-well plates with the rWT infection foci visualized 48 h p.i. using 4 CN Peroxidase Substrate staining Kit (KPL) and anti-SeV primary antibodies. Representative plates are shown. Only large SeV rWT (but not mutant) infectious foci are visible at this time point. (D-E) Cell pellets were analyzed by Northern blot analysis for genomic RNA using a probe for FL genomic RNA (gRNA) as well as DI genomic RNA (D) or a riboprobe for the SeV NP mRNA as well as the FL antigenomic RNA (agRNA) (E), as described in Materials and Methods. “Vero Mock” sample: total RNA isolated from mock-infected Vero cells. 7 μ g of total RNA was used for each sample. “Vero wt SeV” sample: total RNA isolated from Vero cells infected with SeV rWT and collected at 48 h p.i. “DI gRNA” sample: total RNA isolated from a preparation of SeV DI particles (DI-H).

2.5 Figure 14

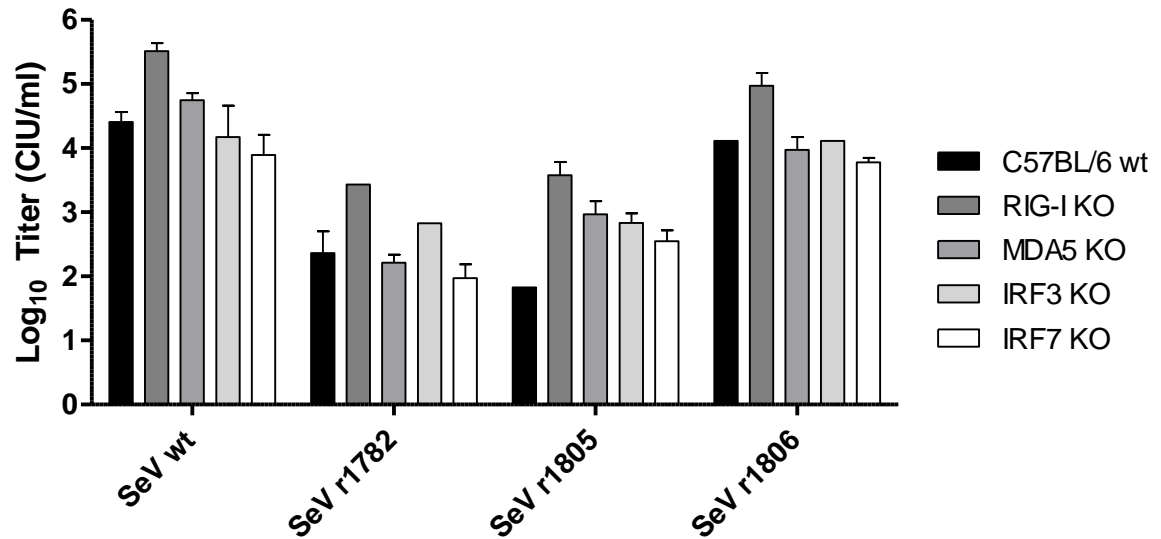


Figure 14. SeV infectivity of MEFs. SeV infectivity, expressed as cell infectious units/ml (CIU/ml), was measured by virus titration on Vero cells and counting infectious foci using immunofluorescence (IF). SFM media from 6-well plates was aspirated 2 or 3 days post infection, cells were washed with PBS, fixed with 3% paraformaldehyde (Sigma) for 10 minutes, and permeabilized for 2 minutes 0.5% Triton-X-100. Cells were then blocked in PBS with 5% bovine serum albumin (BSA, Sigma) for 20 minutes and incubated with anti-SeV primary antibodies (1:100) for 1 h. Cells were washed, incubated with goat anti-rabbit IgG-Alexafluor antibodies (Santa Cruz) for 1 h in the dark, and viewed under a fluorescent microscope to determine virus titer.

2.5 Figure 15

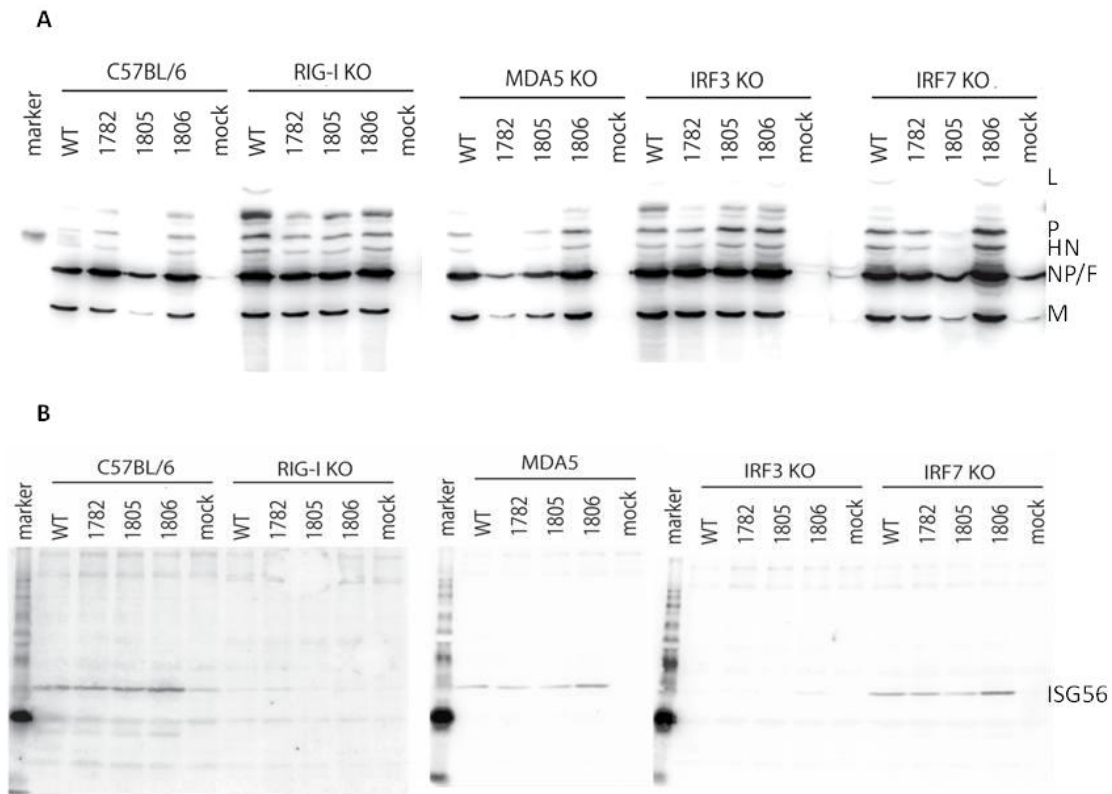


Figure 15. Western blot analysis of MEFs infected with SeV mutants. Six well plates of MEFs were infected at an MOI of 10 CIU/cell and cells were harvested for lysates at 24 h p.i. Lysates were prepared directly in the 6 well plates in 1X SDS sample buffer and 5 μ l (of a total of 150 μ l) of each sample was separated by 10% SDS-PAGE and electroblotted onto PVDF membranes. Membranes were blocked with 5% non-fat dry milk and membranes were incubated with (A) rabbit anti-SeV antibodies (1:5000) or (B) rabbit anti-IFIT-1 (ISG56, 1:500) followed by incubation with goat anti-rabbit IgG-HRP secondary antibodies (1:5000).

2.6 Table 1. Sequences of primers used in this study to generate SeV mutant L genes. Capital letters show substituted nucleotides resulting in the aa change.

L mutant	L changes	Silent Site	Primer sequences
L-1777A	S1777A	AatII	(+) ctctttggcatcaac GCG acgtcctgcttgaaagcacttg (-) caagtgccttcaagcaggacgtcgcttgatgccaaagag
L-1782A	K1782A	AfeI	(+) catcaacagtactagctgcttg GC agcgcttgaacttacctactatt (-) caataggtaggttaagttcaagcgctgccaaagcagctagctactgttgat
L-1795A	D1795A	StyI	(+) gagccccttagttg C caaggataaagatagggc (-) gcctatctttatccttggcaactaaggggctc
L-1796A	K1796A	SalI	(+) ctattgagccccttagtcgac GC ggataaagatagggc (-) gcctatctttatccgctcgactaaggggctcaatag
L-1797A	D1797A	SalI	(+) gagccccttagtcgacaag CT aaagatagctatattagggg (-) cccctaaatatagcctatctttagccttgcgactaaggggctc
L-1798A	K1798A	RsrII	(+) ccccttagttgacaaggat GCG gaccggctatatttagg (-) cctaaatatagcgggtccgcatccttgcactaagggg
L-1799A	D1799A	StyI	(+) gttgacaaggataaag CT aggctatacctaggggaaggagctg (-) cagctcctcccctaggtatagcctagctttatccttgcacac
L-1800A	R1800A	MluI	(+) gttgacaaggataaagac GC gttatatttaggggaag (-) ctcccctaaatataacgcgtctttatccttgcacac
L-1802A	Y1802A	StyI	(+) ggataaagataggctc GC Cttgggggaaggagctggggc (-) gccccagctcctcccccaagggcagcctatctttatcc
L-1804A	G1804A	EaeI	(+) gataggctatatttg CC gaaggagctggggccatg (-) catggccccagctccttcggccaaatagcctatc
L-1804L	G1804L	XbaI	(+) gataaagataggctatattct CTA gaaggagctggggccatg (-) catggccccagctccttcggaagatagcctatctttatc
L-1805A	E1805A	AvrII	(+) gataaagataggctatacctagggg C aggagctggggccatg (-) gcatggccccagctcctgccctaggtatagcctatctttat
L-1805L	E1805L	StyI	(+) gataggctatatttaggc CT aggagctggggccatgc (-) gcatggccccagctcctaggcctaaatagcctatc
L-1805V	E1805V	AvrII	(+) gataaagataggctatacctagggg T aggagctggggccatg (-) gcatggccccagctcctaccctaggtatagcctatctttat
L-1806A	G1806A	AvrII	(+) gataaagataggctatacctaggggaag C agctggggccatgcttc (-) gaaagcatggccccagctcccctaggtatagcctatctttatc
L-1806L	G1806L	SacI	(+) ggctatatttaggggag CTC gctggggccatgctttc (-) gaaagcatggccccagcagctcccctaaatagcctatc
L-1804A/ 1806A	G1804A/ G1806A	PstI	(+) gataggctatatttag CggaagCT gcaggggccatgctttc (-) gaaagcatggccccctgcagctcccctaaatagcctatc
L-1808A	G1808A	PstI	(+) tttaggggaaggagctg CA gcatgctttcctgtt (-) aacaggaaagcatggctgcagctcctcccctaaa
L-1808L	G1808L	HaeII	(+) tatttaggggaaggagcg CT ggccatgctttcctgttatg (-) cataacaggaaagcatggccagcgcctcccctaaa
L-1804A/ 1806A/ 1808A	G1804A/ G1806A/ G1808A	PstI	(+) gataggctatatttag CggaagCagctgCA gcatgctttcctgtt (-) aacaggaaagcatggctgcagctgctcccctaaatagcctatc
L-1810A	M1810A	AfeI	(+) gaaggagctggggca GC gcttctctgttatgacg (-) cgtcataacaggaaagcgtgccccagctcctc
L-1825A/ 1826A/ 1827A	Y1825A/ N1826A/ S1827A	NotI	(+) gccatgcatcaactat GCGGCcGc aggggtatactctgtg (-) cacaagagtatacccctgcccgcgcatagttgatgatgggc
L-1876A	W1876A	HincII	(+) gaatcctgggtcgaca GC gattgggaatgatgagtg (-) cactcatcatccaatcgetgctgacccaggatt

2.6 Table 1 continued.

L mutant	L changes	Silent Site	Primer sequences
L-1875A/ 1876A	T1875A/W187 6A	PstI	(+) cgggaatcctggctct GcaGC gattgggaatgatgagtg (-) cactcatcatccaatcgctgcagagccaggattcccg
L-1901A	D1901A	FspI	(+) aggcctagtccactg cgCA atggaggaggagatc (-) gatctcctccctcattg cg cagtggactaggcct
L-1903A	E1903A	NaeI	(+) gtccactgtgacatg gCC ggcggagatcataaggatg (-) catccttatgatctccg cc gcatgtcacagtggac
L-1938A	K1938A	AfeI	(+) gttgtgcttataagc GCT attgctcccaggctgg (-) ccagcctgggagcaatag cg cttataagcacaac
L-1969A	S1969A	AflII	(+) cctaatagtgcttaagaca Gcta accctgctccacag (-) ctg gga agcagggtagctgtcttaagcactattagg
L-1975A	E1975A	EaeI	(+) ctaaccctgctccacg gCC atgtatcttctatcgag (-) ctcgatagaagatacatg cc gtggaagcagggftag
L-1977A	Y1977A	HaeII	(+) ctgctccacagagatg GCG cttctatcgaggcacc (-) ggtgcctcgatagaag cc atctctgtggaagcag
L-ΔVI	deletion of aa 1777-1976	none	(+) ggctcttggcatcaaccttctatcgaggcacc (-) ggggtgcctcgatagaag gt gatgccaagagcc
Upstream primer VG19 for cloning and sequencing			(+) catacctatgcagctggcagaga
Downstream primer VG20 for cloning and sequencing			(-) taaccctcagttcctgatctcac

2.6 Table 2. Comparative titers of recombinant Sendai viruses in Vero or HEp2 cells at 34°C or 40°C

Virus	Virus titer (CIU/ml) in Vero cells		Virus titer (CIU/ml) in HEp-2	Titer ratio 34°C/40°C in Vero	Titer ratio at 34°C Vero/HEp-2
	34°C	40°C	34°C		
SeV rWT	2.0×10^8	3.4×10^7	8.8×10^7	5.9	2.3
SeV r1782A	4.0×10^5	$<10^3$	4.0×10^3	$>1.2 \times 10^3$	100
SeV r1804A	1.5×10^7	3.2×10^6	5.3×10^6	4.7	2.8
SeV r1805A	3.6×10^8	$<10^3$	1.6×10^8	$>3.6 \times 10^5$	2.3
SeV r1806A	2.4×10^8	1.6×10^7	1×10^8	15	2.4
SeV r1804A/1806A	5.0×10^7	8.0×10^6	2.5×10^7	6.3	2.0
SeV r WT-GFP	1.9×10^8	7.0×10^6	1.0×10^8	27.1	1.9
SeV r1805A-GFP	8.3×10^7	$<10^3$	3.3×10^7	$>8.3 \times 10^4$	2.5
SeV r1806A-GFP	1.3×10^8	4.6×10^6	4.4×10^7	28.3	3.0
rVSV wt	2.4×10^9	1.0×10^7	3.2×10^7	240	75
rVSV <i>hrl</i>	6.0×10^7	$<10^3$	$<10^3$	$> 6 \times 10^4$	$> 6 \times 10^4$

2.6 Table 3. Cap methylation analysis using SeV detergent-activated purified virions

VIRUSES	Virus stock infectivity (CIU/ml)	Txn - AdoHcy (% of rWT - AdoHcy)	Txn + AdoHcy (% of rWT - AdoHcy)	† Cap Methylation - AdoHcy (% of rWT - AdoHcy)	† Cap Methylation + AdoHcy (% of rWT - AdoHcy)
rWT	3.8 x 10 ⁸	100.0	67.0 ± 26.0	100.0	2.7 ± 0.2
rS1777A	4 x 10 ⁷	100.0 ± 25.8	70.3 ± 5.2	45.8 ± 11.9	0.7 ± 0.2
rK1782A	2 x 10 ⁵	25.8 ± 2.6	32.8 ± 11.7	6.6 ± 1.2	1.4 ± 0.7
rD1795A	8 x 10 ⁷	55.4 ± 12.4	51.3 ± 17.0	51.6 ± 16.9	1.7 ± 0.6
rK1796A	8 x 10 ⁷	54.0 ± 13.5	41.6 ± 3.9	82.2 ± 13.2	1.7 ± 0.3
rD1797A	8 x 10 ⁷	79.4 ± 0.5	64.4 ± 25.2	120.9 ± 20.8	2.7 ± 0.1
rK1798A	1 x 10 ⁸	48.9 ± 7.1	24.8 ± 0.5	104.0 ± 0.8	4.2 ± 0.6
rD1799A	1.4 x 10 ⁷	64.2 ± 12.7	53.1 ± 15.1	80.2 ± 19.8	2.7 ± 0.4
rR1800A	4.8 x 10 ⁷	70.1 ± 7.3	70.7 ± 9.9	48.5 ± 17.8	1.5 ± 1.0
rY1802A	1.4 x 10 ⁸	14.6 ± 5.6	15.4 ± 3.0	7.2 ± 0.5	1.8 ± 1.7
rG1804A	3.4 x 10 ⁷	nd	nd	nd	nd
rG1804L	1 x 10 ⁶	27.9 ± 4.6	30.1 ± 5.8	9.9 ± 0.7	1.2 ± 0.5
rE1805A	3.2 x 10 ⁷	34.0 ± 15.8	50.0 ± 2.8	22.8 ± 5.2	5.3 ± 5.7
rE1805L	NR	NR	NR	NR	NR
rG1806A	2.2 x 10 ⁸	nd	nd	nd	nd
rG1806L	<10 ²	nd	nd	nd	nd
rG1808A	8 x 10 ⁷	21.8 ± 8.2	18.1 ± 6.3	31.4 ± 0.1	1.8 ± 1.5
rG1808L	NR	NR	NR	NR	NR
rG1804A/G1806A	8 x 10 ⁷	114.8 ± 5.9	86.8 ± 12.8	50.9 ± 1.6	12.5 ± 0.3
rG1804A/G1806A/ G1808A	1.4 x 10 ⁸	25.0 ± 5.0	17.2 ± 3.1	36.8 ± 5.0	2.1 ± 0.5
rY1825A/N1826A/ S1827A	NR	NR	NR	NR	NR
rW1876A	1.6 x 10 ⁸	20.3 ± 2.8	21.9 ± 6.2	46.8 ± 10.3	1.5 ± 0.3
rT1875A/W1876A	NR	NR	NR	NR	NR
rD1901A	1.4 x 10 ⁷	37.4 ± 5.7	27.3 ± 4.9	2.1 ± 0.5	0.2 ± 0.3
rE1903A	4 x 10 ⁵	26.1 ± 4.4	27.3 ± 3.5	7.3 ± 2.4	0.2 ± 0.5
rK1938S	1.2 x 10 ⁶	91.0 ± 12.7	60.1 ± 3.1	8.1 ± 0.9	2.2 ± 0.6
rK1938A/I1939L	1.2 x 10 ⁶	46.9 ± 23.2	28.4 ± 16.1	2.4 ± 0.5	1.1 ± 0.4
rS1969A	4.4 x 10 ⁷	71.5 ± 10.1	67.0 ± 12.4	73.7 ± 20.9	2.1 ± 0.1
rE1975A	NR	NR	NR	NR	NR
rY1977A	8 x 10 ⁷	55.5 ± 16.7	48.5 ± 23.2	28.6 ± 5.7	5.1 ± 3.3

- AdoHcy: in vitro transcription in the absence of S-adenosylhomocysteine (AdoHcy)

+ AdoHcy: in vitro transcription in the presence of 100 μM AdoHcy

† methylation of viral mRNA (NP + P) produced in vitro is expressed as the ratio (% of rWT) of [H3]-AdoMet incorporation into viral mRNA by scintillation counting to the mRNA levels determined analyzed by Northern blot (mRNA levels are shown in the “Txn” columns) .

NR = not rescued (unable to rescue after multiple attempts)

nd = not determined

CIU = cell infectious units

The data represent the mean ± standard deviation of two independent experiments.

CHAPTER 3: VESICULAR STOMATITIS VIRUS AS AN ONCOLYTIC AGENT AGAINST PANCREATIC DUCTAL ADENOCARCINOMA

3.1 Objective of the Study

Oncolytic virus (OV) therapy is an anticancer approach that utilizes replication-competent viruses to specifically kill tumor cells (Russell and Peng 2007; Vähä-Koskela et al. 2007; Breitbach et al. 2010). Such selectivity is possible because many tumors are characterized by defective innate immune responses or tumor-related abnormalities in regulation of mRNA translation or certain cellular signaling pathways, facilitating selective replication of viruses in cancer cells. OV can infect, replicate within and kill tumor cells and successful virus replication in leads to the release of newly formed infectious virus particles that go on to infect neighboring tumor cells.

VSV is a promising OV and has demonstrated preclinical success against a variety of malignancies, including prostate (Ahmed et al. 2004; Chang et al. 2010; Moussavi et al. 2010), breast (Fernandez et al. 2002; Obuchi et al. 2003; Shi et al. 2009; Ahmed et al. 2010), melanoma (Fernandez et al. 2002; Galivo et al. 2010), colorectal (Huang et al. 2003; Shinozaki et al. 2005; Edge et al. 2008), liver (Wu 2008; Altomonte et al. 2009; Ausubel et al. 2011), glioblastoma (Ozduman et al. 2008; Wollmann 2010; Cary et al. 2011) and other cancers (Barber 2004). However, VSV oncolytic potential has never been studied in any pancreatic cancer models. Pancreatic ductal adenocarcinoma (PDA) is the most common form of pancreatic cancer and is characterized as being locally invasive with aggressive local growth and rapid metastases to surrounding tissues

(Stathis and Moore 2010). PDA is considered one of the most lethal abdominal malignancies with annual deaths closely matching the annual incidence of the disease (Lindsay et al. 2005; Farrow et al. 2008), resulting in a 5-year survival rate of merely 8-20%. Several cancer therapies proven successful in other tumor types have shown little efficacy in treating PDA. Chemotherapy is the primary treatment available; however, patients exhibit little improvement or develop chemoresistance (Stathis and Moore 2010). Therefore, development of new treatment strategies for patients suffering from PDA is of utmost importance.

OV therapy with several viruses, including adenoviruses (Kuhlmann et al. 2008; He et al. 2009; Huch 2009), herpesviruses (Sarinella et al. 2006; Kasuya et al. 2007; Nakao et al. 2007; Watanabe et al. 2008; Eisenberg et al. 2010) and reoviruses (Etoh et al. 2003; Himeno et al. 2005; Hirano et al. 2009), has recently shown promise in several PDA tumor models. However, there are several advantages of using VSV as an anticancer therapy. VSV is the prototypic nonsegmented negative-strand RNA (NNS) virus (order *Mononegavirales*, family *Rhabdoviridae*), and its basic biology and interactions with host immune responses have been extensively studied (Lyles 2007). This knowledge has led to the development of rationally designed VSV vectors for use in vaccines, gene therapy and OV therapy (Barber 2004; von Messling and Cattaneo 2004). While VSV is very sensitive to IFN-mediated antiviral responses (and therefore unable to productively infect healthy cells), it can specifically infect and kill tumor cells, majority of which are believed to be defective in Type I IFN production and responses (Barber 2004; Lichty et al. 2004). Also, the mechanisms of VSV-mediated killing by apoptosis have been established (Gaddy and Lyles 2007). In addition to tumor specificity, VSV has

several important advantages as an OV: (i) replication occurs in the cytoplasm of host cells with no risk of host cell transformation, (ii) cellular uptake in many mammalian cell types occurs rapidly and there is no cell cycle dependency, (iii) the genome is easily manipulated with the possibility for strong and adjustable levels of foreign gene expression to enhance oncolysis and specificity, and (iv) there is no preexisting immunity against VSV in humans (Barber 2004). While VSV is not considered a significant human pathogen, it can cause neurotoxicity in mice, nonhuman primates and even humans (Quiroz et al. 1988). However, several VSV mutants have been generated which are not neurotropic but retain their oncolytic activity (Ahmed 2008; Kelly et al. 2010; Wollmann 2010). In this study, we focused on two such VSV mutants, VSV- Δ M51-GFP and VSV-p1-GFP (Wollmann 2010). VSV-p1-GFP has the green fluorescent protein (GFP) open reading frame (ORF) inserted at position one of the viral genome resulting in slower viral replication kinetics reducing VSV-p1-GFP abilities to evade innate immune responses (Wollmann 2010). VSV- Δ M51-GFP has a deletion at amino acid position 51 of the matrix (M) protein, as well as the GFP ORF inserted in position 5 of the viral genome (Wollmann 2010). The wt M protein plays a role in inhibiting transport of host mRNAs from the nucleus to the cytoplasm and thereby downregulating IFN production. The single deletion at the M51 position knocks out this important function of M and allows for a more robust IFN response from normal healthy tissue while the M51 deletion mutant is still affective against tumor cells. Both attenuated VSV recombinants have shown a desirable phenotype characterized by retention of their oncolytic activities but lack of neurotoxicity in vivo (Ahmed 2008; Wollmann 2010).

In our study, the oncolytic potential of VSV variants was analyzed in a panel of 13 clinically relevant human PDA cell lines and compared to conditionally replicative adenoviruses (CRAds), SeV, and respiratory syncytial virus (RSV). VSV showed superior oncolytic abilities compared to all other viruses tested, and was effective in killing the majority of tested PDA cell lines. However, we identified some PDA cell lines that showed general resistance to oncolysis by all tested viruses. These results were confirmed for several PDA cell lines in vivo in nude mice. We also conducted initial analysis of PDA resistance to virus-induced cell death. Our in vitro and in vivo results demonstrate that VSV has good potential as an OV against PDA, while further studies are needed to better understand the molecular mechanisms of resistance of some PDA cell lines to virotherapy.

3.2 Materials and Methods

Cell lines.

Human PDA cell lines used in this study: CFPAC-1 (ATCC CRL-1918), Hs766T (ATCC HTB-134), Capan-2 (ATCC HTB-80), T3M4 (Okabe et al. 1983), AsPC-1 (ATCC CRL-1682), HPAF-II (ATCC CRL-1997), Suit2 (Iwamura et al. 1987), HPAC (ATCC CRL-2119), BxPC-3 (ATCC CRL-1687), MIA PaCa2 (ATCC CRL-1420), SU.86.86 (ATCC CRL-1837), Capan-1 (ATCC HTB-79), and Panc-1 (ATCC CRL-1469) (Table 4). In addition, the immortal human pancreatic duct epithelial cell line (HPDE) (Furukawa et al. 1996) was used in this study and maintained in Keratinocyte-SFM (Gibco). This cell line, which was generated by introduction of the E6 and E7 genes of human papillomavirus 16 into normal adult pancreas epithelia, retains a genotype similar to pancreatic duct epithelia and is non-tumorigenic in nude mice (Furukawa et al. 1996). The mouse breast cancer cell line 4T1 (ATCC CRL-2539), the baby hamster kidney fibroblasts BHK-21 (ATCC CCL-10), the human cervix adenocarcinoma cell line HeLa (ATCC CCL-2), the African green monkey kidney cells Vero (ATCC CCL-81) and the human epidermoid cancer cells Hep-2 (ATCC CCL-23) were used to grow viruses and/or as controls for viral replication. CFPAC-1, Suit2, HPAC, MIA PaCa2, Capan-1, Panc-1, 4T1, and Vero cells were all maintained in Dulbecco's modified Eagle's medium (DMEM, Cellgro). Capan-2, T3M4, AsPC-1, BxPC-3 and SU.86.86 cells were maintained in Roswell Park Institute medium-1640 (RPMI, Hyclone). HPAF-II, Hs766T, BHK-21, A549 and HeLa cells were maintained in modified Eagle's medium (MEM, Cellgro). All cell lines were supplemented with 9% fetal bovine serum (Gibco). For all experiments, PDA cell lines were passaged no more than 10 times.

Viruses.

The following viruses were used in this study: recombinant wild-type (wt) VSV (Indiana serotype) (Lawson et al. 1995); VSV-p1-GFP; VSV- Δ M51-GFP (p5); CRAd-dl1520 (“ONYX-015”); CRAd-hTERT (Adv-TERTp-E1A); SeV-GFP; and RSV-GFP. VSV-p1-GFP has GFP ORF inserted at position one of the viral genome (Wollmann 2010). VSV- Δ M51-GFP has a deletion at amino acid position 51 of the matrix (M) protein, as well as the GFP ORF inserted in position 5 of the viral genome (Wollmann 2010). Both attenuated VSV recombinants have been shown to retain their oncolytic activity while lacking neurotoxicity in vivo (Ahmed 2008; Wollmann 2010). CRAd-dl1520 is attenuated by deletion of a large part of the coding sequence for the E1b55k viral gene product and selectively replicates in and kills cancer cells (Bischoff et al. 1996; Crompton and Kirn 2007). CRAd-hTERT is a human telomerase reverse transcriptase (hTERT)-promoter-dependent CRAd, which selectively replicates in and kill cells with active hTERT (85–90% of tumor cells) (Huang et al. 2003). SeV-GFP (SeV-GFP-F_{mut}) has the GFP ORF at position one of the viral genome and a mutation in the cleavage site of the fusion (F) protein allowing for F activation and production of infectious virus particles in cells without acetylated trypsin in the medium through a ubiquitous furin-like protease (Wiegand et al. 2007). RSV-GFP has the GFP ORF at position one of the viral genome (Hallak et al. 2000) (Fig. 16). All VSV variants were grown in BHK-21 cells, SeV-GFP was grown in Vero, CRAds were grown in HeLa, and RSV-GFP was grown in Hep-2 cells. For animal experiments, VSV- Δ M51-GFP was dialyzed (Slide-A-Lyzer, Pierce) in 2 L chilled dialysis buffer [25 mM Tris pH 7.4, 140 mM NaCl, 5 mM KCl, 0.6 mM Na₂HPO₄, 0.5 mM MgCl₂, 0.9 mM CaCl₂, and 5% (w/v) sucrose] for 2 hour (h) at

4°C and then 4 h at 4°C in fresh dialysis buffer. CRAd-dl1520 was dialyzed in 10 mM Tris pH 8, 135 mM NaCl, 1 mM MgCl₂ and 50% (v/v) glycerol three times for 1 h each at 4°C. Dialyzed viruses were tested for infectivity on A549 cells.

Cell viability assay.

Cells were seeded in 96-well plates so that they reached 80% confluency at 24 h, and then virus-infected at a multiplicity of infection (MOI) of 1 or 0.01 CIU (cell infectious units) per cell (based on VSV titration on 4T1 cells) or mock infected in MegaVir HyQSFM4 serum-free media (SFM, Hyclone). One h post infection (p.i.) virus was aspirated and cells were incubated in growth media containing 5% FBS. Cell viability was analyzed at 5 days (d) p.i. by an MTT cell viability assay (Biotium). To determine the kinetics of virus-associated cytopathogenicity, cells were seeded in 96-well plates so that they reached 50% confluency at 24 h. Cells were then mock infected or infected with VSV-ΔM51-GFP at low (0.001 CIU/cell), intermediate (0.1 CIU/cell), or high MOI (1 CIU/cell). At 1 h p.i., virus was aspirated and cells were overlaid with growth media containing 5% FBS. An MTT cell viability assay was performed at 1, 16, 24, 48, and 72 h p.i.

Permissiveness of cells to virus infection.

Cells were incubated with serial dilutions of VSV-wt, VSV-GFP(p1), VSV-ΔM51-GFP, SeV-GFP, CRAd-dl1520, or CRAd-hTERT in SFM for 1 h. At 1 h p.i., virus was aspirated and growth media containing 5% FBS was added to each well. The infectious foci of VSV-ΔM51-GFP, VSV-GFP(p1) and SeV-GFP were analyzed by fluorescent microscopy at 24 and 48 h p.i. respectively. The infectious foci of CRAd-dl1520 and CRAd-hTERT were analyzed by immunocytochemistry (ICC) at 5 d p.i.

Briefly, cells were washed with phosphate buffered saline (PBS) and fixed in 3% paraformaldehyde (PFA, Sigma) for 10 min followed by permeabilization for 2 min on ice with a solution containing 20 mM HEPES (pH 7.5), 300 mM sucrose, 50 mM NaCl, 3 mM MgCl₂, and 0.5% Triton X-100. Cells were then blocked with 5% bovine serum albumin (BSA, Sigma) in PBS for 20 min and incubated with anti-adenovirus hexon primary antibodies (1:600, US Biologicals, Cat # A0880-14) for 1.5 h. Cells were washed, incubated with peroxidase conjugated goat anti-mouse IgG antibodies (1:300, Jackson ImmunoResearch) for 1.5 h, and detected by addition of the peroxidase substrate 3,3'-diaminobenzidine tetrahydrochloride hydrate (DAB, Amresco). The infectious foci of VSV-wt were also analyzed by ICC as described above but using 1:100 rabbit polyclonal anti-VSV antibodies (raised against VSV virions) and anti-rabbit secondary antibodies. Cells were infected with serial dilutions of VSV-wt in triplicate and infectious foci were analyzed by ICC at 48 h p.i.

One-step virus growth kinetics.

Selected PDA cells were seeded in 96-well plates to reach confluency at 24 h. They were infected in duplicate with VSV-wt, VSV- Δ M51-GFP, or VSV-p1-GFP at MOI 10 CIU/cell based on the reference cell line 4T1. At 1 h p.i. virus was aspirated, cells were washed twice with PBS (to prevent carryover of virions) and overlaid with growth media containing 5% FBS. At 1, 24, 50 and 72 h p.i. supernatant was collected from wells and flash frozen at -80°C. Virus titers were later determined by plaque assay analysis. Briefly, BHK-21 cells were incubated with serial dilutions of the samples for 1 h. Virus was aspirated and cells were overlaid with a SFM / 2% BactoAgar mixture to

limit virus spread. Infectious foci were counted by light and fluorescence microscopy at 16 h p.i.

Type I interferon sensitivity and production.

Cells were seeded in 96-well plates so that they reached 80% confluency at 24 h. For Type I interferon sensitivity, cells were either treated with 5000 U/ml interferon alpha (IFN- α , Calbiochem, Cat # 407294) in SFM or with SFM only. Twenty-four h post treatment, cells were infected with serial dilutions of VSV- Δ M51-GFP, and infectious foci were analyzed 16 h p.i. by fluorescent microscopy. Treatments and infections were performed in duplicate. For Type I interferon production, cells were infected with VSV- Δ M51-GFP at MOI 10 CIU/cell or mock-treated with SFM only. One h p.i. virus was aspirated and cells were incubated in SFM. Eighteen h p.i. supernatant was harvested and analyzed by ELISA for production of human IFN- β (PBL, Cat # 41410-1) or human IFN- α (multi-subtype, PBL, Cat # 41105-1) per manufacturer's instructions (PBL InterferonSource). Infections were performed in triplicate.

Western blot.

Cellular lysates were prepared by mock infecting cells or infecting them with VSV- Δ M51-GFP at MOI 1 or 10 CIU/cell. One h p.i. virus was aspirated, cells were extensively washed and incubated in growth media containing 5% FBS. Cells were harvested at 16 h p.i. and lysed in lysis buffer containing 1% Triton-X-100, 20mM Hepes, 0.15 M NaCl, 2 mM EDTA and supplemented with c-inhibitor (2X, Roche). Total protein concentration was determined by Bradford assay. Three μ g (for VSV detection) or 30 μ g (for GFP detection) of total protein was separated by electrophoresis on 10% or 12% SDS-PAGE gels respectively, and electroblotted to polyvinylidene

difluoride (PVDF) membranes. Membranes were blocked using 5% non-fat powdered milk in TBS-T [0.5 M NaCl, 20 mM Tris (pH 7.5), 0.1% Tween20], which was also used for antibody dilutions. Membranes were incubated with 1:10000 rabbit polyclonal anti-VSV antibodies (raised against VSV virions) or 1:3000 mouse anti-GFP clone 9F9.F9 (Rockland). Detection was with 1:5000 goat anti-rabbit or 1:5000 goat anti-mouse horseradish peroxidase-conjugated secondary antibodies (Jackson ImmunoResearch) using the Enhanced Chemiluminescence Plus (ECL+) protein detection system (GE Healthcare). Membranes were reprobbed with mouse anti-actin clone C4 (Moyer et al. 1986) to verify sample loading. Image capture and densitometry analysis were performed using VisionWorksLS v6.8 software (UVP).

Northern blot.

The pVSVFL(+).g.1 plasmid, which encodes a complete cDNA copy of the VSV (Indiana strain) antigenome (Lawson et al. 1995), was used as a template for addition of a SP6-promotor to the 3' end of a 279 bp fragment of N by PCR using the following primers: 5'-ATCCAGTGGAATACCCGGCAGATT-3' and 5'-ATTAGGTGACACTATAGAAGTGCTCGTCAGATTCAAGCTCAGGCTG-3'. A probe for detection of N mRNA and VSV anti-genomic RNA was synthesized from the PCR product by in vitro transcription in the presence of ³²P-UTP using the MAXIscript T7 kit (Ambion). Cells were mock treated or treated with 100 µg/ml cycloheximide for 30 min prior to mock infection or infection with VSV-ΔM51-GFP at MOI 10 and continuing treatment with cycloheximide. At 4 h p.i. cells were collected and total RNA extracted using the Quick-RNA MiniPrep kit (Zymo Research). For each sample, 1 µg of RNA was separated on a 1.2% agarose-formaldehyde gel containing ethidium bromide

for confirmation of RNA loading by visualization of rRNA. The RNA was transferred to a nylon membrane and incubated with probe overnight at 58°C. Bands were detected using a phosphorimager and quantitated using Image Quant 5.2 (Molecular Dynamics).

Surface expression of adenovirus CAR receptor.

Single cell suspensions were obtained by detaching cells using cell scrapers without trypsin to rule out potential proteolytic effect of trypsin on surface proteins. Cells then were incubated with Fc block at a concentration of 0.5ug/mL at room temperature for 30 min. Cells were stained for cellular receptor for adenovirus and coxsackievirus (CAR) using anti-CAR antibody (clone RmCB, Millipore) for 30 min (or mock-treated), washed, and subsequently stained with secondary antibody, goat anti-mouse IgG-FITC (Santa Cruz, 0.5 ug/ml) for 30 min. Expression of CAR was determined by flow cytometry (Beckman Coulter). Analysis was conducted using FlowJo (Treestar, Ashland, OR).

Animal experiments.

Mice were handled and maintained under veterinary supervision in accordance with institutional guidelines and under a University of North Carolina at Charlotte Animal Care and Use Committee (IACUC) approved protocol. 6-8 week old, male, athymic nude mice (Hsd:Athymic Nude-Foxn1^{nu}, Harlan Laboratories, Inc., Frederick MD) were subcutaneously injected with one of 4 human PDA cell lines. All cell lines used in animal experiments were tested negative for an extended panel of pathogens (MIA PaCa2, SU.86.86, and Panc-1 were tested by Charles River Laboratories and HPAF-II was tested by Bioreliance). Based on preceding titration experiments (data not shown), mice were injected with: 5×10^6 Mia PaCa2, 5×10^6 Panc-1, 3×10^6 HPAF-II, and

3×10^6 SU.86.86 cells (in 100 μ l of PBS) into the right flank (n=18 per group). Two additional untreated age-matched mice were used in this experiment to compare body weights with the treated experimental mice. Mice were palpated starting at 9 d post tumor injection. Tumors were established by day 13 and mice were randomly divided into 3 groups (n=6 per group). One group served as a control and received one intratumoral (IT) administration of 50 μ l PBS only. The other two groups were administered once with VSV- Δ M51-GFP or CRAd-dl1520 IT with a dose of 5×10^7 CIU in 50 μ l PBS. Dose was determined based on CIU established on A549 cells for both viruses. Tumor size was monitored by caliper measurements every other day, and body weight was measured once weekly. Tumor weight was calculated according to the formula: grams = [(length in cm) x (width in cm)²]/2. Upon sacrifice, tumor and brain tissue were harvested and tested for the presence of VSV- Δ M51-GFP. Data were analyzed using GraphPad software and are expressed as mean \pm standard deviation.

3.3 Results

Susceptibility of PDA cell lines to viral oncolysis.

The susceptibility of human PDA cells to virus-mediated oncolysis was tested in a panel of 13 clinically relevant PDA cell lines derived from primary PDA tumors or PDA metastases to the liver and lymph nodes. In addition to PDA cell lines, the immortal human pancreatic duct epithelial cell line (HPDE), which retains a genotype similar to pancreatic duct epithelia and is non-tumorigenic in nude mice (Furukawa et al. 1996), was employed as a “benign” control cell line to determine virus specificity towards PDA cells. In addition to VSV-wt, we tested two additional VSV variants: VSV- Δ M51-GFP and VSV-p1-GFP (Fig. 16), with a particular focus on VSV- Δ M51-GFP (Wollmann 2010). Several previous studies showed that VSV mutants with the deletion of methionine at position 51 (Δ M51) of the matrix (M) protein exhibited good oncolytic potential but lack undesirable neurotoxicity (Stojdl 2003; Ebert et al. 2005; Goel et al. 2007; Ahmed 2008; Wu 2008; Wollmann 2010). A similar phenotype was recently demonstrated for VSV-p1-GFP (Wollmann 2010). To evaluate the relative efficacy of VSV as an OV, we compared VSV variants to four other viruses: SeV-GFP, RSV-GFP, CRAd-dl1520, and CRAd-hTERT (Fig. 16). SeV-GFP and RSV-GFP are also NNS RNA viruses shown to have oncolytic potential (Kinoh 2004; Kinoh 2008; Yonemitsu 2008; Echchgadda et al. 2009; Komaru 2009; Echchgadda et al. 2011), while CRAbs have shown some success in several PDA cell lines in vitro and in vivo (Kuhlmann et al. 2008; He et al. 2009; Huch 2009), although they have not been tested in most of the PDA cell lines used in this study. The inclusion of additional viruses would also help to

discriminate between a virus-specific and general resistance phenotype if any PDA cell lines were identified as non-permissive to VSV.

To analyze the ability of viruses to kill cancer cells, PDA cell lines were infected at either a low MOI (0.01 CIU/cell) or a higher MOI (1.0 CIU/cell) and at 5 d p.i. an MTT cell viability assay was performed. The MOI values for each virus/cell line combination are relative and calculated based on titration of all VSV variants and SeV on 4T1 cells, and RSV and CRAds on HeLa cells. These two reference cell lines (4T1 and HeLa) were selected based on their abilities to support robust replication of viruses used in this study. Therefore, for each MOI, the same amount of virus stock was added to each cell line. VSV-wt, VSV- Δ M51-GFP, and VSV-p1-GFP all caused significant death in the majority of cell lines at both high (Fig. 17A) and low (Fig. 17B) MOI compared to mock infected cells. In general, at the higher MOI, VSVs and CRAds caused more significant cell death than to SeV-GFP and RSV-GFP (Fig. 17A). At the lower MOI VSVs caused more significant cell death compared to all other viruses including CRAds (Fig. 17B).

Several PDA cell lines showed varying degrees of resistance to oncolysis by VSVs, with HPAF-II, Hs766T and BxPC-3 displaying the strongest resistance. Interestingly, we observed a substantial difference in susceptibilities of HPAF-II, Hs766T and “benign” HPDE to oncolysis with different VSV variants. These cell lines were effectively killed by VSV-wt (both MOIs) and VSV-p1-GFP (HPAF-II at high MOI only) at 5 d p.i. but were resistant to VSV- Δ M51-GFP, even at MOI 1. Importantly, all these three PDA cell lines were also among the most resistant to other tested viruses suggesting that general antiviral mechanisms may contribute to their phenotype (addressed later).

To analyze the kinetics of PDA cell death following VSV- Δ M51-GFP (Fig. 18) or VSV-wt (data not shown) infection, cells were infected at MOI 0.001, 0.1 or 1 CIU/cell (Fig. 18) and cell viability was analyzed at different time points. The majority of cell lines had significantly decreased viability after infection with VSV- Δ M51-GFP at any tested MOI. Consistent with the data presented in Figure 17, HPAF-II, Hs766T and BxPC-3 were most resistant to VSV-mediated cell death in the presence of any amount of VSV- Δ M51-GFP. CFPAC-1, HPAC and “benign” HPDE cells were resistant to VSV- Δ M51-GFP only when infected with the lowest MOI (0.001).

Permissiveness of PDA cell lines to viral infection.

The failure of OVVs to kill cancer cells can be explained by their inability to infect and/or replicate in these cells, although cellular defects in apoptosis may also be responsible for the defect in virus-mediated oncolysis. To determine whether variations in viral oncolysis observed between different PDA cell lines were due to different permissiveness of these cell lines to virus infection, monolayer cultures of PDA cells were infected with serial virus dilutions. To test whether the differences between cell line permissiveness to virus infection were specific for VSVs or general (e.g. if they have intact antiviral responses), we examined all viruses (Fig. 16) except for RSV. The infectious foci of VSV- Δ M51-GFP, VSV-p1-GFP and SeV-GFP were analyzed by fluorescent microscopy at 24 (VSV) or 48 (SeV) h p.i., respectively. The number and size of viral plaques produced by VSV-wt, CRAd-d11520 and CRAd-hTERT were analyzed by ICC as described in Materials and Methods. Virus permissiveness in Figure 19 is expressed as the ratio of virus titer on the pancreatic cell line under study to the titer on a

reference cell line (4T1 or HeLa) such that higher numbers indicate greater permissiveness.

The degree of curvature in Figure 19 indicates that that the adenoviruses have less variability among PDA cells than VSV and SeV. Interestingly, while BxPC-3 and Hs766T were resistant to all tested viruses, HPAF-II showed an intermediate permissiveness to infection by both adenoviruses (Fig. 19; Fig. 20 for CRAd-d11520), although this PDA cell line was resistant to virus-mediated oncolysis by either CRAd (Fig. 17). As shown in Figure 19, the majority of cell lines were highly permissive to VSV- Δ M51-GFP infection with a relative ratio greater than or close to 1 ($\log_{10}=0$) (AsPC-1, SU.86.86, Capan-1, Panc-1, MIA PaCa2, Suit2 and Capan-2). In these cell lines, we observed rapid spread of VSV- Δ M51-GFP forming large infectious foci (filled circle symbol in Fig. 19; large GFP foci in Fig. 20). Cell lines less permissive to VSV- Δ M51-GFP infection include “benign” HPDE cells (6.6 times less with very small foci) as well as T3M4 (2.2 times less than 4T1), CFPAC-1 (3.8 times less), and HPAC (10 times less), all of which also formed smaller infectious foci at 16 h p.i. BxPC-3, HPAF-II and Hs766T appeared highly resistant to VSV- Δ M51-GFP infection, with relative susceptibilities much less than 4T1 (62,971 and 25,385 times less, respectively) and infectious foci being much smaller in size than all other cell lines tested (Fig. 20). VSV- Δ M51-GFP was also analyzed at 5 d p.i., when the majority of cell lines highly permissive to VSV- Δ M51-GFP infection were no longer viable and detached from the culture plastic. However, HPAF-II, BxPC-3 and Hs766T cells remained attached to the plastic with decreased GFP intensity; again indicating VSV- Δ M51-GFP infection is restricted in these cell lines (data not shown).

SU.86.86 showed a very intriguing phenotype by being highly permissive to VSVs and SeV, but resistant to both CRAd-dl1520 and CRAd-hTERT. To test whether this cell line may lack Coxsackievirus and adenovirus receptor (CAR) required for adenovirus attachment (which would explain this phenotype) (Kuhlmann et al. 2008; He et al. 2009; Huch 2009), we analyzed all PDA cell lines for CAR expression by flow cytometry and found that SU.86.86 was the only cell line completely lacking CAR (Fig. 21), while all other cell lines (including HPAF-II, Hs766T and BXPC-3 displaying general resistance phenotype) had varying but detectable levels of CAR (data not shown), which is in agreement with our data (Figures 19 and 20) that these cell lines (unlike SU.86.86) have reasonably good susceptibility to both adenoviruses, also indicating that they are not defective in CAR expression. Although other factors may also contribute to the resistance of SU86.86 to CRAbs, the lack of CAR expression alone might be a sufficient factor responsible for this phenotype.

To examine if reduced permissiveness to VSV- Δ M51-GFP also resulted in a decrease in new viral protein synthesis, lysates were prepared from uninfected cells and from cells infected with VSV- Δ M51-GFP at MOI 1 and 10 CIU/cell and harvested at 16 h p.i. Equal amounts of total protein were then examined by Western blot for both VSV proteins and GFP expression. Expression levels of viral proteins within the different cell lines were in agreement with GFP protein expression (Fig. 22). Protein expression (see GFP level measurements in Fig. 22) was also generally consistent with cell line permissiveness and oncolysis, especially when protein accumulation is compared after lower MOI infection. Viral protein expression was strongly reduced in BxPC-3, HPAF-II, Hs766T and “benign” HPDE cells which are the most “non-permissive” and all

demonstrated small foci sizes when infected with VSV- Δ M51-GFP (Fig. 19). Viral protein expression was also reduced in CFPAC-1 and HPAC cells which had reduced permissiveness and medium foci sizes.

To directly examine growth potential of VSVs in resistant cell lines, we tested all 3 VSVs in the majority of PDA cell lines (and in “benign” HPDE cells) using a standard one-step growth kinetics assay (Fig. 23). In general, our data show that while all tested cell lines were able to support productive replication of VSVs, the lowest production was observed in “benign” HPDE cells and in most PDA cell lines displaying resistant phenotype. Also, most cells showed very similar growth kinetics for all 3 viruses, while HPAF-II supported significantly lower level of VSV- Δ M51-GFP production compared to other VSVs. This result may explain at least partially why HPAF-II cells were particularly resistant to VSV- Δ M51-GFP (Fig. 17A) BxPC-3 cells showed surprisingly high level of new particle production when infected at MOI 10. However, it is important to note that MOI 10 used for one-step growth kinetics is never attainable during oncolytic treatment in vivo. The experiments on virus-mediated cell death shown in Figures 73 and 18 were conducted at more realistic MOIs 0.001 to 1 (maximum).

Timing and cellular factors of resistance of PDA cell lines to VSV- Δ M51-GFP

To analyze why PDA cells differ in their permissiveness to VSV- Δ M51-GFP, we looked at the early stages of virus infection and at cellular characteristics that could explain the observed differences. Antigenome and VSV N mRNA synthesis was determined by Northern blot of total RNA isolated at 4 h p.i. from cells untreated or treated with cycloheximide and infected with VSV- Δ M51-GFP at MOI 10 (Fig. 24 and Table 5). Cycloheximide blocks new protein synthesis and thereby viral genome

synthesis and secondary transcription. Expression of both VSV N mRNA and anti-genomic RNA were strongly reduced in BxPC-3, HPAC, HPAF-II, Hs766T and somewhat reduced in CFPAC-1 cells, consistent with the reduced viral protein synthesis and permissiveness to VSV- Δ M51-GFP infection seen in these cell lines. Interestingly, RNA synthesis in “benign” HPDE cells was quite robust despite low protein synthesis 16 h p.i. (Fig. 22) and reduced permissiveness in this cell line, suggesting a block at a later stage of viral infection. In all cases where secondary transcription was reduced, primary transcription was reduced proportionately (Table 5). This suggests that in cell lines with lower mRNA synthesis, viral genome release into the cytoplasm was inhibited, and that for genomes that were released, early infection proceeded normally.

VSV is sensitive to Type I IFN responses. However, many different tumor types are known to lack these responses, allowing VSV to productively infect cancer cells while sparing healthy cells (Lichty et al. 2004; Barber 2005). Here, we wanted to test the hypothesis that the resistance of some PDA cell lines to VSV (and other viruses) was a result of their intact IFN responses. To determine if PDA cell lines were sensitive to Type I IFN, all cells were mock treated or treated with 5000 U/ml IFN- α for 24 h prior to infection with serial dilutions of VSV- Δ M51-GFP. A titer ratio for mock treated to IFN- α treated cells was determined for each PDA cell line (Fig. 25). We observed that certain cell lines did not significantly suppress VSV- Δ M51-GFP infection in response to IFN- α . VSV- Δ M51-GFP titers were no more than 26-fold reduced following IFN treatment in Panc-1, SU.86.86, MIA PaCa2, and HPAC cells, while Capan-2, Hs766T, T3M4 and “benign” HPDE cells showed an intermediate sensitivity to IFN- α . HPAC displayed an interesting phenotype with comparable titers with or without IFN treatment; however,

IFN treated HPAC cells required an additional day for visible foci to appear.

Surprisingly, several PDA cancer cell lines were highly responsive to IFN- α (Capan-1, AsPC-1, HPAF-II, BxPC-3, Suit2 and CFPAC-1). Among these IFN-sensitive cells are AsPC-1, Capan-1 and Suit2, which support robust infection of VSV- Δ M51-GFP in the absence of IFN- α pre-treatment.

To further study the role of IFN in the resistance of PDA cells to VSV, we examined the abilities of PDA cell lines to produce IFN alpha and/or beta in response to VSV- Δ M51-GFP infection (MOI of 10 CIU per cell) at 18 h p. i. As expected, significant amounts of IFN-beta were produced by “benign” HPDE cells, which are expected to retain normal antiviral responses (Fig. 26). Importantly, all three cell lines (HPAF-II, HPAC and Hs766T) producing significant amount of IFN-beta at 18 h p.i. were among the most resistant cell lines (Fig. 26). As illustrated in Table 6, except for BxPC-3, all PDA cell lines highly resistant to VSV show an HPDE-like phenotype characterized by both the production of IFN-beta and sensitivity to IFN treatment. In addition, our data experimentally explain the phenotypes AsPC-1, Suit2, and Capan-1 which are sensitive to IFN but support robust virus infection without added IFN, as they all are defective in IFN production. Interestingly, we were unable to detect any significant production of IFN-alpha in response to virus infection by any tested cell line at 18 h p.i. (data not shown), however it is produced later than IFN-beta. Future experiments will analyze PDA cells for production of various IFNs at different time points after infection.

Together, our data show surprising diversity among PDA cells in regards to their ability to produce and respond to Type I IFN. Moreover, we demonstrate that a

combination of IFN sensitivity and IFN-beta production may be used to predict responsiveness of most PDA cells to oncolytic treatment.

Efficacy of VSV-ΔM51-GFP and CRAd-dl1520 in nude mice bearing human PDA tumors.

To test the efficacy of VSV-ΔM51-GFP *in vivo* and to determine the relevance of our *in vitro* results to an *in vivo* situation, we chose four cell lines for *in vivo* testing based on our *in vitro* virus permissiveness and oncolysis experiments. MIA PaCa2 and Panc-1 are highly permissive to both VSV-ΔM51-GFP and CRAd-dl1520, SU.86.86 is highly permissive to VSV-ΔM51-GFP but not CRAd-dl1520, and HPAF-II has limited permissiveness to both VSV-ΔM51-GFP and CRAd-dl1520 (Fig. 17-20). These human pancreatic cancer cell lines were injected subcutaneously into the right flank of male nude mice (n=18 per cell line). Once the mice developed palpable tumors (5-7 mm) they were divided equally into three groups (n=6). A control group received an IT injection of PBS, one group received an IT injection of 5×10^7 CIU VSV-ΔM51-GFP, and one group received an IT injection of 5×10^7 CIU CRAd-dl1520. The mice were monitored daily for signs of distress and tumor size was measured every other day for 14 days. VSV-ΔM51-GFP and CRAd-dl1520 had the greatest therapeutic effect in mice bearing Panc-1 and MIA PaCa2 tumors (Fig. 27). VSV-ΔM51-GFP seemed to stabilize SU.86.86 tumor growth compared to treatment of SU.86.86 tumors with CRAd-dl1520 and PBS, which had no effect on tumor growth (Fig. 27). SU.86.86 grew more rapidly than all other cell lines *in vivo* and several tumors became ulcerated over the course of the experiment (Fig. 27). While mice bearing SU.86.86 tumors showed no signs of distress at any point during the experiment, several were euthanized at an earlier time point due to large tumor size

(day 21 instead of day 25). Tumor growth continued in the presence or absence of VSV- Δ M51-GFP and CRAd-dl1520 for mice bearing HPAF-II tumors (Fig. 27). In general, our in vivo experiments closely mimicked our in vitro results. Fourteen days post injection with VSV- Δ M51-GFP, CRAd-dl1520 or PBS, all mice were euthanized and tumors were harvested and wet weight and presence of virus was determined.

It has been demonstrated that VSV-wt can cause encephalitis in mice; however, VSV- Δ M51-GFP is a non-neurotropic OV (Wollmann 2010). In agreement with this, animals infected with VSV- Δ M51-GFP showed no signs of encephalitis or distress over the course of the experiment. Nevertheless, brain tissues of VSV- Δ M51-GFP-infected animals were analyzed for the presence of virus by standard plaque assay on BHK-21 cells with no VSV- Δ M51-GFP being detected. Interestingly, despite the robust oncolytic effect achieved for animals bearing Panc-1 and MIA PaCa2 following IT infection with VSV- Δ M51-GFP, when a similar analysis was conducted on tumor samples, only two samples (one SU.86.86 and one MIA PaCa2 sample) had detectable VSV- Δ M51-GFP present at 14 d p.i. (data not shown).

3.4 Conclusions

In this study, we have evaluated for the first time VSV as an OV against pancreatic cancer cells. VSV variants showed superior oncolytic abilities compared to other viruses and were effective against the majority of the 13 tested human PDA cell lines. We also identified several cell lines highly resistant to oncolytic virotherapy by VSV and/or other tested viruses.

Among VSV variants, we focused primarily on VSV- Δ M51-GFP because several previous studies showed that VSV variants with Δ M51 mutation were effective OVs with no neurotoxicity in animals (Stojdl 2003; Ebert et al. 2005; Goel et al. 2007; Ahmed 2008; Wu 2008; Wollmann 2010). To evaluate the relative efficacy of VSV as an OV, we initially compared VSV variants to four other viruses. We chose CRAd-dl1520 (also known as “ONYX-15”) as a relevant control for further in vitro and in vivo experiments, as this DNA virus is unrelated to VSV, has been tested in several clinical trials, and has shown some success in previous PDA studies (Kasuya et al. 2005; Crompton and Kirn 2007). It is important to point out that although our in vitro data suggest a possible use of CRAds for PDA treatment, any viable strategy for treatment of patients using CRAds remains to be determined due to some of their reported limitations, including their dependence of CAR expression in target cells, their quick elimination from the bloodstream by the liver, inactivation by binding to blood cells and other components of the immune system, as well as their limited spread throughout the tumor (Kuhlman et al. 2008; He et al. 2009; Huch 2009).

Our in vitro experiments indicated a great variability in permissiveness of PDA cell lines to all viruses. Overall, VSV variants were the most effective, but even for VSVs, some cell lines, including HPAF-II, Hs766T and CFPAC-1, were less effectively killed by VSV- Δ M51-GFP than by VSV-wt and VSV-p1-GFP. There are two major hypotheses explaining varying susceptibility of PDA cell lines to oncolysis by a particular virus in vitro. First, PDA cells may differ in their susceptibility to virus infection and/or their ability to support virus replication. This may happen because PDA cells may lack key cellular factors (e.g., receptors) required for successful virus infection or because resistant cells have intact antiviral responses preventing successful virus spread. Alternatively, some PDA cells may have defective apoptotic pathways, so that even if a virus can successfully infect and replicate in these cells, they are not efficiently killed by apoptosis.

The oncolytic potential of viruses is generally contingent on their ability to infect and replicate in these cells. In our study, PDA cell permissiveness to all viruses closely mirrored our cell death analysis, with several cell lines (HPAF-II, Hs766T and BxPC-3) showing varying degrees of resistance to all tested viruses. The six least permissive cell lines were all defective in cell killing for at least some of the MOIs tested. Five of these cell lines, BxPC-3, HPAF-II, HPAC, Hs766T and CFPAC showed low levels of early (4 h p.i.) viral RNA synthesis (including primary transcription of viral genome) when infected with VSV- Δ M51-GFP compared to the more permissive cell lines, indicating a possible defect at very early stage in infection, such as attachment, entry or endosomal escape. Experiments are underway in these PDA cell lines to further define the affected steps in viral infection and the responsible cellular mechanisms. In contrast to VSV-

resistant PDA cell lines, in “benign” HPDE cells (also resistant to VSV), early viral mRNA and genome synthesis equaled that found in many permissive cell lines, but viral protein synthesis at 16 h p.i and virion production were sharply reduced, suggesting a defect at later stages of viral infection. This phenotype is expected for “benign” cells with intact innate antiviral responses.

To address differences in permissiveness to VSV in PDA cell lines, we also looked at their abilities to produce and respond to Type I IFN. In general, many tumor cells are defective in producing Type I IFNs but may remain sensitive to Type I IFN, which could be produced by infected benign cells that surround the tumor. Still other tumor cells may retain the ability to produce their own IFN (Stojdl et al. 2000; Naik and Russell 2009). Responsiveness of cancer cells to IFN could be an important factor in predicting their behavior in vivo, where VSV infection would induce IFN production in surrounding healthy tissues, thus limiting oncolytic potential towards cancer cells sensitive to IFN. Our data showed surprising diversity among PDA cells in regard to their ability to produce and respond to Type I IFN (Table 6). With the exception of BxPC-3, all other VSV-resistant PDA cell lines were characterized by both the production of IFN-beta and sensitivity to IFN treatment. The same phenotype was shown by “benign” HPDE cells, which are expected to retain normal antiviral responses. The VSV-resistant phenotype of BxPC-3 in vitro (sensitive to IFN but does not produce IFN-beta) could be due to an IFN-independent block of virus infection. Interestingly, we identified some PDA cell lines (AsPC-1, Suit2, and Capan-1) that are responsive to IFN, but highly susceptible to infection in vitro (without added IFN) as they all are defective in IFN production. High heterogeneity in response to type I IFN has been reported in

several other cancer types, including mesothelioma (Saloura et al. 2010), melanomas (Linge et al. 1995; Wong et al. 1997), lymphomas (Sun et al. 1998), bladder cancers (Matin et al. 2001), renal cancers (Pfeffer et al. 1996), and likely in other types (Stojdl 2003). Our data suggest that a combination of IFN sensitivity and IFN-beta production may be used to predict responsiveness of most PDA cells to oncolytic treatment.

Together, our data suggest that VSV-resistant cell lines have more than one “defect” responsible for their virus resistant phenotype. If their resistance was solely dependent on their intact IFN pathway, we would expect them to have phenotype similar to “benign” HPDE cells. HPDE cells do not have any defects in early steps of VSV infection (demonstrated by “normal” RNA synthesis including primary transcription of viral genome at 4 h p.i.), but robust Type I IFN responses inhibit consequent virus replication resulting in very low protein accumulation at 16 h p.i. However, unlike HPDE cells, all PDA cell lines highly resistant to VSV also showed defective early viral RNA synthesis suggesting that they have some defects inhibiting early steps of VSV infection (e.g. attachment or entry).

Most of our data show a correlation between permissibility of PDA cells to VSV infection and its oncolytic potential. However, if cells are successfully infected at high MOI (one-step infection), they are able to successfully produce new viral particles. BxPC-3 showed surprisingly high production of new particle when infected at MOI 10. Interestingly, it is also the only one of the most resistant cell lines that did not produce significant amounts of IFN-beta (Fig. 26 and Table 6). At the same time, BxPC-3 were characterized by deficient RNA synthesis at 4 h p.i. suggesting that BxPC-3 have some defects in virus attachment/internalization or other early step in VSV infection. It also

showed a low levels of viral (and GFP) protein synthesis when BxPC-3 were infected at lower MOI of 1 (compare Figure 18 for AsPC1 and BxPC-3 at MOI 1 and 10). It is important to note that MOI 10 infection used in Figure 23 for one-step growth kinetics is never attainable during oncolytic treatment *in vivo*. The experiments on virus-mediated cell death shown in Figures 17 and 18 were conducted at more realistic MOIs between 0.001 and 1.

Previous studies have shown that many cancer cells are able to inhibit apoptosis to allow for prolonged proliferation (Hamacher et al. 2008). As VSV has been shown to cause cell death by apoptosis via either the intrinsic or extrinsic pathway or both (Gaddy and Lyles 2005; Gaddy and Lyles 2007; Sharif-Askari et al. 2007; Cary et al. 2011), cell lines with decreased expression or activation of certain apoptotic proteins have the potential of limiting/delaying cell death following VSV infection. Furthermore, differences in permissiveness to the VSV variants could be due to differences in their mechanisms of cell death induction. It has been demonstrated that VSV-wt induces apoptosis via the mitochondrial pathway due to wt M protein inhibiting gene expression, while VSV- Δ M51-GFP, with a mutant M protein, induces apoptosis primarily via the death receptor pathway (Gaddy and Lyles 2005). While we cannot fully address these possibilities at this point, our preliminary experiments show significant increases in caspase-3 cleavage following VSV- Δ M51-GFP infection in all cell lines except Hs766T and HPAC at 17 h p.i. (data not shown). More studies are needed to determine whether reduced level of apoptotic response or the delayed induction of apoptosis in some of these cell lines plays a role in restricting VSV oncolysis. These defects could also (in addition

to intact IFN pathways) explain why cell lines resistant to VSV are also resistant to other, unrelated, viruses.

Based on our in vitro studies we chose 4 cell lines with varying permissiveness to VSV- Δ M51-GFP and CRAAd-dl1520 to determine if our in vitro studies are relevant in vivo. We observed in vitro that MIA PaCa2 and Panc-1 are highly permissive to both VSV- Δ M51-GFP and CRAAd-dl1520, SU.86.86 is highly permissive to VSV- Δ M51-GFP but not CRAAd-dl1520, and HPAF-II has limited permissiveness to both. The induced tumors in nude mice showed the same permissiveness pattern as observed in vitro indicating in vitro testing can be used to identify cancers resistant to a particular virus. It is important to emphasize that the ability of a virus to kill cancer cells in vitro or even in vivo (in nude mice) would not guarantee its efficacy in cancer patients due to complex tumor microenvironments and compromised immune responses (Breitbach et al. 2010). However, our data clearly show that if cells are resistant to viral oncolysis in vitro, it is highly unlikely that they could be effectively eliminated in vivo, suggesting the importance of in vitro pretesting (when possible) in identifying virus-resistant cancers.

There are several important characteristics of VSV which in combination make it more attractive candidate for PDA treatment compared to other tested viruses: (i) there are few if any restrictions to VSV attachment and entry as it is believed to be not dependent on any host receptor in target cells; (ii) there is no preexisting immunity against VSV in humans; (iii) VSV is not considered a significant human pathogen, and several VSV mutants, including VSV- Δ M51-GFP and VSV-p1-GFP, are not neurotropic but retain their oncolytic activity; (iv) cellular uptake in many mammalian cell types occurs very rapidly and there is no cell cycle dependency; (v) our comparative analysis

here demonstrated that VSV variants showed superior oncolytic abilities compared to other viruses, and some cell lines that exhibited resistance to other viruses were successfully killed by VSV.

There are several potential options for virus-resistant cancer cells. Prescreening cells against an array of different OVs could identify the best option for treating a particular tumor. For example, VSV- Δ M51-GFP is more suitable than CRAds for treating PDAs similar to SU.86.86 cells which showed a complete lack of CAR expression required for adenovirus attachment (data not shown). In the cases where cells are less permissive to VSV- Δ M51-GFP than VSV-wt or VSV-p1-GFP (HPAF-II and Hs766T), the use of VSV-p1-GFP might be a better option, especially because this virus is also non-neurotoxic *in vivo*. Combination therapies have also demonstrated some success. Virotherapy in combination with chemotherapy can enhance the oncolytic effect compared to either treatment alone (Ottolino-Perry et al. 2010). Treating tumors with more than one OV (combined virotherapy) could also potentially lead to enhanced oncolysis (Le Boeuf et al. 2010). Importantly, understanding the mechanisms and identifying potential biomarkers of resistance is critical for the development of prescreening approaches and individualized oncolytic virotherapy against PDA.

3.5 Figure 16

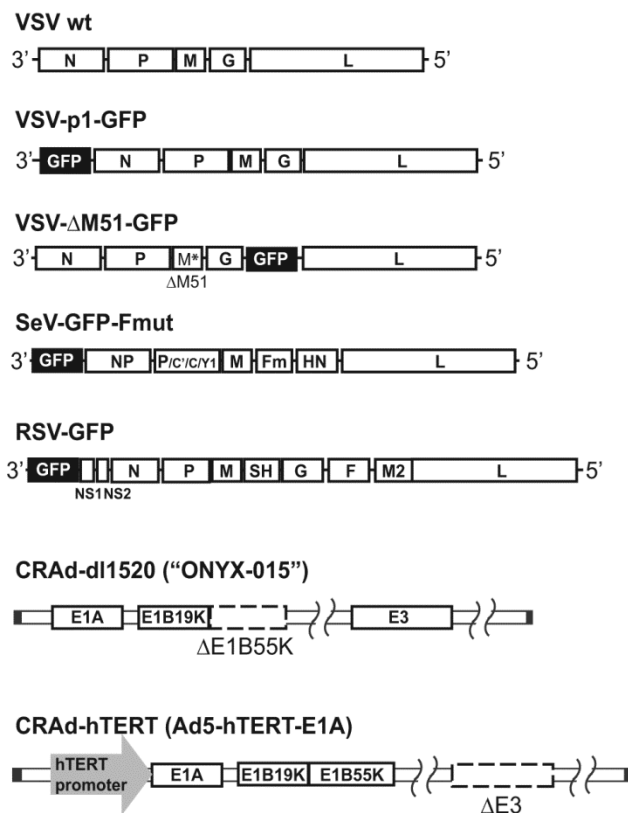


Figure 16. Viruses used in this study. VSV-p1-GFP has the GFP ORF inserted in position one of the viral genome resulting in attenuation of the virus. VSV- Δ M51-GFP has a deletion at amino acid position 51 of the matrix (M) protein reducing its ability to suppress host immunity. In addition, VSV- Δ M51-GFP has the GFP ORF inserted in position 5 of the viral genome. SeV-GFP has the GFP ORF inserted at position one of the viral genome and a mutation in the cleavage site of the fusion (F) protein allowing for F activation and production of infectious virus particles in cell without trypsin addition. RSV-GFP has GFP ORF inserted at position one of the viral genome. CRAd-dl1520 is attenuated by deletion of a large part of the coding sequence for the E1b55k viral gene product. CRAd-hTERT is a human telomerase reverse transcriptase (hTERT)-dependent CRAd.

3.5 Figure 17

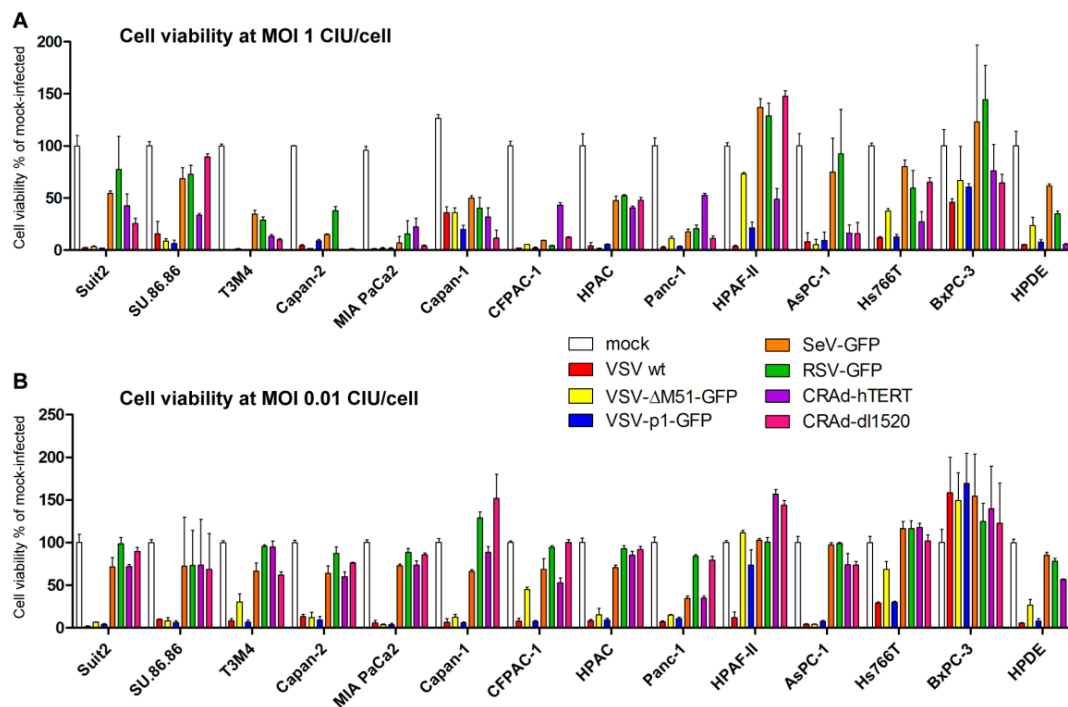


Figure 17. PDA cell viability following infection with viruses. PDA cell lines and HPDE were seeded in 96-well plates so that they reached 80% confluency at 24 h. The cells were infected with the indicated viruses at MOI of 1 (A) or 0.01 (B) CIU/cell or mock infected. Cell viability was analyzed at 5 d p.i. by an MTT cell viability assay and expressed as a ratio of virus-treated to mock-treated cells for each time point. All MTT assays were done in triplicate and the data represent the mean \pm standard deviation. Cell lines are grouped arbitrarily based on their susceptibility to virus-induced oncolysis.

3.5 Figure 18

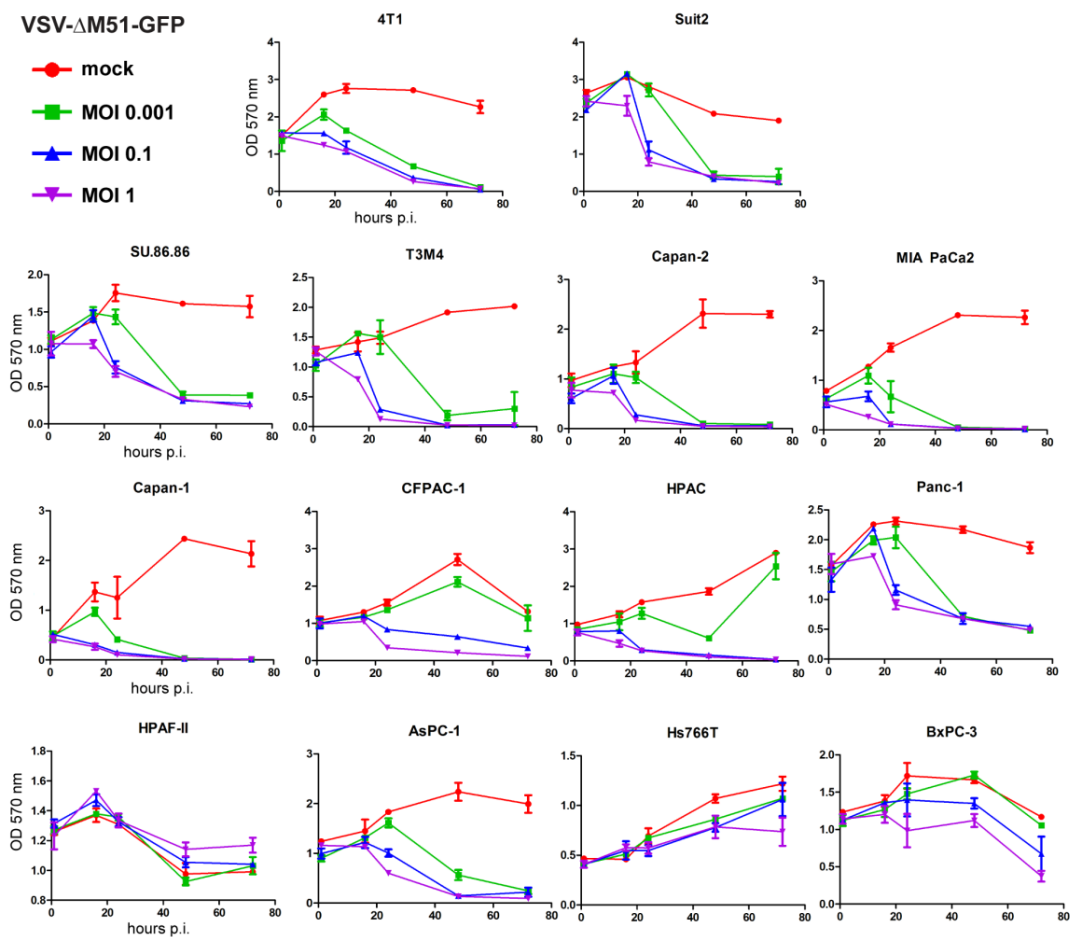


Figure 18. Kinetics of cytopathogenicity of VSV- Δ M51-GFP in PDA cells. Cells were seeded in 96-well plates so that they reached 50% confluency at 24 h. Cells were then mock infected or virus infected at low (0.001 CIU/cell), intermediate (0.1 CIU/cell), or high MOI (1 CIU/cell). An MTT cell viability assay was performed at 1, 16, 24, 48, and 72 h p.i. Cell viability is expressed as the % of mock-infected at 1 h p.i. All MTT assays were done in triplicate and the data represent the mean \pm standard deviation.

3.5 Figure 19

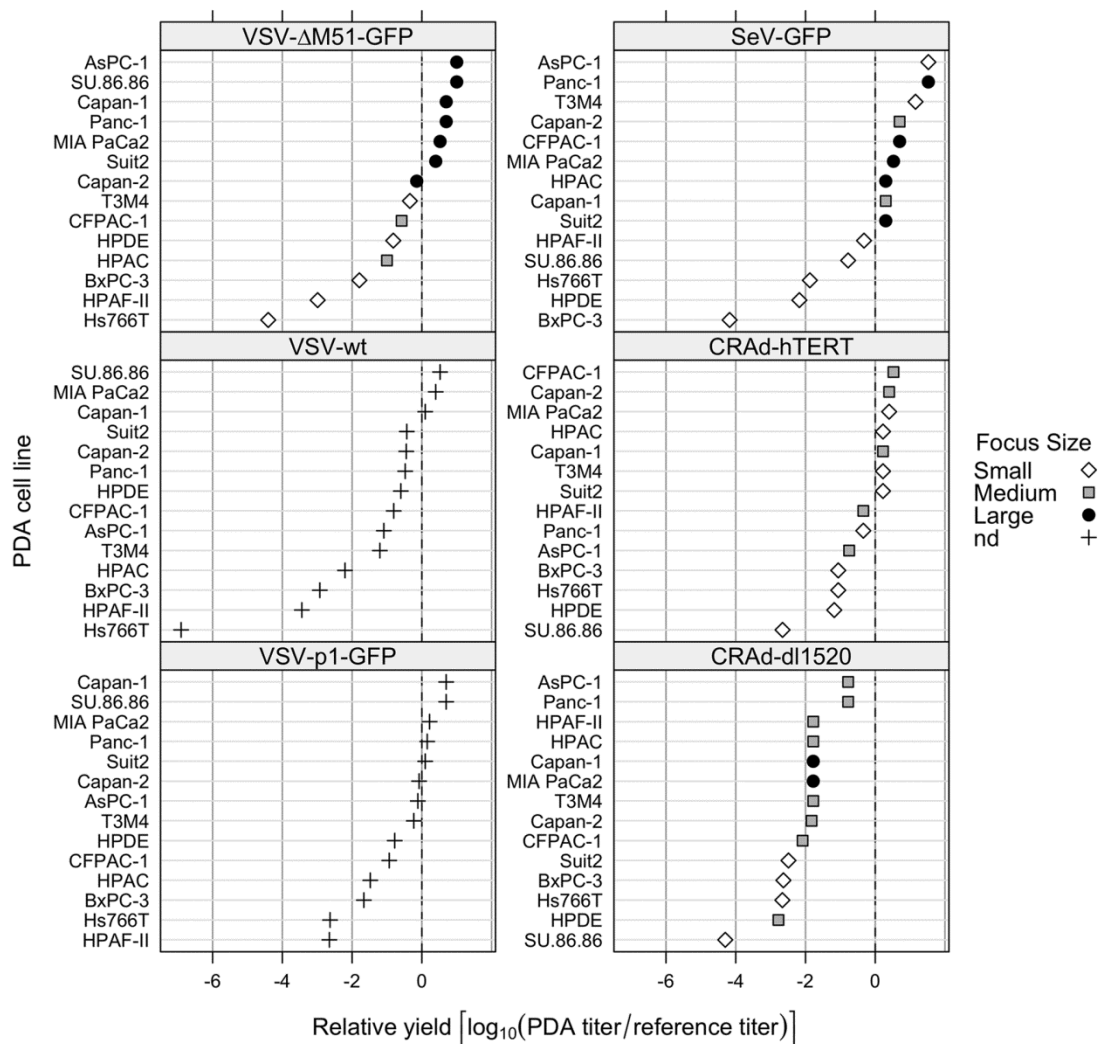


Figure 19. Permissiveness of PDA cell lines to different viruses. PDA cell lines and HPDE were incubated with serial dilutions of viruses. The infectious foci of VSV- Δ M51-GFP, VSV-GFP(p1) (24 h p.i.) and SeV-GFP (48 h p.i.) were analyzed by fluorescent microscopy. The infectious foci of VSV-wt, CRAd-dl1520 and CRAd-hTERT were analyzed by ICC as described in Materials and Methods. Virus permissiveness (relative yield) is expressed as the \log_{10} of the ratio of virus titer on the pancreatic cell line under study to the titer on a reference cell line (4T1 for VSV and SeV; HeLa for CRAds). The following titers were observed on reference cell lines: VSV-wt (1.6×10^9 CIU/ml on 4T1), VSV- Δ M51-GFP (3.3×10^8 CIU/ml on 4T1), VSV-p1-GFP (3×10^7 CIU/ml on 4T1), SeV-GFP (1.5×10^7 CIU/ml on 4T1), CRAd-hTERT (1.5×10^7 CIU/ml on HeLa) and CRAd-dl1520 (4×10^8 CIU/ml on HeLa). Relative yield 0 indicates that the PDA cell line is equally permissive to the virus as a reference cell line, while higher numbers indicate greater permissiveness. Area of infectious foci was analyzed using Image J software (NIH): "Small = area <10 (surface area units); Medium = area 10-30; Large = area >30. nd = not done.

3.5 Figure 20

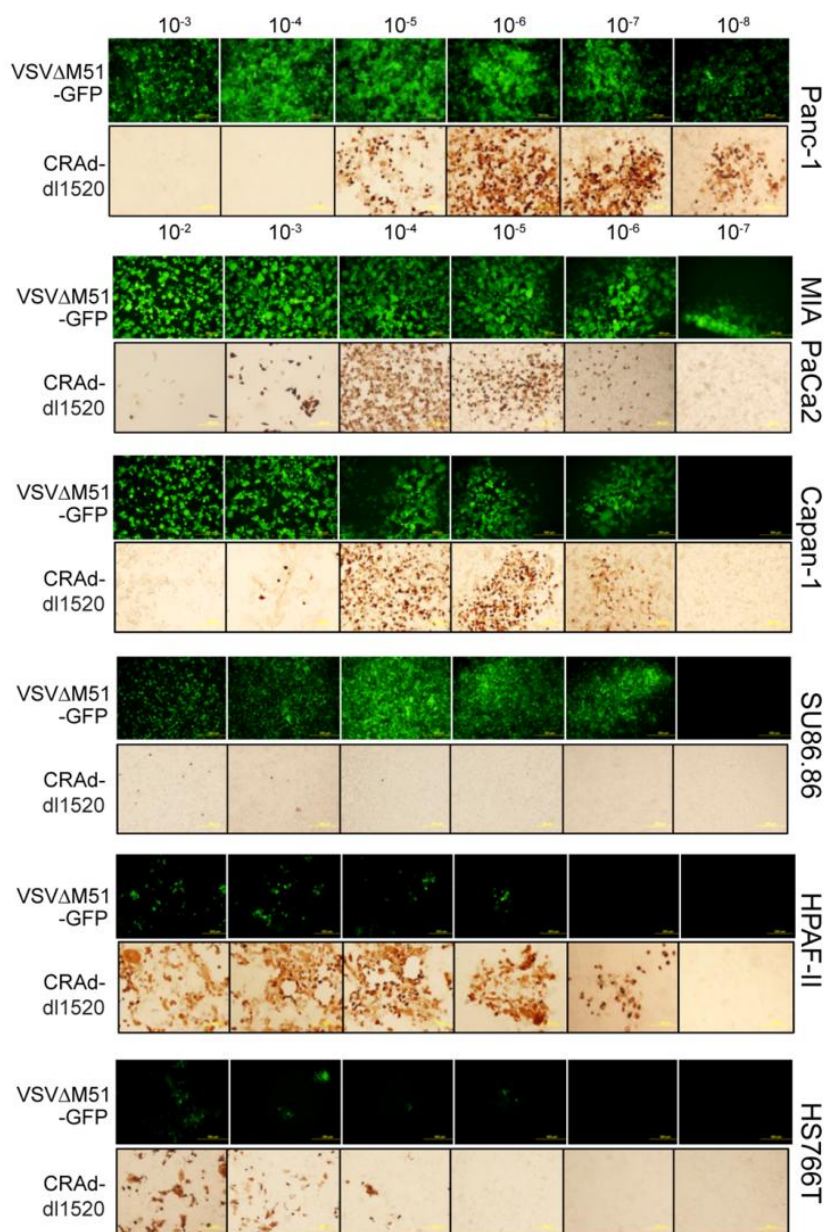


Figure 20. Permissiveness of selected PDA cell lines to virus infection. Representative PDA cell lines (not all shown) were incubated with serial dilutions of VSV- Δ M51-GFP and CRAd-dl1520. The infectious foci of VSV- Δ M51-GFP were analyzed by fluorescent microscopy at 24 h p.i. The infectious foci of CRAd-dl1520 were analyzed by ICC at 5 d p.i as described in Materials and Methods.

3.5 Figure 21

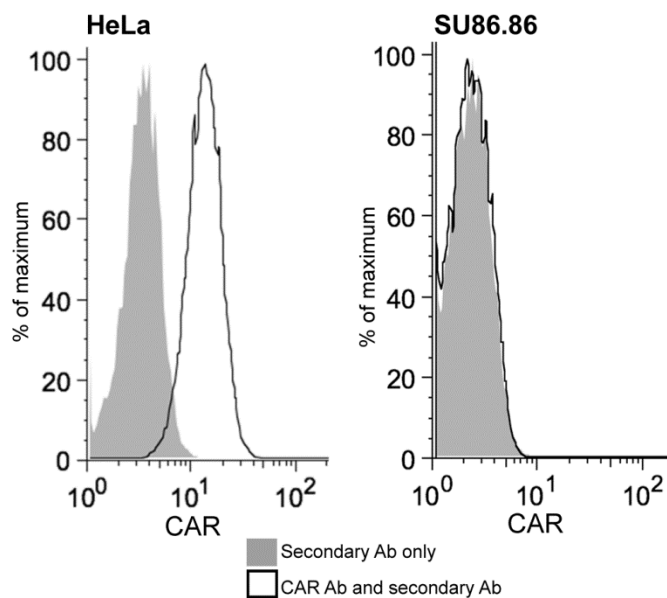


Figure 21. Surface expression of adenovirus CAR receptor. Single cell suspensions of HeLa (positive control) and SU.86.86 cells (obtained without trypsin) were analyzed for adenovirus CAR receptor using anti-CAR antibody and secondary IgG-FITC antibody (solid lines) or secondary IgG-FITC antibody only (gray area). Expression of CAR was determined by flow cytometry (Beckman Coulter) and analyzed using FlowJo (Treestar, Ashland, OR) as described in Materials and Methods.

3.5 Figure 22

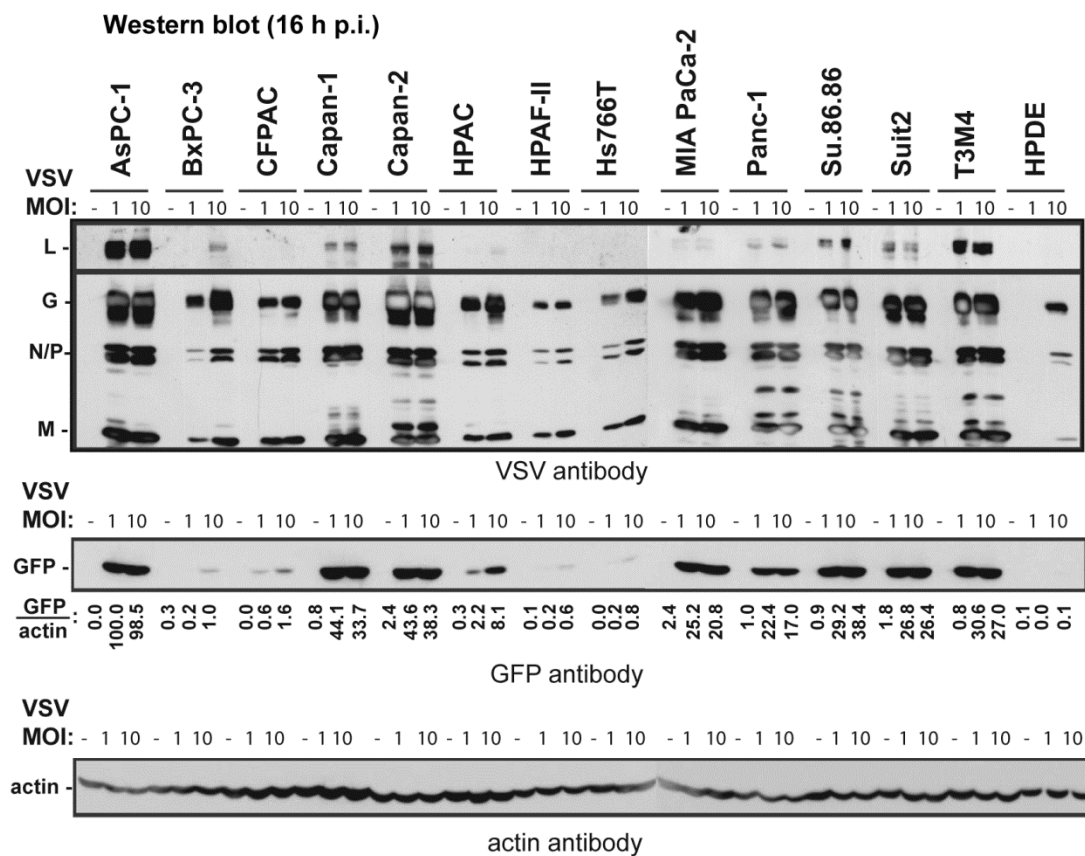


Figure 22. Analysis of viral protein accumulation in cells at 16 h p.i. Cells were mock infected or infected them with VSV- Δ M51-GFP at MOI 1 or 10 CIU/cell. Cells were harvested at 16 h p.i. and cell lysates were analyzed by western blot for VSV proteins, GFP or actin.

3.5 Figure 23

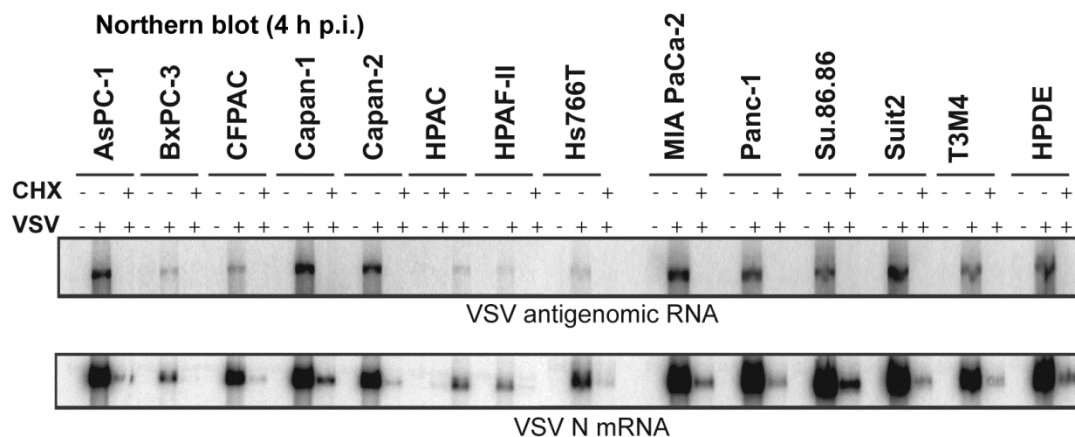


Figure 23. Early viral RNA levels in infected cells. Cells were mock treated or treated with 100 $\mu\text{g/ml}$ cycloheximide (CHX) for 30 min prior to mock infection or infection with VSV- $\Delta\text{M51-GFP}$ at MOI 10 and continuing treatment with CHX. At 4 h p.i., cells were collected and total RNA extracted and analyzed by Northern blot for VSV antigenome RNA (upper panel) or N mRNA (lower panel).

3.5 Figure 24

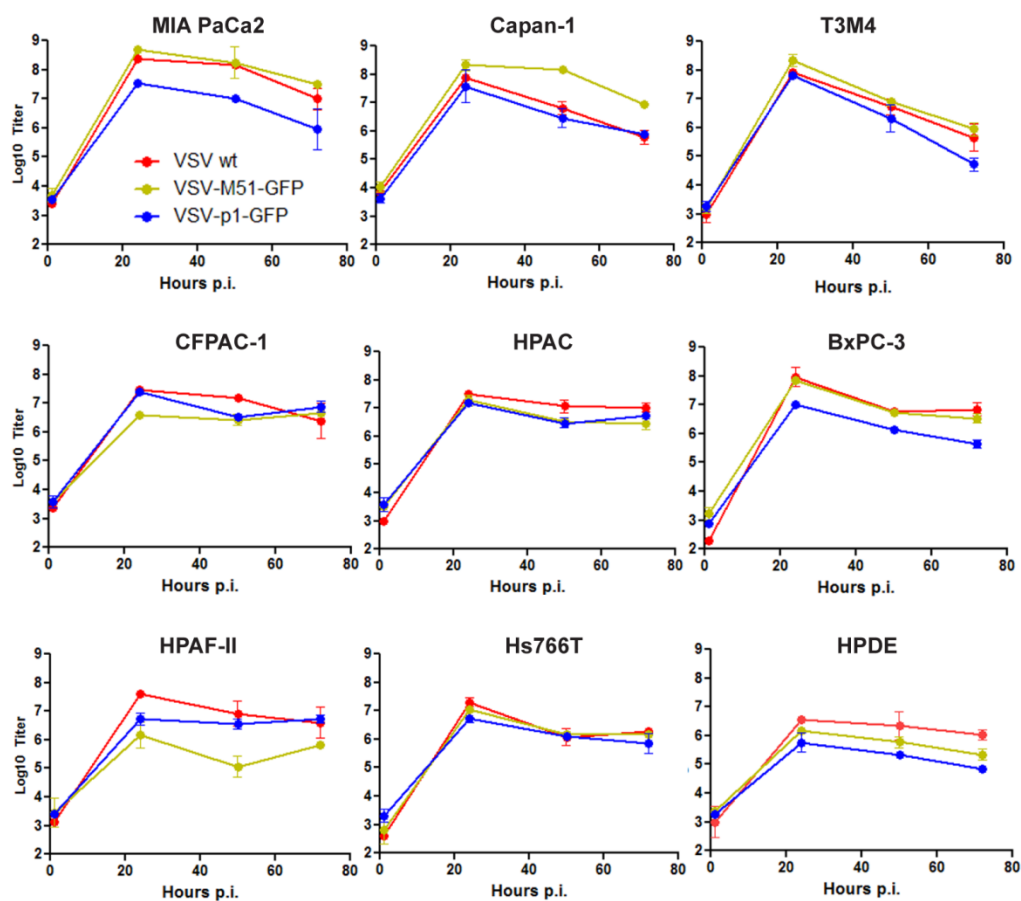


Figure 24. One-step growth kinetics of VSVs in PDA cell lines. PDA cells were infected with VSV-wt, VSV- Δ M51-GFP, or VSV-p1-GFP at MOI 10 CIU/cell that was calculated based on the reference cell line 4T1. At 1 h p.i. virus was aspirated and cells were washed and overlaid with 5% growth media. At 1, 24, 50 and 72 h p.i. supernatant was collected and virus titers determined by plaque assay on BHK-21 cells. All infections were done in duplicate and the data represent the mean \pm standard deviation.

3.5 Figure 25

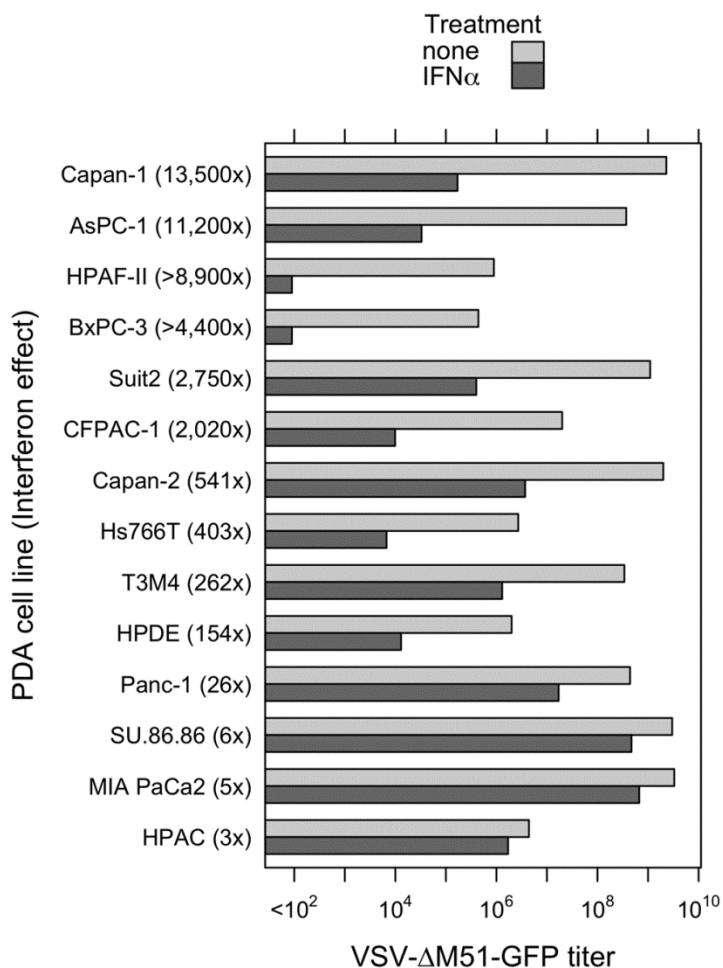


Figure 25. Type I interferon sensitivity of PDA cell lines. PDA cell lines and HPDE were either treated with 5000 U/ml IFN- α in SFM or mock-treated with SFM only. Twenty-four h post treatment, cells were infected with serial dilutions of VSV- Δ M51-GFP, and infectious foci were analyzed 16 h p.i. by fluorescent microscopy to calculate virus titer under these conditions. Treatments and infections were performed in duplicate and average values are shown. For HPAC cells pretreated with IFN- α , virus-driven GFP signal was delayed by 24 h p.i.

3.5 Figure 26

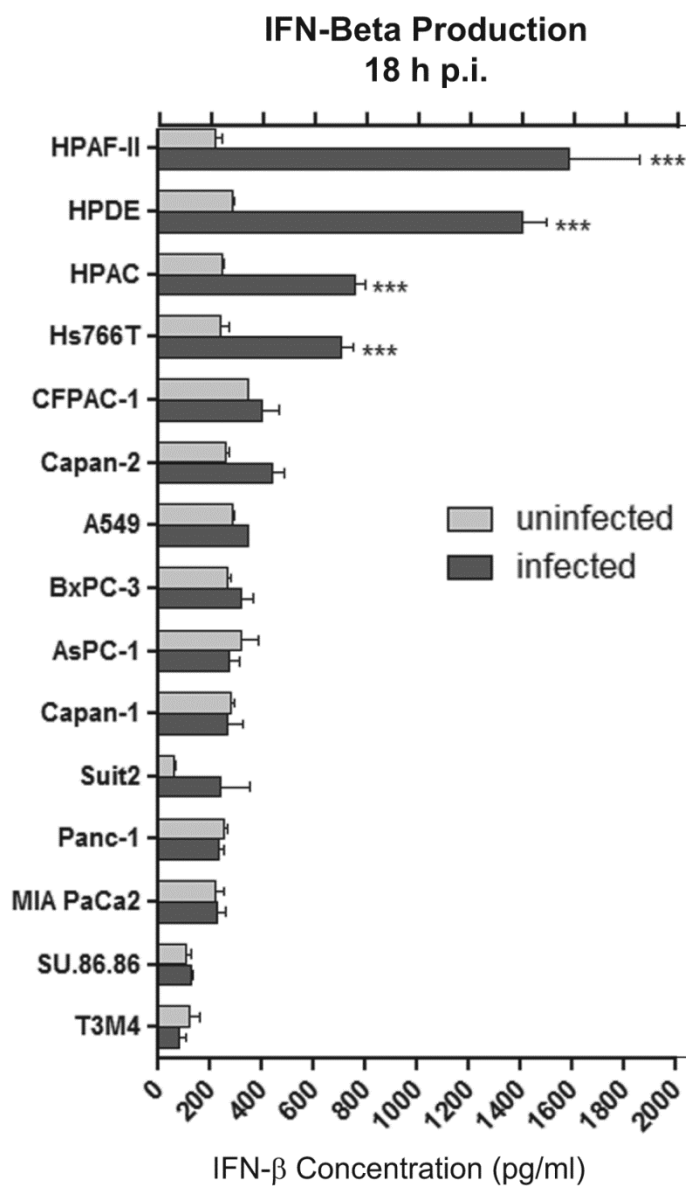


Figure 26. Type I interferon production by PDA cell lines. Cells were infected with VSV- Δ M51-GFP at MOI of 10 CIU/cell or mock-treated with SFM only. One h p.i. virus was aspirated and supernatant was harvested and analyzed by ELISA for production of human IFN- β . Infections were performed in triplicate and the data represent the mean \pm standard deviation. Comparison of groups was done by using 2-way ANOVA followed by the Bonferroni posttest for multiple comparisons (***, $P < 0.001$).

3.5 Figure 27

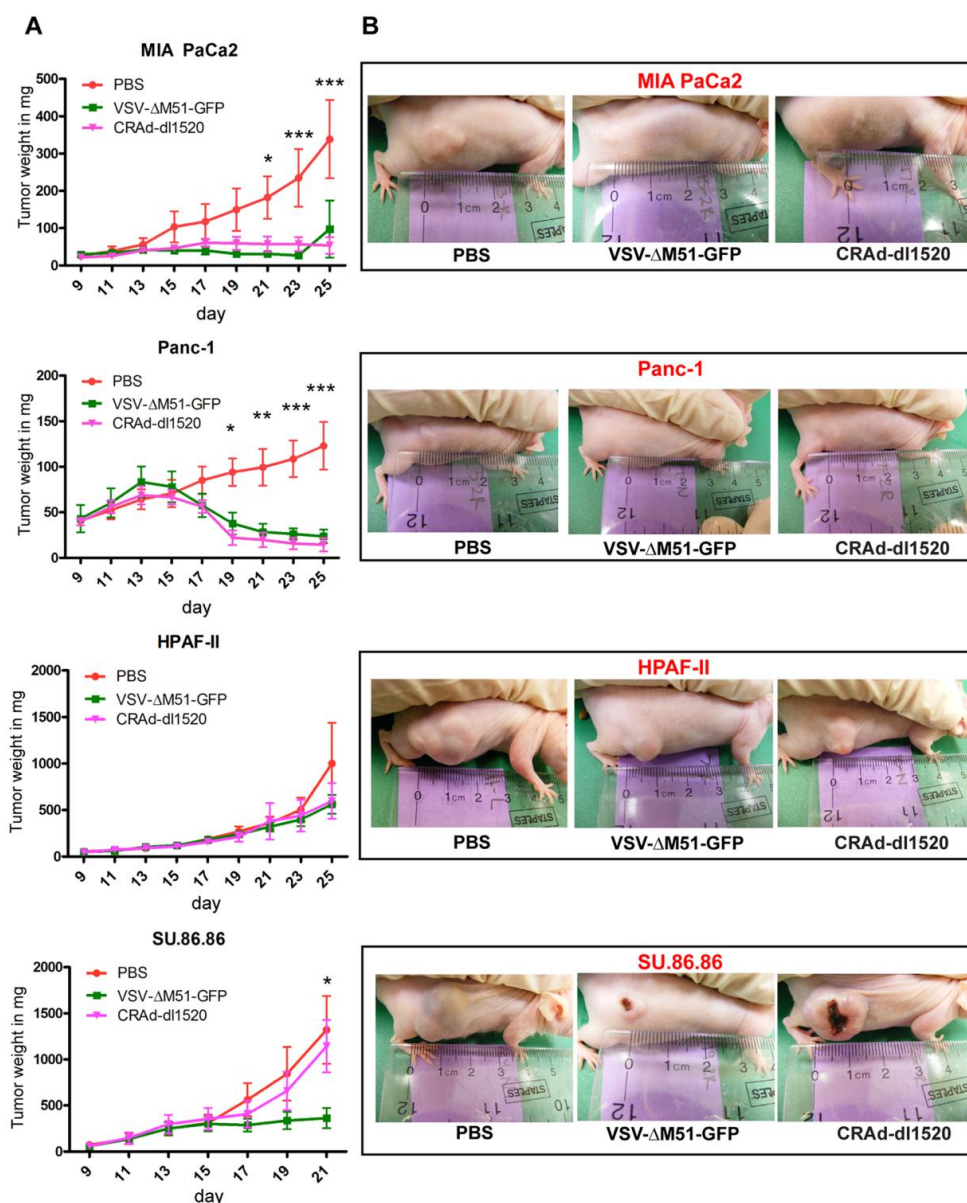


Figure 27. Efficacy of VSV-ΔM51-GFP and CRAd-dl1520 in nude mice bearing human PDA tumors. 6-8 week old, male, athymic nude mice were subcutaneously injected with Mia PaCa2, Panc-1, HPAF-II, or Su.86.86 cells into the right flank (n=18 per group). Tumors were established by day 13 and mice were randomly divided into 3 groups (n=6 per group). One group served as a control and received one IT administration of 50 μl PBS only. The other two groups were administered IT once with VSV-ΔM51-GFP or CRAd-dl1520 at a dose of 5×10^7 CIU in 50 μl PBS. Tumor size was monitored by caliper measurements and tumor weight was calculated according to the formula: grams = (length in centimeters x (width)²)/2. Comparison of groups was done by using 2-way ANOVA followed by the Bonferroni posttest for multiple comparisons (*, P < 0.05, **, P < 0.01, ***, P < 0.001).

3.6 Table 4. PDA cell lines used in this study.

PDA cell line	Origin	Tumor type
AsPC-1	Human	Ascites
BxPC-3	Human	Primary
CFPAC	Human	Primary
Capan-1	Human	Liver metastasis
Capan-2	Human	Primary
HPAC	Human	Primary
HPAF-II	Human	Primary
Hs766T	Human	Lymph node metastasis
MIA PaCa2	Human	Primary
Panc-1	Human	Primary
Su.86.86	Human	Liver metastasis
Suit2	Human	Liver metastasis
T3M4	Human	Lymph node metastasis
HPDE	Human	Non-malignant pancreatic ductal epithelia

3.6 Table 5. Early viral RNA synthesis in cells infected with VSV- Δ M51-GFP.

Cell Line	Primary TXN ^a	Total TXN ^b	Total TXN / Primary TXN	Antigenome RNA ^c	Total TXN / Antigenome RNA
AsPC-1	668	29232	44	1276	23
BxPC-3	37	1517	41	40	38
CFPAC	172	10911	63	230	47
Capan-1	1728	31394	18	2205*	14
Capan-2	249	14807	59	1401*	11
HPAC	56	1549	28	60*	26
HPAF-II	27	899	34	18*	49
Hs766T	181	3891	22	86	45
MIA PaCa2	1520	31434	21	1857	17
Panc-1	1126	34698	31	1401	25
Su.86.86	5162	46195	9	1428	32
Suit2	854*	41203*	48	2988*	14
T3M4	378	14363	38	1051	14
HPDE	1682	32759	19	1803	18

^a VSV N mRNA transcription (TXN) level 4 h p.i. in the presence of cycloheximide

^b VSV N mRNA transcription (TXN) level 4 h p.i. in the absence of cycloheximide

^c VSV antigenome RNA synthesis level 4 h p.i. in the absence of cycloheximide

*values are for RNA bands detected using a phosphoimager and quantitated using Image Quant software, the average of two independent repeats except as indicated

3.6 Table 6. Correlation between IFN sensitivity, production and resistance of PDA cells to VSV.

	IFN sensitivity (24 h p.i.)	IFN- β production (18 h p.i.)	In vitro resistance to VSV- Δ M51-GFP
AsPC-1	+++	-	-
Su.86.86	-	-	-
Capan-1	+++	-	-
Panc-1	-	-	-
MIA PaCa2	-	-	-
Suit2	++	-	-
Capan-2	+	-	-
T3M4	+	-	-
CFPAC	++	-	++
HPDE	+	+++	+++
HPAC	-	+++	++
BxPC-3	+++	-	+++
HPAF-II	+++	+++	+++
Hs766T	+	+++	+++

- +++ high levels of IFN sensitivity, IFN production, or virus resistance
- ++ intermediate levels of IFN sensitivity, IFN production, or virus resistance
- + low levels of IFN sensitivity, IFN production, or virus resistance
- no detectible levels of IFN sensitivity, IFN production, or virus resistance

CHAPTER 4: DISSERTATION SUMMARY

VSV and SeV are the prototypic members of the NNS RNA viruses of the order *Mononegavirales* and are related to many medically important human and animal pathogens. Understanding the molecular biology of VSV and SeV is an important step in understanding the biology of these more dangerous viruses, and additionally VSV and SeV have great potential as vectors for vaccine development, gene therapy and oncolytic virus (OV) therapy. This dissertation analyzed the cap methylation function of the SeV L protein in comparison to what has been previously shown for the VSV L protein we identified several aa residues required for SeV cap methylation function. In addition, we analyzed for the first time, the oncolytic potential of VSV in a pancreatic ductal adenocarcinoma (PDA) model and we observed that VSV can be a highly effective oncolytic agent against PDA.

Sequence-function analysis of the Sendai virus L protein domain VI

To begin our comparative analysis of domain VI of the VSV and SeV L proteins, we hypothesized that domain VI of VSV and SeV had similar importance in cap methylation function. We performed a sequence alignment and targeted aa residues that are highly conserved in *Mononegavirales*, were shown to effect cap methylation function in VSV (positions of the KDKE catalytic tetrad and glycine-rich motif), and are present in other MTases. Using site-directed mutagenesis, targeted aa residues were substituted

for alanines (and in some cases leucines) and twenty-nine mutant SeV L proteins were generated (all mutations were in domain VI). Our focus was on the aa residues of the KDKE catalytic tetrad and the glycine-rich motif (the putative methyl donor binding site), in addition to several other highly conserved aa residues in domain VI of the L protein. We targeted residues D1799 and Y1802 located just upstream of the glycine-rich motif and conserved only in some paramyxoviruses. Many classes of MTases of known structure contain either a conserved aspartate or glutamate, or a tyrosine residue within the beta strand that precedes the conserved glycine-rich motif, but rarely do they contain both these residues. A polar residue in this position has been implicated in reaction mechanism as the fifth catalytic entity (Kozbial and Mushegian 2005), and we were interested in determining whether one or both of these aa may play a functional role in SeV MTase. We also targeted the unusual DKDKD sequence located immediately upstream of the residue D1799. Although this DKDKD sequence is present only in some paramyxoviruses, we wanted to determine whether such high concentration of aspartates and lysines and its close proximity to the glycine-rich motif may play some role in cap methylation catalysis. All viruses with mutations in this motif were easily rescued and had wt-like levels of transcription, replication and cap methylation functions indicating these individual positions do not play an important role in L protein function.

All L protein mutations were cloned into a SeV FL genomic plasmid and using a reverse genetics system, this plasmid along with plasmids encoding L, P, and N (the proteins necessary for an successful virus replication cycle) were transfected into a mammalian cell line (BSR-T7). Twenty-four infectious mutant SeV were generated using this system and these mutant viruses contained the specific mutations in their L proteins

within the infectious virus particles. We were unable to generate infectious viruses containing certain specific L mutations, therefore we tested these mutant L proteins for their ability to catalyze genome replication and mRNA synthesis. We found that certain mutations completely inactivated the enzymatic function of these L proteins and therefore infectious virus particles could not be recovered. We were not surprised that the L- Δ VI mutant was not functional because deletion of an entire portion of the L would affect protein folding, allosteric interactions with other domains, or interactions with other viral proteins. The inactivation of the L-E1805V protein was more surprising as a similar substitution in the VSV *hr1* mutant (D1671V), while abolishing cap methylation, had no effect on VSV mRNA synthesis (Grdzlishvili et al. 2005). It is likely that the aa substitution in the L-E1805V protein negatively affected L protein folding resulting in a complete inactivation of this protein. Interestingly, we also observed varying transcription and replication levels for other mutants which indicates these specific mutations also negatively affected L protein folding or allosteric interactions with other domains.

Infectious SeV with specific mutations within domain VI of the L protein were further characterized in cell culture and analyzed for their ability to infect and replicate in Vero cells, which are known to support robust replication of SeV. It was shown previously for VSV that defects in cap methylation led to attenuation in certain nonpermissive cell lines while still retaining the ability to grow to high titers in permissive cell lines. We expected to see similar levels of virus replication between different SeV mutant viruses in Vero cells because these cells are known to be highly permissive to SeV. We found that several SeV mutants had similar infectivity as rWT,

however several mutants also exhibited no cytopathic effects in Vero cells. Infection of Vero cells by these mutants could be detected by immunofluorescence and were shown to be highly attenuated compared to rWT. This result was confirmed in a virus replication kinetics experiment. The same SeV mutants that were attenuated in Vero cells demonstrated lower titers and delayed infection compared to rWT. We had hypothesized that SeV infection in Vero cells would mimic what has been shown for VSV infection in BHK cells. Previous studies linked the inability of VSV cap methylation defective mutants to grow in nonpermissive cells to a viral defect in mRNA cap G-N7 methylation and consequent nontranslatability of primary VSV transcripts (Horikami and Moyer 1982; Horikami et al. 1984; Grdzlishvili et al. 2005; Grdzlishvili et al. 2006). It was also suggested that host cells methylate viral mRNA in permissive cell lines through an unknown mechanism (Horikami et al. 1984). The exact mechanism is unknown; however, permissive cells can have trans acting MTases present in the cytoplasm possibly due to contamination with other viruses or bacteria present in these cells. Therefore, SeV mutants being attenuated in Vero cells indicates that this cell line lacks the ability to complement cap methylation function as was observed in BHK cells.

We performed a biochemical analysis of cap methylation status of our mutant SeV using an in vitro transcription assay with purified virions in the presence of a radiolabeled methyl donor (AdoMet). We observed a correlation between mutant SeV attenuation in Vero cells and defective cap methylation especially for viruses carrying mutations in the KDKE catalytic tetrad. We also observed that SeV exhibits more tolerance to aa substitutions to alanine in the glycine-rich motif as compared to VSV. The slight differences in aa residues surrounding the glycine-rich motif of SeV might play a

role in the observed tolerance. However, this motif was still shown to be important to SeV cap methylation function when we generated mutant viruses with substitutions to leucines and observed severe attenuation in cell culture. Unfortunately, in contrast to our previous VSV studies (Grzelishvili et al. 2005; Grzelishvili et al. 2006), we were unable to conduct a very detailed analysis of the SeV cap structure because of very low levels of viral mRNA produced in vitro (about 200-fold less viral mRNA compared to VSV in vitro transcription system). Nevertheless, our assays (supported by the described virus growth analysis) allowed us to make general conclusions about cap methylation function in all tested SeV mutants.

Cap methylation defective viruses (VSV, SeV, or any other *Mononegavirales*) have never been tested in any animal system or primary cells. It is possible that cap methylation defective viruses will be attenuated in vivo; however, it is unclear if infectious viruses carrying these specific mutations will exhibit any unusual tissue specificity as compared to their wild type counterpart. Further studies of cap methylation defective viruses in vivo can lead to the rational design of vectors for vaccine, gene therapy and oncolytic virotherapy development. Additionally, studying cap methylation defective SeV mutants in mice (the natural host of SeV) would provide the unique ability to analyze the effect of defective cap methylation over the course of natural infection at the organismal level.

Despite some observed differences between VSV and SeV (more tolerance of SeV to aa substitutions in the glycine-rich motif), our analysis identified several aa residues required for successful cap methylation and virus replication and clearly showed the importance of a putative catalytic tetrad and methyl donor binding site in SeV cap

methylation. This study is the first extensive sequence analysis of the L protein domain VI in the family *Paramyxoviridae*, and it confirms structural and functional similarity of this domain across different families of the order *Mononegavirales*.

VSV as an oncolytic agent against pancreatic ductal adenocarcinoma

We also analyzed for the first time VSV as an oncolytic agent against pancreatic ductal adenocarcinoma (PDA). PDA remains one of the most challenging malignancies to treat due to aggressive growth and rapid metastases to surrounding tissues. Other oncolytic viruses have had preclinical success in pancreatic cancer however VSV (or any VSV variants) has never been tested in any pancreatic cancer model. We chose to focus on VSV- Δ M51-GFP, a recombinant VSV that retains its oncolytic activities but lacks neurotoxicity in vivo (Ahmed 2008; Wollmann 2010) and is being widely used in other oncolytic VSV studies. In addition, we compared VSV to other oncolytic viruses (CRAds, SeV, and RSV). There are several important characteristics of VSV which in combination make it a more attractive candidate for PDA treatment compared to other tested viruses: (i) there are few if any restrictions to VSV attachment and entry as it is believed to be not dependent on any specific host receptor in target cells; (ii) there is no preexisting immunity against VSV in humans; (iii) VSV is not considered a significant human pathogen, and several VSV mutants, including VSV- Δ M51-GFP and VSV-p1-GFP, are not neurotropic but retain their oncolytic activity; (iv) cellular uptake in many mammalian cell types occurs very rapidly and there is no cell cycle dependency; (v) our comparative analysis here demonstrated that VSV variants showed superior oncolytic abilities compared to other tested viruses, and some cell lines that exhibited resistance to other viruses were successfully killed by VSV. Based on these characteristics, we

hypothesized that VSV would be an effective oncolytic agent against PDA. In this study, VSV variants and other oncolytic viruses were tested for their ability to infect, replicate and cause cell death in a panel of 13 clinically relevant PDA cell lines. VSV variants showed superior oncolytic abilities compared to other viruses, and some cell lines that exhibited resistance to other viruses were successfully killed by VSV. However, PDA cells were highly heterogeneous in their susceptibility to virus-induced oncolysis and several cell lines were resistant to all tested viruses (resistance discussed below).

Four cell lines that varied in their permissiveness to VSV- Δ M51-GFP and CRAd-d11520 were tested in nude mice, and in vivo results closely mimicked those in vitro, indicating in vitro testing can be used to identify cancers resistant to a particular virus. However, the ability of a virus to kill cancer cells in vitro or even in vivo (in nude mice) would not guarantee its efficacy in cancer patients due to complex tumor microenvironments and compromised immune responses (Breitbach et al. 2010). Lack of relevant mouse models has contributed to the challenge of developing effective therapies for patients suffering from PDA. Until recently, much PDA research has been conducted in immunocompromised mouse models that lack important immunologic components and signaling pathways which cannot give a clear picture of tumor growth with respect to an intact immune system (Clark et al. 2009). Currently there are strategies to better understand tumor-immune system interactions using immunocompetent mouse models. Mice with induced PDA tumors are created by injecting malignant murine PDA cell lines into a particular immunocompetent strain of mice which then develop palpable tumors at the site of injection. This system is useful in studying the interactions between the tumor microenvironment and host immunity however it is an artificial system in the sense that

tumors do not develop orthotopically and injected tumor cells need to be of mouse origin (human cell lines would most likely be rejected). In addition to induced mouse models, there are a variety of immunocompetent mouse models that have been recently described that mimic the natural progression of preinvasive to invasive PDA as observed in human patients. Studying these mice has led to a better understanding of the dynamics of the tumor microenvironment and host immune interactions (Hingorani et al. 2003).

Hingorani et al. (2003) developed PDA mice which have a point mutation in one *Kras* allele (LSL-KRAS^{G12D}) that is activated upon breeding with mice expressing *Cre* recombinase under control of the pancreas specific p48 promoter (P48-Cre) (Kawaguchi et al. 2002). Analyzing VSV-ΔM51-based virotherapy in immunocompetent mice that closely mimic human progression of PDA would give a clearer picture of the efficacy of VSV-ΔM51 against PDA. While VSV is one of the most promising oncolytic viruses, several obstacles remain to be addressed. Use of an orthotopic model of PDA would require intravenous delivery of VSV-ΔM51. Intravenous delivery of VSV-ΔM51 would ideally target only cancer cells (primary tumor and metastases), but there are several obstacles to this mode of virus delivery. Delivery of VSV-ΔM51 into the bloodstream can lead to inactivation of the virus by neutralizing antibodies, complement molecules, and other immune components prior to delivery to the tumor. The dose of virus particles delivered will also play a major role in the efficacy of VSV-ΔM51. There is little seroprevalence of VSV in the human population, therefore VSV-ΔM51 would be most effective upon primary administration, but further administration can lead to faster neutralization and clearance of the virus before full oncolytic potential can be achieved. One strategy to overcome this would be to deliver multiple doses of VSV-ΔM51 within a

few days prior to the induction of immune responses. Combination therapies with multiple oncolytic viruses might also achieve greater efficacy by eliminating the need to administer multiple doses of a single virus. Because of its preclinical success, at least two VSV OV_s have been considered for clinical trials by the NIH Recombinant-DNA Advisory Committee (Cary et al. 2011) and these trials will determine the fate of VSV-based oncolytic virotherapy.

While our results demonstrate VSV is a promising oncolytic agent against PDA, further studies are needed to better understand the molecular mechanisms of resistance of some PDAs to oncolytic virotherapy. There are two major hypotheses explaining varying susceptibility of PDA cell lines to oncolysis by VSV *in vitro*. First, PDA cells may differ in their susceptibility to virus infection and/or their ability to support virus replication. This may happen because PDA cells may lack key cellular factors (e.g., receptors) required for successful virus infection or because resistant cells have intact antiviral responses preventing successful virus spread. Alternatively, some PDA cells may have defective apoptotic pathways, so that even if a virus can successfully infect and replicate in these cells, they are not efficiently killed by apoptosis.

Resistant PDA cells in this study showed low levels of very early VSV RNA synthesis, indicating possible defects at initial stages of infection. VSV infects a wide range of cell types, and while there is no distinct receptor identified for VSV, it is thought that VSV enters cells through recognition of ubiquitous cell surface molecules or even electrostatic interactions (Schlegel et al. 1983; Bailey et al. 1984; Coil and Miller 2004). It is possible that VSV entry can be inhibited by steric hindrance by cell surface molecules such as mucins, large cell surface molecules that are highly glycosylated and

often overexpressed in human cancers (Tinder et al. 2008). Heavily glycosylated mucins in pancreatic cancer also create a highly acidic tumor microenvironment (Moniaux et al. 2004; Wojton and Kaur 2010) which can inhibit the effects of oncolytic virotherapy.

Unlike permissive PDA cell lines, most of the resistant cell lines were able to both produce and respond to Type I IFN, suggesting that intact IFN responses contributed to their resistance phenotype. A hallmark of many cancers is a loss of chromosome arm 9p where many important tumor suppressor genes, genes for cell cycle control, and the Type I IFN genes (IFN- α/β) reside (Vitale et al. 2007). The loss of these important gene products provide growth advantages to the tumor however the inability to produce Type I IFN renders tumor cells susceptible to virus infections (Stojdl et al. 2000). While the majority of cancer cells lack Type I IFN signaling and production, certain cancer cell types retain this function and OV's such as VSV would not be an effective therapy. While VSV is an effective OV against tumors that lack Type I IFN, other OV's that utilize different mechanisms of oncolysis might be more effective for patients with tumors with intact IFN responses. For example, CRA's are OV's that target cancer cells that have dysfunctional p53 molecules (also a hallmark of many cancers). However, our results demonstrate cells that are resistant to VSV are also resistant to other OV's, including CRA's, which indicates multiple mechanisms are involved in resistant cancer cells. Prescreening patient samples for production of Type I IFN would be a useful biomarker for determining patients that would respond to VSV-based OV therapy.

Many cancer cells are also defective in apoptosis, which could delay or prevent cell death following infection (Hamacher et al. 2008). As VSV has been shown to cause cell death by apoptosis via either the intrinsic and/or extrinsic pathway (Gaddy and Lyles

2005; Gaddy and Lyles 2007; Sharif-Askari et al. 2007; Cary et al. 2011), cell lines with decreased expression or activation of certain apoptotic proteins have the potential of limiting/delaying cell death following VSV infection. Furthermore, differences in permissiveness to the VSV variants could be due to differences in their mechanisms of cell death induction. Our preliminary analysis of the apoptosis regulatory proteins Bax and Bcl-2 failed to show an association with resistance, and in most PDA cell lines caspase-3 was activated in a caspase-8 dependent manner following VSV- Δ M51 infection (data not shown). More studies are needed to determine whether reduced level of apoptotic response or the delayed induction of apoptosis in some of these cell lines plays a role in restricting VSV oncolysis. These defects could also (in addition to intact IFN pathways) explain why cell lines resistant to VSV are also resistant to other, unrelated, viruses.

Cancer cells exhibiting resistance might not be candidates for OV therapy, or alternative strategies can be employed to aggressively target resistant cells. There are several potential options for virus-resistant cancer cells. Prescreening cells against an array of different OVs could identify the best option for treating a particular tumor. Combination therapies have also demonstrated some success. Virotherapy in combination with chemotherapy can enhance the oncolytic effect compared to either treatment alone (Ottolino-Perry et al. 2010). Treating tumors with more than one OV (combined virotherapy) could also potentially lead to enhanced oncolysis (Le Boeuf et al. 2010). Importantly, understanding the mechanisms and identifying potential biomarkers of resistance is critical for the development of prescreening approaches and individualized oncolytic virotherapy against PDA.

In summary, the current study analyzed for the first time domain VI of the L protein in SeV, and we demonstrated structural and functional similarities between two distantly related families of *Mononegavirales* – rhabdoviruses and paramyxoviruses. This region of the L protein plays a role in several aspects of cap methylation of viral mRNAs. Additionally, we analyzed the potential of using VSV as an oncolytic agent against PDA. While we demonstrated that VSV has superior oncolytic abilities compared to other viruses used in our study, further analysis of the molecular mechanisms of resistance of certain cell lines can lead to a better understanding of viral infection and oncolysis and development towards an improved anticancer therapy.

REFERENCES

- Abraham, G. and A. K. Banerjee (1976). "Sequential transcription of the genes of vesicular stomatitis virus." Proc.Natl.Acad.Sci.U.S.A **73**(5): 1504-1508.
- Abraham, G., D. P. Rhodes, et al. (1975). "The 5' terminal structure of the methylated mRNA synthesized in vitro by vesicular stomatitis virus." Cell **5**(1): 51-58.
- Abraham, G., D. P. Rhodes, et al. (1975). "Novel initiation of RNA synthesis in vitro by vesicular stomatitis virus." Nature **255**(5503): 37-40.
- Ahmed M, Cramer SD, et al. (2004). "Sensitivity of prostate tumors to wild type and M protein mutant vesicular stomatitis viruses." Virology **330**(1): 34-49.
- Ahmed, M. and D. S. Lyles (1998). "Effect of vesicular stomatitis virus matrix protein on transcription directed by host RNA polymerases I, II, and III." J.Virol. **72**(10): 8413-8419.
- Ahmed M, M. T., Puckett S, Kock ND, Lyles DS. (2008). "Immune response in the absence of neurovirulence in mice infected with m protein mutant vesicular stomatitis virus." Journal of Virology **82**(18): 9273-9277.
- Ahmed, M., S. Puckett, et al. (2010). "Susceptibility of breast cancer cells to an oncolytic matrix (M) protein mutant of vesicular stomatitis virus." Cancer Gene Ther **17**(12): 883-892.
- Alberts B, Johnson A, et al. (2002). Molecular Biology of the Cell, 4th Edition. New York, Garland Science.
- Altomonte, J., L. Wu, et al. (2009). "Enhanced oncolytic potency of vesicular stomatitis virus through vector-mediated inhibition of NK and NKT cells." Cancer Gene Ther **16**(3): 266-278.
- Andrejeva, J., K. S. Childs, et al. (2004). "The V proteins of paramyxoviruses bind the IFN-inducible RNA helicase, mda-5, and inhibit its activation of the IFN-beta promoter." Proc Natl Acad Sci U S A **101**(49): 17264-17269.
- Ausubel, L. J., M. Meseck, et al. (2011). "Current good manufacturing practice production of an oncolytic recombinant vesicular stomatitis viral vector for cancer treatment." Hum Gene Ther **22**(4): 489-497.
- Bailey, C. A., D. K. Miller, et al. (1984). "Effects of DEAE-dextran on infection and hemolysis by VSV. Evidence that nonspecific electrostatic interactions mediate effective binding of VSV to cells." Virology **133**(1): 111-118.

- Ball, L. A. (1977). "Transcriptional mapping of vesicular stomatitis virus in vivo." J.Virol. **21**(1): 411-414.
- Ball, L. A. and C. N. White (1976). "Order of transcription of genes of vesicular stomatitis virus." Proc.Natl.Acad.Sci.U.S.A **73**(2): 442-446.
- Barber, G. N. (2004). "Vesicular stomatitis virus as an oncolytic vector." Viral Immunology **17**(4): 516-527.
- Barber, G. N. (2005). "VSV-tumor selective replication and protein translation." Oncogene **24**(52): 7710-7719.
- Barik, S. (1993). "The structure of the 5' terminal cap of the respiratory syncytial virus mRNA." J.Gen.Virol. **74 (Pt 3)**: 485-490.
- Ben-Baruch, A. (2006). "Inflammation-associated immune suppression in cancer: the roles played by cytokines, chemokines and additional mediators." Seminars in Cancer Biology **16**(1): 38-52.
- Bergmann, J. E., K. T. Tokuyasu, et al. (1981). "Passage of an integral membrane protein, the vesicular stomatitis virus glycoprotein, through the Golgi apparatus en route to the plasma membrane." Proc Natl Acad Sci U S A **78**(3): 1746-1750.
- Bischoff, J. R., D. H. Kirn, et al. (1996). "An adenovirus mutant that replicates selectively in p53-deficient human tumor cells." Science **274**(5286): 373-376.
- Bishop, D. H. and P. Roy (1971). "Kinetics of RNA synthesis by vesicular stomatitis virus particles." J Mol Biol **57**(3): 513-527.
- Black, B. L. and D. S. Lyles (1992). "Vesicular stomatitis virus matrix protein inhibits host cell-directed transcription of target genes in vivo." J.Virol. **66**(7): 4058-4064.
- Bossow, S., C. Grossardt, et al. (2011). "Armed and targeted measles virus for chemovirotherapy of pancreatic cancer." Cancer Gene Ther **18**(8): 598-608.
- Bray, M., J. Driscoll, et al. (2000). "Treatment of lethal Ebola virus infection in mice with a single dose of an S-adenosyl-L-homocysteine hydrolase inhibitor." Antiviral Res. **45**(2): 135-147.
- Breitbach, C. J., T. Reid, et al. (2010). "Navigating the clinical development landscape for oncolytic viruses and other cancer therapeutics: no shortcuts on the road to approval." Cytokine Growth Factor Rev **21**(2-3): 85-89.

- Brown, E. L. and D. S. Lyles (2003). "A novel method for analysis of membrane microdomains: vesicular stomatitis virus glycoprotein microdomains change in size during infection, and those outside of budding sites resemble sites of virus budding." Virology **310**(2): 343-358.
- Brown, E. L. and D. S. Lyles (2003). "Organization of the vesicular stomatitis virus glycoprotein into membrane microdomains occurs independently of intracellular viral components." J Virol **77**(7): 3985-3992.
- Buchholz, U. J., S. Finke, et al. (1999). "Generation of bovine respiratory syncytial virus (BRSV) from cDNA: BRSV NS2 is not essential for virus replication in tissue culture, and the human RSV leader region acts as a functional BRSV genome promoter." J Virol **73**(1): 251-259.
- Bujnicki, J. M. and L. Rychlewski (2002). "In silico identification, structure prediction and phylogenetic analysis of the 2'-O-ribose (cap 1) methyltransferase domain in the large structural protein of ssRNA negative-strand viruses." Protein Eng **15**(2): 101-108.
- Bukreyev, A., M. H. Skiadopoulos, et al. (2006). "Nonsegmented negative-strand viruses as vaccine vectors." J Virol **80**(21): 10293-10306.
- Canter, D. M. and J. Perrault (1996). "Stabilization of vesicular stomatitis virus L polymerase protein by P protein binding: a small deletion in the C-terminal domain of L abrogates binding." Virology **219**(2): 376-386.
- Carlsen, S. R., R. W. Peluso, et al. (1985). "In vitro replication of Sendai virus wild-type and defective interfering particle genome RNAs." J. Virol. **54**(2): 493-500.
- Carlson SK, C. K., Hadac EM, Dingli D, Bender CE, Kemp BJ, Russell SJ. (2009). "Quantitative molecular imaging of viral therapy for pancreatic cancer using an engineered measles virus expressing the sodium-iodide symporter reporter gene." American Journal of Roentgenology **192**(1): 279-287.
- Cartee, T. L., A. G. Megaw, et al. (2003). "Identification of a single amino acid change in the human respiratory syncytial virus L protein that affects transcriptional termination." J. Virol. **77**(13): 7352-7360.
- Cary, Z. D., M. C. Willingham, et al. (2011). "Oncolytic Vesicular Stomatitis Virus Induces Apoptosis in U87 Glioblastoma Cells by a Type II Death Receptor Mechanism and Induces Cell Death and Tumor Clearance In Vivo." J Virol **85**(12): 5708-5717.
- Chandrika, R., S. M. Horikami, et al. (1995). "Mutations in conserved domain I of the Sendai virus L polymerase protein uncouple transcription and replication." Virology **213**(2): 352-363.

- Chang, G., S. Xu, et al. (2010). "Enhanced oncolytic activity of vesicular stomatitis virus encoding SV5-F protein against prostate cancer." J Urol **183**(4): 1611-1618.
- Clark CE, Beatty GL, and Vonderheide RH (2009). "Immunosurveillance of pancreatic adenocarcinoma: insights from genetically engineered mouse models of cancer." Cancer Letters **279**(1):1-7.
- Coil, D. A. and A. D. Miller (2004). "Phosphatidylserine is not the cell surface receptor for vesicular stomatitis virus." J Virol **78**(20): 10920-10926.
- Colonno, R. J. and H. O. Stone (1976). "Newcastle disease virus mRNA lacks 2'-O-methylated nucleotides." Nature. **261**(5561): 611-614.
- Conzelmann, K. K. (2005). "Transcriptional activation of alpha/beta interferon genes: interference by nonsegmented negative-strand RNA viruses." J Virol **79**(9): 5241-5248.
- Cortese, C. K., J. A. Feller, et al. (2000). "Mutations in domain V of the Sendai virus L polymerase protein uncouple transcription and replication and differentially affect replication in vitro and in vivo." Virology **277**(2): 387-396.
- Cowling, V. H. (2010). "Regulation of mRNA cap methylation." Biochem J **425**(2): 295-302.
- Crompton, A. M. and D. H. Kirn (2007). "From ONYX-015 to armed vaccinia viruses: the education and evolution of oncolytic virus development." Curr Cancer Drug Targets **7**(2): 133-139.
- Cureton, D. K., R. H. Massol, et al. (2009). "Vesicular stomatitis virus enters cells through vesicles incompletely coated with clathrin that depend upon actin for internalization." PLoS Pathog **5**(4): e1000394.
- Curran, J., R. Boeck, et al. (1991). "The Sendai virus P gene expresses both an essential protein and an inhibitor of RNA synthesis by shuffling modules via mRNA editing." Embo J **10**(10): 3079-3085.
- Daffis, S., K. J. Szretter, et al. (2010). "2'-O methylation of the viral mRNA cap evades host restriction by IFIT family members." Nature **468**(7322): 452-456.
- De, B. P., A. Lesoon, et al. (1991). "Human parainfluenza virus type 3 transcription in vitro: role of cellular actin in mRNA synthesis." J Virol **65**(6): 3268-3275.
- De Clercq, E. (1998). "Carbocyclic adenosine analogues as S-adenosylhomocysteine hydrolase inhibitors and antiviral agents: recent advances." Nucleosides Nucleotides **17**(1-3): 625-634.

- Decroly, E., I. Imbert, et al. (2008). "Coronavirus nonstructural protein 16 is a cap-0 binding enzyme possessing (nucleoside-2'O)-methyltransferase activity." J Virol.
- Duprex, W. P., F. M. Collins, et al. (2002). "Modulating the function of the measles virus RNA-dependent RNA polymerase by insertion of green fluorescent protein into the open reading frame." J.Virol. **76**(14): 7322-7328.
- Ebert O, Harbaran S, et al. (2005). "Systemic therapy of experimental breast cancer metastases by mutant vesicular stomatitis virus in immune-competent mice." Cancer Gene Therapy **12**(4): 350-358.
- Echchgadda I, Chang TH, et al. (2011). "Oncolytic targeting of androgen-sensitive prostate tumor by the respiratory syncytial virus (RSV): consequences of deficient interferon-dependent antiviral defense." BMC Cancer **28**(11): 43.
- Echchgadda I, Kota S, et al. (2009). "Anticancer oncolytic activity of respiratory syncytial virus." Cancer Gene Ther **16**(12): 923-935.
- Edge RE, Falls TJ, et al. (2008). "A let-7 MicroRNA-sensitive vesicular stomatitis virus demonstrates tumor-specific replication." Molecular Therapy **16**(8): 1437-1443.
- Egloff, M. P., D. Benarroch, et al. (2002). "An RNA cap (nucleoside-2'-O)-methyltransferase in the flavivirus RNA polymerase NS5: crystal structure and functional characterization." EMBO J. **21**(11): 2757-2768.
- Eisenberg, D. P., S. G. Carpenter, et al. (2010). "Hyperthermia potentiates oncolytic herpes viral killing of pancreatic cancer through a heat shock protein pathway." Surgery **148**(2): 325-334.
- Emerson, S. U. and R. R. Wagner (1972). "Dissociation and reconstitution of the transcriptase and template activities of vesicular stomatitis B and T virions." J.Virol. **10**(2): 297-309.
- Etoh, T., Y. Himeno, et al. (2003). "Oncolytic viral therapy for human pancreatic cancer cells by reovirus." Clin Cancer Res **9**(3): 1218-1223.
- Farrow B, Albo D, et al. (2008). "The role of the tumor microenvironment in the progression of pancreatic cancer." Journal of Surgical Research **149**(2): 319-328.
- Fernandez M, Porosnicu M, et al. (2002). "Genetically engineered vesicular stomatitis virus in gene therapy: application for treatment of malignant disease." Journal of Virology **76**(2): 895-904.
- Ferran, M. C. and J. M. Lucas-Lenard (1997). "The vesicular stomatitis virus matrix protein inhibits transcription from the human beta interferon promoter." J Virol **71**(1): 371-377.

- Ferron, F., S. Longhi, et al. (2002). "Viral RNA-polymerases -- a predicted 2'-O-ribose methyltransferase domain shared by all Mononegavirales." Trends Biochem.Sci. **27**(5): 222-224.
- Finke, S. and K. K. Conzelmann (2005). "Recombinant rhabdoviruses: vectors for vaccine development and gene therapy." Curr Top Microbiol Immunol **292**: 165-200.
- Flood, E. A. and D. S. Lyles (1999). "Assembly of nucleocapsids with cytosolic and membrane-derived matrix proteins of vesicular stomatitis virus." Virology **261**(2): 295-308.
- Fuerst, T. R., E. G. Niles, et al. (1986). "Eukaryotic transient-expression system based on recombinant vaccinia virus that synthesizes bacteriophage T7 RNA polymerase." Proc.Natl.Acad.Sci.U.S.A **83**(21): 8122-8126.
- Furuichi, Y., A. LaFiandra, et al. (1977). "5'-terminal structure and mRNA stability." Nature (London) **266**: 235-239.
- Furukawa T, Duguid WP, et al. (1996). "Long-term culture and immortalization of epithelial cells from normal adult human pancreatic ducts transfected by the E6E7 gene of human papilloma virus 16." The American Journal of Pathology **148**(6): 1763-1770.
- Gaddy DF and D. S. and Lyles (2005). "Vesicular stomatitis viruses expressing wild-type or mutant M proteins activate apoptosis through distinct pathways." Journal of Virology **79**(7): 4170-4179.
- Gaddy DF and D. S. and Lyles (2007). "Oncolytic vesicular stomatitis virus induces apoptosis via signaling through PKR, Fas, and Daxx." Journal of Virology **81**(6): 2792-2804.
- Galivo F, Diaz RM, et al. (2010). "Interference of CD40L-mediated Tumor Immunotherapy by Oncolytic VSV." Human Gene Therapy.
- Galloway, S. E., P. E. Richardson, et al. (2008). "Analysis of a structural homology model of the 2'-O-ribose methyltransferase domain within the vesicular stomatitis virus L protein." Virology **382**(1): 69-82.
- Garcia-Sastre, A. (2004). "Identification and characterization of viral antagonists of type I interferon in negative-strand RNA viruses." Curr Top Microbiol Immunol **283**: 249-280.

- Gerlier, D. and D.S. Lyles. (2011). "Interplay between innate immunity and negative-strand RNA viruses: towards a rational model." Micro and Mol Bio Rev **75**: 468-490.
- Gingras, A. C., B. Raught, et al. (1999). "eIF4 initiation factors: effectors of mRNA recruitment to ribosomes and regulators of translation." Annu.Rev.Biochem. **68**: 913-963.
- Goel, A., S. K. Carlson, et al. (2007). "Radioiodide imaging and radiovirotherapy of multiple myeloma using VSV(Delta51)-NIS, an attenuated vesicular stomatitis virus encoding the sodium iodide symporter gene." Blood **110**(7): 2342-2350.
- Gotoh, B., K. Takeuchi, et al. (2003). "The STAT2 activation process is a crucial target of Sendai virus C protein for the blockade of alpha interferon signaling." J Virol **77**(6): 3360-3370.
- Grdzlishvili, V. Z., S. Smallwood, et al. (2005). "A single amino acid change in the L-polymerase protein of vesicular stomatitis virus completely abolishes viral mRNA cap methylation." J.Virol. **79**(12): 7327-7337.
- Grdzlishvili, V. Z., S. Smallwood, et al. (2006). "Identification of a new region in the vesicular stomatitis virus L polymerase protein which is essential for mRNA cap methylation." Virology **350**(2): 394-405.
- Grinnell, B. W. and R. R. Wagner (1985). "Inhibition of DNA-dependent transcription by the leader RNA of vesicular stomatitis virus: role of specific nucleotide sequences and cell protein binding." Mol.Cell Biol. **5**(10): 2502-2513.
- Gupta, K. C., D. H. Bishop, et al. (1979). "5'-Terminal Sequences of Spring Viremia of Carp Virus RNA Synthesized In Vitro." J Virol **30**(3): 735-745.
- Hager, J., B. L. Staker, et al. (2002). "Active site in RrmJ, a heat shock-induced methyltransferase." J Biol Chem **277**(44): 41978-41986.
- Hallak LK, Collins PL, et al. (2000). "Iduronic acid-containing glycosaminoglycans on target cells are required for efficient respiratory syncytial virus infection." Virology **271**(2): 264-275.
- Hamacher, R., R. M. Schmid, et al. (2008). "Apoptotic pathways in pancreatic ductal adenocarcinoma." Mol Cancer **7**: 64.
- Hammond, D. C. and J. A. Lesnaw (1987). "The fates of undermethylated mRNA cap structures of vesicular stomatitis virus (New Jersey) during in vitro transcription." Virology **159**(2): 229-236.

- Harty, R. N., M. E. Brown, et al. (2001). "Rhabdoviruses and the cellular ubiquitin-proteasome system: a budding interaction." J Virol **75**(22): 10623-10629.
- Harty, R. N., J. Paragas, et al. (1999). "A proline-rich motif within the matrix protein of vesicular stomatitis virus and rabies virus interacts with WW domains of cellular proteins: implications for viral budding." J Virol **73**(4): 2921-2929.
- He, X., C. Su, et al. (2009). "E1B-55kD-deleted oncolytic adenovirus armed with canstatin gene yields an enhanced anti-tumor efficacy on pancreatic cancer." Cancer Letters **285**: 89-98.
- Hercyk, N., S. M. Horikami, et al. (1988). "The vesicular stomatitis virus L protein possesses the mRNA methyltransferase activities." Virology **163**(1): 222-225.
- Higuchi, R., B. Krummel, et al. (1988). "A general method of in vitro preparation and specific mutagenesis of DNA fragments: study of protein and DNA interactions." Nucleic Acids Res **16**(15): 7351-7367.
- Himeno, Y., T. Etoh, et al. (2005). "Efficacy of oncolytic reovirus against liver metastasis from pancreatic cancer in immunocompetent models." Int J Oncol **27**(4): 901-906.
- Hingorani SR, Petricoin EF, Maitra A, Rajapakse V, King C, Jacobetz MA, et al. (2003). "Preinvasive and invasive ductal pancreatic cancer and its early detection in the mouse." Cancer Cell **4**(6):437-50.
- Hirano, S., T. Etoh, et al. (2009). "Reovirus inhibits the peritoneal dissemination of pancreatic cancer cells in an immunocompetent animal model." Oncol Rep **21**(6): 1381-1384.
- Hodel, A. E., P. D. Gershon, et al. (1998). "Structural basis for sequence-nonspecific recognition of 5'-capped mRNA by a cap-modifying enzyme." Mol Cell **1**(3): 443-447.
- Horikami, S. M., J. Curran, et al. (1992). "Complexes of Sendai virus NP-P and P-L proteins are required for defective interfering particle genome replication in vitro." J.Virol. **66**(8): 4901-4908.
- Horikami, S. M., F. De Ferra, et al. (1984). "Characterization of the infections of permissive and nonpermissive cells by host range mutants of vesicular stomatitis virus defective in RNA methylation." Virology **138**(1): 1-15.
- Horikami, S. M. and S. A. Moyer (1982). "Host range mutants of vesicular stomatitis virus defective in in vitro RNA methylation." Proc.Natl.Acad.Sci.U.S.A **79**(24): 7694-7698.

- Huang TG, Savontaus MJ, et al. (2003). "Telomerase-dependent oncolytic adenovirus for cancer treatment." Gene Therapy **10**(15): 1241-1247.
- Huang, T. G., O. Ebert, et al. (2003). "Oncolysis of hepatic metastasis of colorectal cancer by recombinant vesicular stomatitis virus in immune-competent mice." Mol Ther **8**(3): 434-440.
- Huch M, G. A., José A, González JR, Alemany R, Fillat C. (2009). "Urokinase-type plasminogen activator receptor transcriptionally controlled adenoviruses eradicate pancreatic tumors and liver metastasis in mouse models." Neoplasia **11**(6): 518-528.
- Ingrosso, D., A. V. Fowler, et al. (1989). "Sequence of the D-aspartyl/L-isoaspartyl protein methyltransferase from human erythrocytes. Common sequence motifs for protein, DNA, RNA, and small molecule S-adenosylmethionine-dependent methyltransferases." J.Biol.Chem. **264**(33): 20131-20139.
- Irie, T., J. M. Licata, et al. (2004). "Functional analysis of late-budding domain activity associated with the PSAP motif within the vesicular stomatitis virus M protein." J Virol **78**(14): 7823-7827.
- Irie, T., J. M. Licata, et al. (2004). "Budding of PPxY-containing rhabdoviruses is not dependent on host proteins TGS101 and VPS4A." J.Virol. **78**(6): 2657-2665.
- Iwamura T, Katsuki T, et al. (1987). "Establishment and characterization of a human pancreatic cancer cell line (SUIT-2) producing carcinoembryonic antigen and carbohydrate antigen 19-9." Jpn J Cancer Res. **78**(1): 54-62.
- Jayakar, H. R., K. G. Murti, et al. (2000). "Mutations in the PPPY motif of vesicular stomatitis virus matrix protein reduce virus budding by inhibiting a late step in virion release." J Virol **74**(21): 9818-9827.
- Kasuya H, Takeda S, et al. (2005). "The potential of oncolytic virus therapy for pancreatic cancer." Cancer Gene Therapy **12**(9): 725-736.
- Kasuya, H., Y. Nishiyama, et al. (2007). "Suitability of a US3-inactivated HSV mutant (L1BR1) as an oncolytic virus for pancreatic cancer therapy." Cancer Gene Ther **14**(6): 533-542.
- Kato, H., O. Takeuchi, et al. (2006). "Differential roles of MDA5 and RIG-I helicases in the recognition of RNA viruses." Nature **441**(7089): 101-105.
- Kawaguchi Y, Cooper B, Gannon M, Ray M, MacDonald RJ, and Wright CV (2002). "The role of the transcriptional regulator Ptf1a in converting intestinal to pancreatic progenitors." Nature Genetics. **32**(1):128-34.

- Kelly EJ, Nace R, et al. (2010). "Attenuation of vesicular stomatitis virus encephalitis through microRNA targeting." Journal of Virology **84**(3): 1550-1562.
- Kinoh H, I. M. (2008). "New cancer therapy using genetically-engineered oncolytic Sendai virus vector." Frontiers in Bioscience **13**: 2327-2334.
- Kinoh H, I. M., Washizawa K, Yamamoto T, Fujikawa S, Tokusumi Y, Iida A, Nagai Y, Hasegawa M. (2004). "Generation of a recombinant Sendai virus that is selectively activated and lyses human tumor cells expressing matrix metalloproteinases." Gene Therapy **11**(14): 1137-1145.
- Kiyotani, K., S. Takao, et al. (1990). "Immediate protection of mice from lethal wild-type Sendai virus (HVJ) infections by a temperature-sensitive mutant, HVJpi, possessing homologous interfering capacity." Virology **177**(1): 65-74.
- Knipe, D. M., D. Baltimore, et al. (1977). "Separate pathways of maturation of the major structural proteins of vesicular stomatitis virus." J Virol **21**(3): 1128-1139.
- Komaru A, U. Y., Furuya A, Tanaka S, Yoshida K, Kato T, Kinoh H, Harada Y, Suzuki H, Inoue M, Hasegawa M, Ichikawa T, Yonemitsu Y. (2009). "Sustained and NK/CD4+ T cell-dependent efficient prevention of lung metastasis induced by dendritic cells harboring recombinant Sendai virus." Journal of Immunology **183**(7): 4214-4219.
- Kozbial, P. Z. and A. R. Mushegian (2005). "Natural history of S-adenosylmethionine-binding proteins." BMC.Struct.Biol. **5**:19.: 19-.
- Kuhlmann, K. F., D. J. Gouma, et al. (2008). "Adenoviral gene therapy for pancreatic cancer: where do we stand?" Dig Surg **25**(4): 278-292.
- Lamb, R. A. and G. D. Parks (2007). Paramyxoviridae: The viruses and their replication. Fields Virology. e. In: D.M.Knipe and P.M.Howley, Lippincott Williams & Wilkins, Philadelphia, 5th edition.: 1449-1496.
- Lawson, N. D., E. A. Stillman, et al. (1995/5/9). "Recombinant vesicular stomatitis viruses from DNA." Proc.Natl.Acad.Sci.U.S.A **92**(10): 4477-4481.
- Le Boeuf, F., J. S. Diallo, et al. (2010). "Synergistic interaction between oncolytic viruses augments tumor killing." Mol Ther **18**(5): 888-895.
- Leyrer, S., W. J. Neubert, et al. (1998). "Rapid and efficient recovery of Sendai virus from cDNA: factors influencing recombinant virus rescue." J Virol Methods **75**(1): 47-58.

- Li, J., J. S. Chorbá, et al. (2007). "Vesicular stomatitis viruses resistant to the methylase inhibitor sinefungin upregulate RNA synthesis and reveal mutations that affect mRNA cap methylation." J Virol **81**(8): 4104-4115.
- Li, J., E. C. Fontaine-Rodriguez, et al. (2005). "Amino acid residues within conserved domain VI of the vesicular stomatitis virus large polymerase protein essential for mRNA cap methyltransferase activity." J.Virol. **79**(21): 13373-13384.
- Li, J., A. Rahmeh, et al. (2008). "A conserved motif in region v of the large polymerase proteins of nonsegmented negative-sense RNA viruses that is essential for mRNA capping." J Virol **82**(2): 775-784.
- Li, J., J. T. Wang, et al. (2006). "A unique strategy for mRNA cap methylation used by vesicular stomatitis virus." Proc Natl Acad Sci U S A **103**(22): 8493-8498.
- Lichty BD, Power AT, et al. (2004). "Vesicular stomatitis virus: re-inventing the bullet." TRENDS in Molecular Medicine **10**(5): 210-216.
- Lindsay TH, Jonas BM, et al. (2005). "Pancreatic cancer pain and its correlation with changes in tumor vasculature, macrophage infiltration, neuronal innervation, body weight and disease progression." Pain **119**(1-3): 233-246.
- Linge, C., D. Gewert, et al. (1995). "Interferon system defects in human malignant melanoma." Cancer Research **55**(18): 4099-4104.
- Luongo, C. L., C. M. Contreras, et al. (1998). "Binding site for S-adenosyl-L-methionine in a central region of mammalian reovirus lambda2 protein. Evidence for activities in mRNA cap methylation." J.Biol.Chem. **273**(37): 23773-23780.
- Lyles, D., Rupprecht, CE. (2007). Rhabdoviridae. Fields Virology. e. In: DM Knipe and PM Howley, Lippincott Williams & Wilkins, Philadelphia, 5th edition.: 1363-1408.
- Lyles, D. S., M. O. McKenzie, et al. (1996/11/1). "Potency of wild-type and temperature-sensitive vesicular stomatitis virus matrix protein in the inhibition of host-directed gene expression." Virology **225**(1): 172-180.
- Mao, X. and S. Shuman (1996). "Vaccinia virus mRNA (guanine-7-)-methyltransferase: mutational effects on cap methylation and AdoHcy-dependent photo-cross-linking of the cap to the methyl acceptor site." Biochemistry **35**(21): 6900-6910.
- Markwell, M. A., P. Fredman, et al. (1984). "Specific gangliosides are receptors for Sendai virus. Proteins in lipid samples can mask positive biological effects." Adv Exp Med Biol **174**: 369-379.

- Markwell, M. A., A. Portner, et al. (1985). "An alternative route of infection for viruses: entry by means of the asialoglycoprotein receptor of a Sendai virus mutant lacking its attachment protein." Proc Natl Acad Sci U S A **82**(4): 978-982.
- Martin, J. L. and F. M. McMillan (2002). "SAM (dependent) I AM: the S-adenosylmethionine-dependent methyltransferase fold." Curr.Opin.Struct.Biol. **12**(6): 783-793.
- Matin, S. F., R. R. Rackley, et al. (2001). "Impaired alpha-interferon signaling in transitional cell carcinoma: lack of p48 expression in 5637 cells." Cancer Research **61**(5): 2261-2266.
- Matlin, K. S., H. Reggio, et al. (1982). "Pathway of vesicular stomatitis virus entry leading to infection." J Mol Biol **156**(3): 609-631.
- McGowan, J. J., S. U. Emerson, et al. (1982). "The plus-strand leader RNA of VSV inhibits DNA-dependent transcription of adenovirus and SV40 genes in a soluble whole-cell extract." Cell **28**(2): 325-333.
- Mizumoto, K., K. Muroya, et al. (1995). "Protein factors required for in vitro transcription of Sendai virus genome." **117**(3): 527-534.
- Moniaux N, Andrianifahanana M, Brand RE, Batra SK (2004). Multiple roles of mucins in pancreatic cancer, a lethal and challenging malignancy. Br J Cancer **91**(9):1633-8.
- Moussavi, M., L. Fazli, et al. (2010). "Oncolysis of prostate cancers induced by vesicular stomatitis virus in PTEN knockout mice." Cancer Research **70**(4): 1367-1376.
- Moyer, S. A. (1981). "Alteration of the 5' terminal caps of the mRNAs of vesicular stomatitis virus by cycloleucine in vivo." Virology **112**(1): 157-168.
- Moyer, S. A., G. Abraham, et al. (1975). "Methylated and blocked 5' termini in vesicular stomatitis virus in vivo mRNAs." Cell **5**(1): 59-67.
- Moyer, S. A., S. C. Baker, et al. (1990). "Host cell proteins required for measles virus reproduction." J.Gen.Virol. **71**(Pt 4): 775-783.
- Moyer, S. A., S. C. Baker, et al. (1986). "Tubulin: a factor necessary for the synthesis of both Sendai virus and vesicular stomatitis virus RNAs." Proc.Natl.Acad.Sci.U.S.A **83**(15): 5405-5409.
- Murthy, K. G., P. Park, et al. (1991). "A nuclear micrococcal-sensitive, ATP-dependent exoribonuclease degrades uncapped but not capped RNA substrates." Nucleic Acids Res **19**(10): 2685-2692.

- Nagy, P. D., C. D. Carpenter, et al. (1997). "A novel 3'-end repair mechanism in an RNA virus." Proc Natl Acad Sci U S A **94**(4): 1113-1118.
- Naik, S. and S. J. Russell (2009). "Engineering oncolytic viruses to exploit tumor specific defects in innate immune signaling pathways." Expert Opin Biol Ther **9**(9): 1163-1176.
- Nakao, A., S. Takeda, et al. (2007). "Clinical experiment of mutant herpes simplex virus HF10 therapy for cancer." Curr Cancer Drug Targets **7**(2): 169-174.
- Obuchi M, Fernandez M, et al. (2003). "Development of recombinant vesicular stomatitis viruses that exploit defects in host defense to augment specific oncolytic activity." Journal of Virology **77**(16): 8843-8856.
- Odenwald, W. F., H. Arnheiter, et al. (1986). "Stereo images of vesicular stomatitis virus assembly." J Virol **57**(3): 922-932.
- Ogino, T. and A. K. Banerjee (2007). "Unconventional mechanism of mRNA capping by the RNA-dependent RNA polymerase of vesicular stomatitis virus." Mol Cell **25**(1): 85-97.
- Ogino, T. and A. K. Banerjee (2008). "Formation of guanosine(5')tetraphospho(5')adenosine cap structure by an unconventional mRNA capping enzyme of vesicular stomatitis virus." J Virol **82**(15): 7729-7734.
- Ogino, T. and A. K. Banerjee (2010). "The HR motif in the RNA-dependent RNA polymerase L protein of Chandipura virus is required for unconventional mRNA-capping activity." J Gen Virol **91**(Pt 5): 1311-1314.
- Ogino, T. and A. K. Banerjee (2011). "An unconventional pathway of mRNA cap formation by vesiculoviruses." Virus Res **162**(1-2): 100-109.
- Ogino, T., M. Kobayashi, et al. (2005). "Sendai virus RNA-dependent RNA polymerase L protein catalyzes cap methylation of virus-specific mRNA." J.Biol.Chem. **280**(6): 4429-4435.
- Ogino, T., S. P. Yadav, et al. (2010). "Histidine-mediated RNA transfer to GDP for unique mRNA capping by vesicular stomatitis virus RNA polymerase." Proc Natl Acad Sci U S A **107**(8): 3463-3468.
- Ohno, S. and N. Ohtake (1987). "Immunocytochemical study of the intracellular localization of M protein of vesicular stomatitis virus." Histochem J **19**(5): 297-306.

- Okabe T, Yamaguchi N, et al. (1983). "Establishment and characterization of a carcinoembryonic antigen (CEA)-producing cell line from a human carcinoma of the exocrine pancreas." Cancer **51**(4): 662-668.
- Onoguchi, K., M. Yoneyama, et al. (2011). "Retinoic acid-inducible gene-I-like receptors." J Interferon Cytokine Res **31**(1): 27-31.
- Ottolino-Perry, K., J. S. Diallo, et al. (2010). "Intelligent design: combination therapy with oncolytic viruses." Mol Ther **18**(2): 251-263.
- Ozduman, K., G. Wollmann, et al. (2008). "Systemic vesicular stomatitis virus selectively destroys multifocal glioma and metastatic carcinoma in brain." The Journal of Neuroscience : the Official Journal of the Society For Neuroscience **28**(8): 1882-1893.
- Patton, J. T., N. L. Davis, et al. (1984). "N protein alone satisfies the requirement for protein synthesis during RNA replication of vesicular stomatitis virus." J.Virol. **49**(2): 303-309.
- Penheiter, A. R., T. R. Wegman, et al. (2010). "Sodium iodide symporter (NIS)-mediated radiovirotherapy for pancreatic cancer." AJR Am J Roentgenol **195**(2): 341-349.
- Pfeffer, L. M., C. Wang, et al. (1996). "Human renal cancers resistant to IFN's antiproliferative action exhibit sensitivity to IFN's gene-inducing and antiviral actions." J Urol **156**(5): 1867-1871.
- Pillutla, R. C., A. Shimamoto, et al. (1998). "Human mRNA capping enzyme (RNGTT) and cap methyltransferase (RNMT) map to 6q16 and 18p11.22-p11.23, respectively." Genomics **54**(2): 351-353.
- Poch, O., B. M. Blumberg, et al. (1990). "Sequence comparison of five polymerases (L proteins) of unsegmented negative-strand RNA viruses: theoretical assignment of functional domains." J.Gen.Virol. **71** (Pt 5): 1153-1162.
- Quiroz E, Moreno N, et al. (1988). "A human case of encephalitis associated with vesicular stomatitis virus (Indiana serotype) infection." The American Journal of Tropical Medicine and Hygiene **39**(3): 312-314.
- Rahmeh AA, Li J, et al. (2009). "Ribose 2'-O methylation of the vesicular stomatitis virus mRNA cap precedes and facilitates subsequent guanine-N-7 methylation by the large polymerase protein." Journal of Virology **83**(21): 11043-11050.
- Ray, D., A. Shah, et al. (2006). "West Nile virus 5'-cap structure is formed by sequential guanine N-7 and ribose 2'-O methylations by nonstructural protein 5." J Virol **80**(17): 8362-8370.

- Rhodes, D. P. and A. K. Banerjee (1975). "5'-terminal sequence of vesicular stomatitis virus mRNA's synthesized in vitro." J.Virol. **17**(1): 33-42.
- Rigaut, K. D., D. E. Birk, et al. (1991). "Intracellular distribution of input vesicular stomatitis virus proteins after uncoating." J Virol **65**(5): 2622-2628.
- Ruedas JB, P. J. (2009). "Insertion of enhanced green fluorescent protein in a hinge region of vesicular stomatitis virus L polymerase protein creates a temperature-sensitive virus that displays no virion-associated polymerase activity in vitro." Journal of Virology **83**(23): 12241-12252.
- Russell, S. J. and K. W. Peng (2007). "Viruses as anticancer drugs." Trends Pharmacol Sci **28**(7): 326-333.
- Saha, N., S. Shuman, et al. (2003). "Yeast-based genetic system for functional analysis of poxvirus mRNA cap methyltransferase." J.Virol. **77**(13): 7300-7307.
- Saloura, V., L. C. Wang, et al. (2010). "Evaluation of an attenuated vesicular stomatitis virus vector expressing interferon-beta for use in malignant pleural mesothelioma: heterogeneity in interferon responsiveness defines potential efficacy." Hum Gene Ther **21**(1): 51-64.
- Sarinella, F., A. Calistri, et al. (2006). "Oncolysis of pancreatic tumour cells by a gamma34.5-deleted HSV-1 does not rely upon Ras-activation, but on the PI 3-kinase pathway." Gene Therapy **13**(14): 1080-1087.
- Scheid, A. and P. W. Choppin (1974). "The hemagglutinating and neuraminidase protein of a paramyxovirus: interaction with neuraminic acid in affinity chromatography." Virology **62**(1): 125-133.
- Scheid, A. and P. W. Choppin (1974). "Identification of biological activities of paramyxovirus glycoproteins. Activation of cell fusion, hemolysis, and infectivity of proteolytic cleavage of an inactive precursor protein of Sendai virus." Virology **57**(2): 475-490.
- Schlegel, R., T. S. Tralka, et al. (1983). "Inhibition of VSV binding and infectivity by phosphatidylserine: is phosphatidylserine a VSV-binding site?" Cell **32**(2): 639-646.
- Schnell, M. J. and K. K. Conzelmann (1995). "Polymerase activity of in vitro mutated rabies virus L protein." Virology **20**;214(2): 522-530.
- Sharif-Askari, E., P. Nakhaei, et al. (2007). "Bax-dependent mitochondrial membrane permeabilization enhances IRF3-mediated innate immune response during VSV infection." Virology **365**(1): 20-33.

- Shi, W., Q. Tang, et al. (2009). "Antitumor and antimetastatic activities of vesicular stomatitis virus matrix protein in a murine model of breast cancer." J Mol Med **87**(5): 493-506.
- Shinozaki, K., O. Ebert, et al. (2005). "Treatment of multi-focal colorectal carcinoma metastatic to the liver of immune-competent and syngeneic rats by hepatic artery infusion of oncolytic vesicular stomatitis virus." International Journal of Cancer. Journal International Du Cancer **114**(4): 659-664.
- Shinshi, H., M. Miwa, et al. (1976). "A novel phosphodiesterase from cultured tobacco cells." Biochemistry **15**(10): 2185-2190.
- Sidhu, M. S., J. P. Menonna, et al. (1993). "Canine distemper virus L gene: sequence and comparison with related viruses." Virology **193**(1): 50-65.
- Sinkovics JG and J. C. and Horvath (2008). "Natural and genetically engineered viral agents for oncolysis and gene therapy of human cancers." Arch. Immun. Ther. Exp. **56**: 3s-59s.
- Sleat, D. E. and A. K. Banerjee (1993). "Transcriptional activity and mutational analysis of recombinant vesicular stomatitis virus RNA polymerase." J.Virol. **67**(3): 1334-1339.
- Smallwood, S., T. Hovel, et al. (2002). "Different substitutions at conserved amino acids in domains II and III in the Sendai L RNA polymerase protein inactivate viral RNA synthesis." Virology **304**(1): 135-145.
- Stathis A and M. J. Moore (2010). "Advanced pancreatic carcinoma: current treatment and future challenges." Nature Reviews in Clinical Oncology **7**: 163-172.
- Stojdl DF, Lichty B, et al. (2000). "Exploiting tumor-specific defects in the interferon pathway with a previously unknown oncolytic virus." Nature Medicine **6**(7): 821-825.
- Stojdl DF, L. B., tenOever BR, Paterson JM, Power AT, Knowles S, Marius R, Reynard J, Poliquin L, Atkins H, Brown EG, Durbin RK, Durbin JE, Hiscott J, Bell JC. (2003). "VSV strains with defects in their ability to shutdown innate immunity are potent systemic anti-cancer agents." Cancer Cell **4**(4): 263-275.
- Sun, W. H., C. Pabon, et al. (1998). "Interferon-alpha resistance in a cutaneous T-cell lymphoma cell line is associated with lack of STAT1 expression." Blood **91**(2): 570-576.
- Takagi, T., K. Muroya, et al. (1995). "In vitro mRNA synthesis by Sendai virus: isolation and characterization of the transcription initiation complex." J.Biochem.(Tokyo) **118**(2): 390-396.

- Testa, D. and A. K. Banerjee (1977). "Two methyltransferase activities in the purified virions of vesicular stomatitis virus." J.Virol. **24**(3): 786-793.
- Tinder TL, Subramani DB, Basu GD, Bradley JM, Schettini J, Million A, Skaar T, Mukherjee P (2008). "MUC1 enhances tumor progression and contributes toward immunosuppression in a mouse model of spontaneous pancreatic adenocarcinoma." J Immunol **181**(5):3116-25.
- Tsukamoto, T., Y. Shibagaki, et al. (1998). "Cloning and characterization of three human cDNAs encoding mRNA (guanine-7-)-methyltransferase, an mRNA cap methylase." Biochem Biophys Res Commun **251**(1): 27-34.
- Vähä-Koskela MJ, Heikkilä JE, et al. (2007). "Oncolytic viruses in cancer therapy." Cancer Letters **254**(2): 178-216.
- Vitale G, van Eijck CH, van Koetsveld Ing PM, Erdmann JI, Speel EJ, van der Wansem Ing K, et al. (2007). "Type I interferons in the treatment of pancreatic cancer: mechanisms of action and role of related receptors." Annals of Surgery **246**(2):259-68.
- von Messling V and R. Cattaneo (2004). "Toward novel vaccines and therapies based on negative-strand RNA viruses." Current Topics in Microbiology and Immunology **283**(281-312).
- Wang, J. T., L. E. McElvain, et al. (2007). "Vesicular stomatitis virus mRNA capping machinery requires specific cis-acting signals in the RNA." J Virol **81**(20): 11499-11506.
- Wang, S. P. and S. Shuman (1997). "Structure-function analysis of the mRNA cap methyltransferase of *Saccharomyces cerevisiae*." J.Biol.Chem. **272**(23): 14683-14689.
- Watanabe, I., H. Kasuya, et al. (2008). "Effects of tumor selective replication-competent herpes viruses in combination with gemcitabine on pancreatic cancer." Cancer Chemother Pharmacol **61**(5): 875-882.
- Wertz, G. W. (1983). "Replication of vesicular stomatitis virus defective interfering particle RNA in vitro: transition from synthesis of defective interfering leader RNA to synthesis of full-length defective interfering RNA." Journal of Virology **46**(2): 513-522.
- Whelan, S. P., J. N. Barr, et al. (2004). "Transcription and replication of nonsegmented negative-strand RNA viruses." Curr.Top.Microbiol.Immunol. **283:61-119.**: 61-119.

- Whelan, S. P. and G. W. Wertz (1999). "Regulation of RNA synthesis by the genomic termini of vesicular stomatitis virus: identification of distinct sequences essential for transcription but not replication." J. Virol. **73**(1): 297-306.
- Wiegand, M. A., S. Bossow, et al. (2007). "De novo synthesis of N and P proteins as a key step in Sendai virus gene expression." J Virol **81**(24): 13835-13844.
- Wojton J, Kaur B (2010). "Impact of tumor microenvironment on oncolytic viral therapy." Cytokine Growth Factor Rev. **21**(2-3):127-34.
- Wollmann G, R. V., Simon I, Rose JK, van den Pol AN. (2010). "Some attenuated variants of vesicular stomatitis virus show enhanced oncolytic activity against human glioblastoma cells relative to normal brain cells." Journal of Virology **84**(3): 1563-1573.
- Wong, L. H., K. G. Krauer, et al. (1997). "Interferon-resistant human melanoma cells are deficient in ISGF3 components, STAT1, STAT2, and p48-ISGF3gamma." J Biol Chem **272**(45): 28779-28785.
- Wu L, H. T., Meseck M, Altomonte J, Ebert O, Shinozaki K, García-Sastre A, Fallon J, Mandeli J, Woo SL. (2008). "rVSV(M Delta 51)-M3 is an effective and safe oncolytic virus for cancer therapy." Human Gene Therapy **19**(6): 635-647.
- Yamada-Okabe, T., R. Doi, et al. (1998). "Isolation and characterization of a human cDNA for mRNA 5'-capping enzyme." Nucleic Acids Res **26**(7): 1700-1706.
- Yamada-Okabe, T., T. Mio, et al. (1999). "The *Candida albicans* gene for mRNA 5-cap methyltransferase: identification of additional residues essential for catalysis." Microbiology **145** (Pt **11**): 3023-3033.
- Yonemitsu Y, U. Y., Kinoh H, Hasegawa M. (2008). "Immunostimulatory virotherapy using recombinant Sendai virus as a new cancer therapeutic regimen." Frontiers in Bioscience **13**: 4953-4959.
- Zhang, X., Y. Wei, et al. (2010). "Identification of aromatic amino acid residues in conserved region VI of the large polymerase of vesicular stomatitis virus is essential for both guanine-N-7 and ribose 2'-O methyltransferases." Virology **408**(2): 241-252.
- Zhou, Y., D. Ray, et al. (2007). "Structure and function of flavivirus NS5 methyltransferase." J Virol **81**(8): 3891-3903.
- Zust, R., L. Cervantes-Barragan, et al. (2011). "Ribose 2'-O-methylation provides a molecular signature for the distinction of self and non-self mRNA dependent on the RNA sensor Mda5." Nat Immunol **12**(2): 137-143.